RASTA

SO164

R/V SONNE Cruise Report SO164

Rapid Climate Changes in the Western Tropical Atlantic

- Assessment of the biogenous and sedimentary record

Balboa - Balboa. May 22 - June 28, 2002

Edited by
Dirk Nürnberg, Joachim Schönfeld,
Wolf-Christian Dullo and Carsten Rühlemann,
with contributions of cruise participants.
Layout and production by Marcus Regenberg

GEOMAR, Kiel, December 2002

GEOMAR

Universität Bremen

bmb+f
Bundesministerium für Bildung, Wissenschaft, Forschung und Technologie

Contents

Abstract

The Caribbean is an ideal place to study the sensitive and delicate Ocean/Climate System and its response to rapid climate variations during the last, early Glacial (Dansgaard/Oeschger-Cycles) as well as the resulting environmental changes at low latitudes. The scope of the project comprises studies on the interrelated processes of global climate variations, sea level changes, sea surface temperature variations, deep and intermediate water hydrography, and the resulting fluctuations in the assemblage composition of marine biota in a confined marginal sea. Emphasis is given to the paleoceanographical processes during the late Quaternary, in particular during the highly dynamic Oxygen Isotope Stages 2 and 3, and their comparison with the Holocene to recent situation. Two largely interrelated subprojects, and an accompanied pilot study contribute to the achievement of theses goals from different perspectives with innovative methods. The basis for these studies is R/V SONNE cruise SO164 (RASTA) to the Caribbean (May 22nd to June 28th, 2002). The marine-geological expedition comprised hydroacoustic surveys, sampling of bottom sediments, and long piston and gravity coring in the Columbian and Venezuelan Basins, within the Windward Passage, and in the Florida Straits. The deployment of the submersible JAGO allowed a detailed mapping of sea bottom structures, reef morphology, and well-defined sampling at shallow depth around Guadeloupe and Martinique (French Lesser Antilles). Hydrocasts, water sampling and plankton tows accomplished the sedimentological studies with ground-truth data on the recent oceanography.

1. Introduction

Cruise SO164 with R/V SONNE was performed from May 22nd to June 28th, 2002, within the framework of RASTA (Project No. 03G0164 to GE) funded by the German Ministery of Education and Research (BMBF). RASTA consists of two largely interrelated subprojects, and an accompanied pilot study, which will contribute from different perspectives to the understanding of the sensitive climate/ocean system in the low latitude tropical/subtropical Caribbean and western Atlantic Ocean, and its response to rapid climatic changes.

The three subprojects concentrate on the following topics:

- Subproject 1: Sea level variability and carbonate export around the Lesser Antilles
- Subproject 2: Variability of paleo-sea surface temperatures and variations in thermocline depths in the Caribbean
- Pilot study: Impact of the Gulf-Stream on sedimentary environments and benthic communities in the southern Florida Straits (GOLDFLOS)

Variations in thermocline depth, sea surface temperatures, and in global sea level during the last climatic changes are causally connected. In order to better understand their interactions and to become able to assess the anthropogenic effect on climate change, the studies performed within the various subprojects are closely interrelated.

1.1 Sea level variability and carbonate export around the Lesser Antilles (RASTA TP 1)

W.-Chr. Dullo

Carbonate production of coral reefs and carbonate platforms is largely determined by sea level variations. Coral reefs are a main target of studies on sea level variations, as they are forced to follow sea level changes instantanously for biological and ecological reasons. They are therefore considered as past sea level indicators, in particular on-shore terraces (Grossmann et al., 1998) and submarine morphological features (Dullo et al., 1998; Hanebuth et al., 2000). The dynamics of ancient sea level rise is approximated from the reef's growth rate. This is determined by establishing an age/depth relationship of dated corals that either have been collected *in situ* with submersibles (Grammer and Ginsburg, 1992; Colonna et al., 1996; Dullo et al., 1998) or were retrieved from reef-drilling (Eisenhauer et al., 1993; Bard et al., 1996; Zinke et al., 2003). This is only effective if the exact paleobathymetrical range of the taxon is well constrained (Montaggioni et al., 1997).

The average sea level rise during the last deglaciation is estimated to 10 mm a^{-1}. The rise increased intermittently during meltwater pulse Ia (14000 a B.P) to 37 mm a^{-1}, and during the second pulse Ib (11000 a B.P.) to 25 mm a^{-1} (Fairbanks, 1989; Bard et al., 1996, Dullo et al., 1998). Precise ^{14}C- and U/Th (TIMS)-datings of Eemian and Holocene reefs revealed temporal and spatial differences between the individual ocean basins. For instance, the Indian Ocean sea level off western Australia was 1 to 2 m above the present level 6000 years ago, while the Atlantic at Barbados was still 10 m below today's gauges (Fairbanks, 1989; Bard et al., 1990; Eisenhauer et al., 1993; Lambeck and Nakada, 1992; Braithwaite et al., 2000). These differences may be affected by geoid changes, neotectonics, and hydro-isostatical re-equilibrations of oceanic and continental crust (Mitrovica and Peltier, 1991; Eisenhauer et al., 1993).

Corals provide reliable environmental records for the reconstruction of past sea surface temperatures (Pätzold, 1984; Heiss and Dullo, 1997; Fairbanks et al., 1997, and references therein). The proxies comprise the genuine $\delta^{18}O$ method, but new applications based on Sr/Ca and U/Ca relationships are also applied (Beck et. al., 1992, 1997)

Results of the CLIMAP program indicate that tropical sea surface temperatures during the Last Glacial Maximum were only lower by 0 to 2°C than today. Meterological approaches based on snowfall altimetry approximated a surface water cooling of 3 to 6.5°C in

the tropics (Broecker and Denton, 1990). Sr/Ca-records of an 10 ka old *Porites lobata* from Vanuatu (equatorial Pacific) revealed average temperatures that were 5.5°C lower than today in this region. Other Sr/Ca and U/Ca studies from the western Pacifik corroborate these results (McCulloch et al., 1996; Min et al., 1995). Hence, results from geochemical proxies are in better agreement with terrestrial records than with the results of foraminiferal transfer functions (CLIMAP, 1981).

Small scale sea level variations leave a strong imprint on the carbonate export of reef systems. They are recorded in composition variations of sediment export at certain sea level stands. A high aragonite proportion of sediments derived from shallow-water platforms characterises high stands while a high calcite proportion prevailes during sea level lowstands. A substantial export of abiogenous components and fragments of inner-platform organisms is recorded during high stands. Biogenous skeletal components and lithoclasts prevail in talus sediments during lowstands (Westphal, 1998). This concept may be applied to high-resolution studies of late Quaternary sediment production history and cyclic deposits, and it may yield evidences for small-scale sea level variations and their effects on carbonate systems (Kroon et al., 1998; Rendle et al., 1998) influencing the diagenetic overprint (Brachert and Dullo, 2000).

The major objectives of RASTA Subproject TP1 is to assess the amplitude of sea level variations during the last glacial-interglacial cycle with special focus on Oxygen Isotope Stage 3 (Fig. 1).

- How is the carbonate production during this specific time window and how are the sedimentary dynamics?
- Are there sufficient areas available for shallow water production during Isotope Stage 3?
- Are there fossil reefs which can be sampled?

Another important issue addresses the determination of carstification levels attributed to the Last Glacial Maximum. We know several such levels from the Caribbean to occur at 120 m below present day sea level. Since sea level rose quickly during the late Pleistocene, there should be drowned reefs on top of the presently submerged bank margins. To prove their existence is another goal for the *in situ* observations with the submersible.

A key issue focuses on the sampling of sclerosponges. These skeletal, long living organisms are a unique paleoclimatic archive, as they occur in a distinct bathymetric window between 100 and 130 m of present water depth. They monitor precisely the dynamics of the thermocline for at least 600 years.

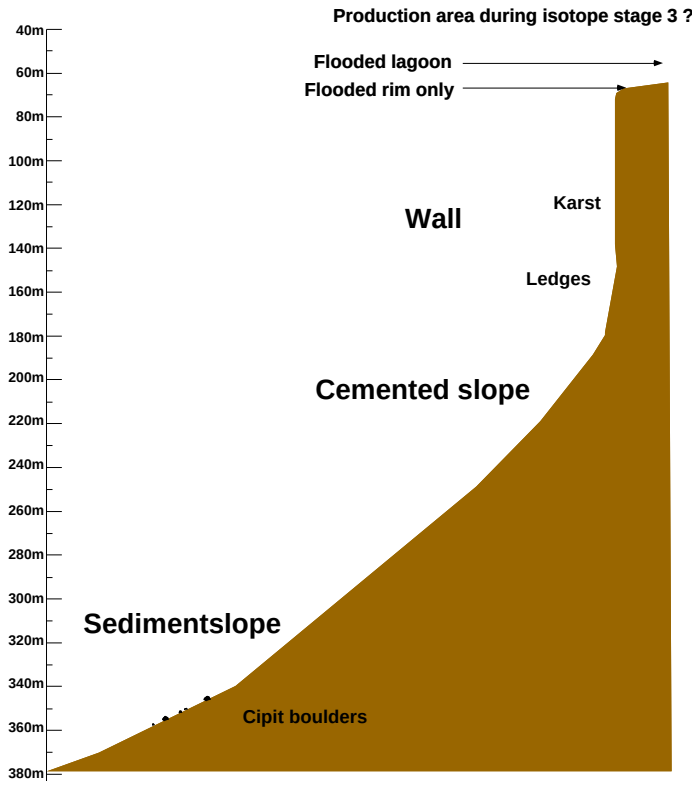

Fig. 1 Schematic sketch of the potential production level for shallow water carbonates during Isotope Stage 3. Minor changes will be reflected in the benthic foraminiferal assemblage (rim *vs*. lagoon)

1.2 Variability of paleo-sea surface temperatures and variations in thermocline depth in the Caribbean (RASTA TP 2)

D. Nürnberg

Currently, scientific efforts concentrate on understanding of how the integrated earth system operates at times of major climatic instability, specifically during very rapid climatic changes. The investigation of high-resolution climatic records from the marine as well as terrestrial realm, the establishment of new proxy records reflecting environmental change, and the improvement of dating methods in order to resolve short-term environmental variability and phasing relationships (leads and lags) are thus of high priority to the scientific community interested in Quaternary climate change.

The temporal evolution of the Western Atlantic Warm Water Pool (WAWP) is crucial in this respect. The WAWP is characterized by extraordinary mean annual sea surface temperatures, which supply tropical heat and moisture to the atmosphere, and related feedback mechanisms (i.e. atmospheric circulation, cloud formation, greenhouse warming, SST-dependant CO_2-uptake) (Tomczak and Godfrey, 1984). This oceanic feature is located mainly in the western tropical-subtropical Atlantic Ocean, Caribbean Sea and Gulf of Mexico (Fig. 2). The WAWP is regarded as the main reservoir of heat to be transferred to the North Atlantic.

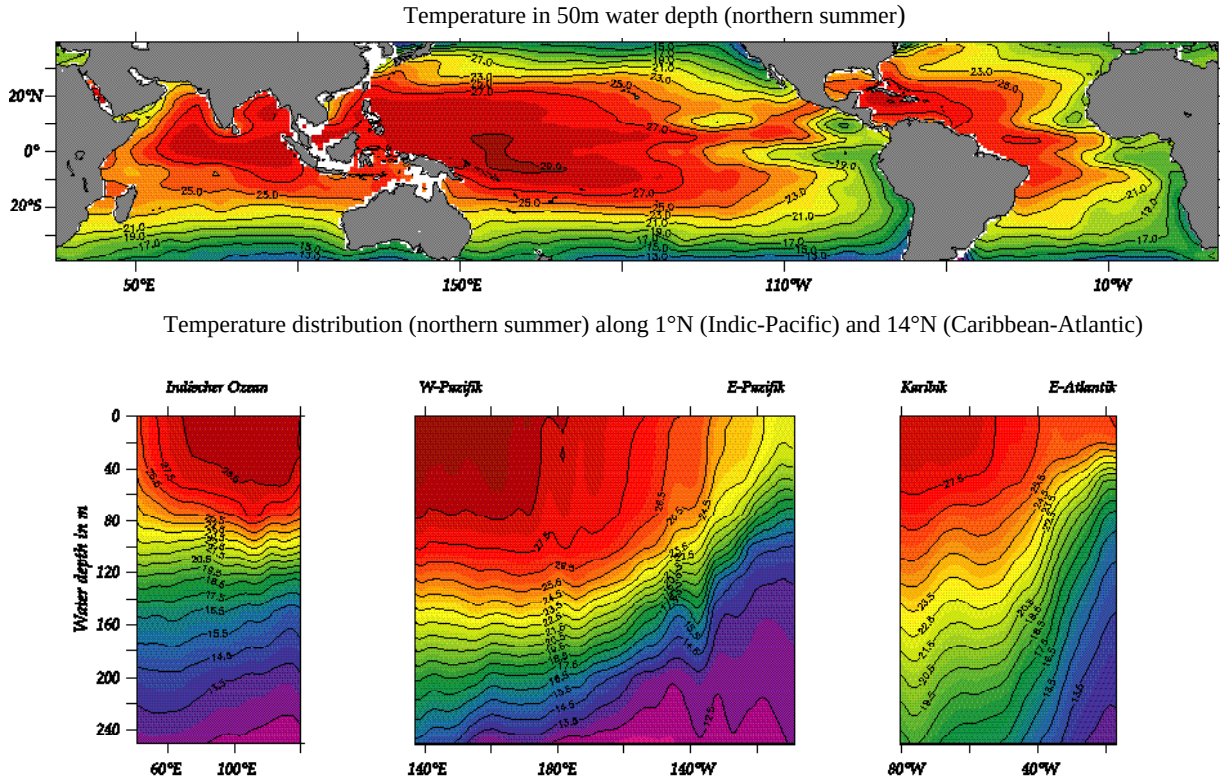

Fig. 2 Modern latitudinal and vertical variability of temperature in subtropical-tropical regions of the World Ocean during northern summer. *Warm water pools* are marked by temperatures of up to 29°C and by a deepening of the thermocline towards the west. Note: The thermocline of the eastern Indian Warm Pool is distinctly shallower than in the W-Pacific and W-Atlantic (Caribbean) warm water pools. Strong upwelling along the Somali and Arabian coasts during the summer monsoon contributes to the cooling of the northwest Indian Ocean. Source: Levitus and Boyer (1994).

It is the source area of the warm Gulf Stream, which is the northward flowing Western Boundary Current in the North Atlantic driven by the western Atlantic equatorial trade winds. Heat release from the WAWP triggered temperature changes even in high latitudes of the North Atlantic region (McIntyre and Molfino, 1996; Rühlemann et al., 1999). Long-term as well as short-term changes in WAWP dynamics, therefore, sensitively affected not only climate in the tropical Atlantic, but also that in the northern Atlantic and in Europe.

The Late Quaternary climate is known to have been unstable and prone to major, rapid changes in climate that occurred within a few decades or less (Kennett et al., 2001). This climatic instability was most pronounced during the last glacial, and implies closely linked changes within the hydrosphere, atmosphere, cryosphere, and biosphere. Stimulated by the findings of millennial to sub-millennial time scale climatic variations in ice core records from Greenland and Antarctica (e.g. Alley et al., 1993), many efforts were undertaken to document the short-term climatic variations also in marine sediment records. The records proved the close relationship of short-term climatic events between the northern and southern hemispheres, and thus teleconnections on suborbital time scales. The oscillations in air temperature recorded in Greenland ice cores apparently correlate with paleoceanographic records in the North Atlantic, known as Dansgaard-Oeschger events (Broecker and Denton, 1989) and Heinrich events (Bond et al., 1993), and in the equatorial Atlantic (Curry and Oppo, 1997). The causes for the rapid climatic Dansgaard-Oeschger variations are largely unknown, although various attempts for explanation were proposed (e.g. Cane and Molnar, 2001; Ganopolski et al, 1998; Ganopolski and Rahmstorf, 2001; van Krefeld et al., 2000). An important mechanism often proposed is the change in the thermohaline circulation (THC). However, Elliot et al. (2002) suggest that only major Dansgaard-Oeschger cooling events, the Heinrich events, were associated with major changes in thermohaline deep-water circulation. The thermohaline circulation, thus, is still questioned as an appropriate global mechanism to explain the rapid climatic Dansgaard-Oeschger variations.

Despite its importance, the dynamics of the WAWP on relatively short time scales and its role for the climatic evolution in the North Atlantic Ocean area are not well understood. The observed time lag between specific SST proxy records (foraminiferal Mg/Ca, alkenones) from various tropical regions (Pacific, Atlantic and Indian oceans) on one hand and stable oxygen isotopes on the other hand, in fact, led Bard et al. (1997), Lea et al. (2000), and Nürnberg et al. (2000) to emphasize the tropical oceans´s role in forcing climate change.

The primary objective of the RASTA subproject TP2 is to document changes in the thermal structure of the Caribbean surface ocean - the source area of the Gulf Stream system - over the last major glacial-interglacial cycles, with specific focus on the last glacial to Holocene period. The reconstruction of sea surface temperatures, the depth of the thermocline, and paleoproductivity will be based primarily on the micropaleontological and geochemical analyses of planktonic foraminifers. The project is in agreement with both the National Climate Program of the German Government and international programs, which focus on Global Change (e.g. Past Global Changes, PAGES). Our attempt to reconstruct SST is in close relationship to the TEMPUS initiative of the European Commission's Environment and Climate Program (Rosell-Mélé et al., 1998). Also, our studies are closely related to the GLAMAP initiative to reconstruct last glacial maximum SST in the Atlantic Ocean (Sarnthein et al., 1998).

In particular, RASTA Subproject TP2 addresses the following topics:

· To define the sea surface temperature variability in the Caribbean during the late Quaternary as revealed by geochemical proxy data.

We will accomplish a combined approach of assessing paleo-SST by applying Mg/Ca paleothermometry, foraminiferal transfer functions, alkenones, Sr/Ca in corals and planktonic foraminifers. In particular, combining both Mg/Ca and $\delta^{18}O$ (reflecting changes in temperature, salinity, and global ice volume) measured on the same planktonic foraminiferal species will allow to separate the temperature signal from the isotope signal and to extract the residual $\delta^{18}O_{seawater}$ record indicative of changes in salinity and ice volume (Nürnberg, 2000). In order to further evaluate and improve the method of Mg/Ca paleothermometry, comparative studies between foraminiferal test chemistry and water chemistry will be carried out. Assessing the impact of carbonate dissolution on the foraminiferal test chemistry is essential and will be approached by core top sediment studies covering a large depth range.

· To reconstruct the spatial and temporal variations in the strength of the WAWP.

Since the depth of the thermocline is indicative for the strengh of warm pools, the reconstruction of sea surface temperatures (SST) and SST gradients in the upper water column is essential for all further reconstructions of warm pool dynamics. Temperature gradients in the upper ocean will be determined by measuring both Mg/Ca and $\delta^{18}O$ in planktonic foraminifers living at different depth levels. In this respect, core-top samples will provide additional data to constrain the existing Mg/SST calibration curves and to establish new species-specific calibration curves.

· To reconstruct lateral changes in the South Equatorial Current and its influence on the thermal structure of the Caribbean.

Selected sediment cores from the outer Lesser Antilles Island Arc will be studied. The according SST records will be compared to the Caribbean records in order to reveal temporal and spatial changes in the surface hydrography. Of particular interest are Termination 1 and Oxygen Isotope Stage 3.

During the expedition SO164 with R/V SONNE, we gathered a suite of sediment cores over a large latitudinal and longitudinal range, which will allow us to establish (high-resolution) time-series and spatial reconstructions of oceanographic and climatic changes in the Caribbean Sea.

1.3 Impact of the Gulf Stream on sedimentary environments and benthic communities in the southern Florida Straits (GOLDFLOS)

W. Kuhnt, J. Schönfeld

The Gulf Stream is the "central heating" of middle and northern Europe and controls to a large extend the recent climate and consequently our living conditions in Cental Europe. The Gulf Stream is part of the trans-equatorial heat transport. Warm ocean surface waters from the equatorial South Atlantic cross the Equator, pass the Caribbean Sea and flow as Gulf Stream into the North Atlantic (Schmitz and McCartney, 1993; Schmitz et al., 1993; Sato and Rossby, 1995). The surface water inflow into the Caribbean Sea passes several straits between the Windward Islands (Wüst, 1964; Stalcup and Metcalf, 1972; Johns et al., 2002). The entire outflow is funnelled, however, in the Florida Straits between Florida, Cuba, and the Little Bahama Bank. The so-called "Florida Stream" constitutes the central core of the Gulf Stream that flows further northwards into the western Atlantic (Pickard and Emery, 1982; Hogg and Johns, 1995). Any change in warm-water transport to the North Atlantic during the late Quaternary should be accompanied with a substantial variation in Florida Straits' throughflow (Lynch-Stieglitz et al., 1999). They are to be monitored with benthic proxies recording the near-bottom flow strength.

Today's structure of the current was extensively studied in the STACS (Subtropical Atlantic Climate Studies) program since 1982 in the northern Florida Straits at 27°N (Molinari et al., 1985), and it is continuously monitored (http://www.pmel.noaa.gov/wbcurrents/cabletransport.html). The main achievement of these studies was an assessment of Gulf Stream's volume and heat transport, and of the short- and long-term variability (Niiller and Richardson, 1973; Schott and Zantop, 1985; Larsen, 1992; Lamb, 1981; Hall and Bryden, 1982; Molinari et al., 1985a). The current velocities are higher than 180 cm s^{-1} in the central core of the Gulf Stream. Close to the sea floor, they vary between 10 and 20 cm s^{-1} (Leaman et al., 1987). Higher near-bottom currents were observed on the northern slope of the Cay Sal Bank where the Florida Stream directly impinges the sea floor with depth-decreasing velocities of 20 to 60 cm s^{-1} (Richardson et al., 1969).

Geological evidence for the imprint of near-bottom currents is provided by sedimentary structures, bedform geometry, and the grain-size distribution of near-surface sediments (e.g. Kennedy, 1964; Faugéres et al., 1984; McCave, 1984; Revel et al., 1996). A calibration to current velocity in the overlying water is achieved by flow experiments and hydrodynamic models (Zanke, 1982; Southard and Boguchwal, 1990).

Water turbulence and near-bottom currents also affect the benthic biota. Hydraulic energy is considered as important environmental factor steering the abundance and species composition of current-swept benthic communities (Mullineaux and Butman, 1990; Bertram and Cowen, 1999). The response of benthic foraminifera to near-bottom currents has been described in several studies from the north-eastern Atlantic (Mackensen et al., 1985; Lutze and Thiel, 1989; Linke and Lutze, 1993; Schönfeld, 1997, 1998, 2002a). A quantification of the relationship between epibenthic foraminiferal abundance and bottom current strength has been attempted in order to constrain the past bottom current activity (Schönfeld and Zahn, 2000). The calibration data available to date are rather limited and show important gaps, in particular at current velocities higher than 20 cm s^{-1} (Schönfeld, 2002a).

The objectives of the GOLDFLOS pilot study are to describe the varying influence of the near-bottom current on recent sediments and benthic communities on a depth transect to the north of Cay Sal Bank, Bahamas. The results will reveal whether a relationship exists between the abundance of passive suspension feeding benthic foraminifers, a certain grain size distribution of the surface sediment, and near-bottom current velocity as inferred from previous hydrographic surveys (Richardson et al., 1969). Once the relationship is assessed, fluctuations of current-sensitive foraminiferal assemblages and grain size properties along sediment cores will depict long-term current variations from the last Glacial to late Holocene. The results are to be compared with evidences from earlier stable isotope studies (Lynch-Stieglitz et al., 1999). Subsequent investigations will focus on a quantification of the Florida Straits throughflow. Ancient current velocities, the cross section of the sea strait at lowered sea level, and paleo-sea surface temperatures from planktonic foraminiferal census data and alkenones may finally allow approximations of water mass transport and heat flow rates during the last Glacial Maximum and Oxygen Isotope Stage 3.

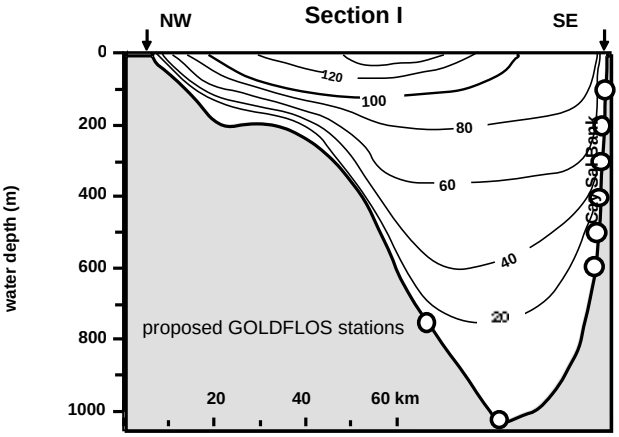

Fig. 3 Morphology and westward current velocities given in cm s^{-1} on the hydrographic „Section I“ (see Fig. 4) at the northern slope of the Cay Sal Bank (Richardson et al., 1969). Our proposed stations are in the immediate vicinity of this transect. Note that the depths of actual stations SO164-09 to SO164-17 differ from this initial proposal (see Fig. 26).

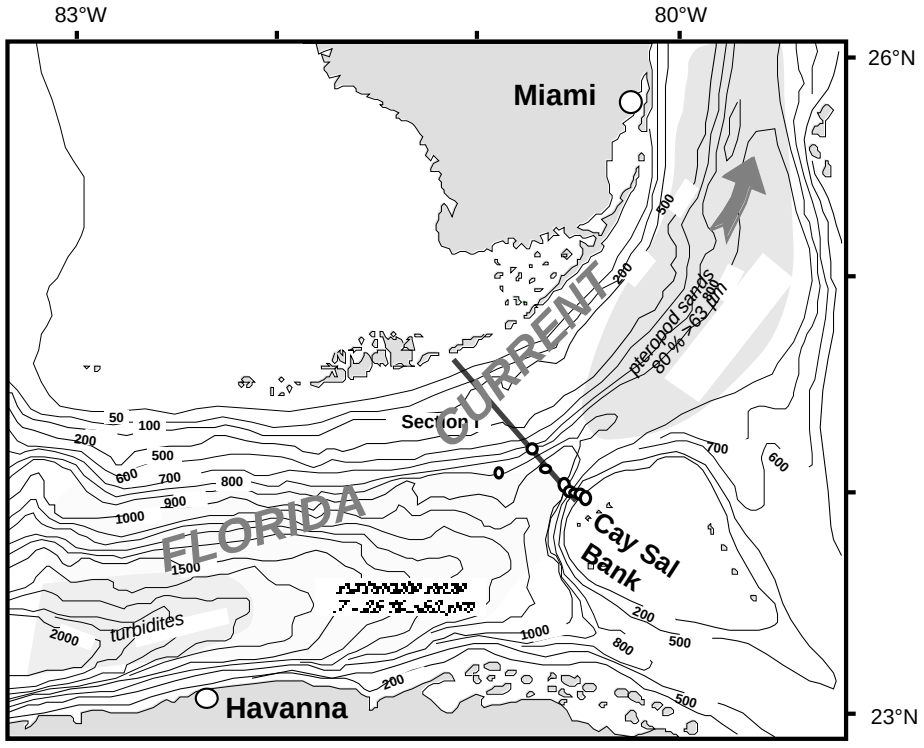

Fig. 4 Bathymetry, bottom sediments and proposed GOLDFLOS stations in the southern Florida Straits. Section 1 according to Richardson et al. (1969). Note that the locations of actual stations SO164-09 to SO164-17 differ from this initial proposal (see Fig. 24 and 28).

2. Background

2.1 Modern hydrographic setting in the study area

D. Nürnberg

Surface currents

The Caribbean hydrography is characterized by the inflow of surface and intermediate water masses from the western North Atlantic Ocean (Fig. 5). The Caribbean surface water masses are part of the anti-cyclonic surface gyre, which dominates the subtropical North Atlantic Ocean. Driven by the eastern trade winds, the water masses of the North and South Equatorial Currents cross the North Brasil Current and the Antilles Current, and enter the Caribbean. They pass the Yucatan channel and flow into the Gulf of Mexico (known as the Loop Current) (Pickard and Emery, 1982). From there, the Florida Current changes into the Gulf Stream, which subsequently exits the Caribbean (Worthington, 1976).

Surface current pattern and hydrography are subject to seasonal fluctuations, which are mainly controlled by the seasonally northward and southward migrations of the Innertropical Convergence Zone (ITCZ). In accordance with the shift of the thermal equator to the south during the northern winter, the ITCZ is located south of the Caribbean at ca. 0° to 5°S. During northern summer, instead, the thermal equator shifts to the north and the ITCZ migrates across the Caribbean to about 6° to 10°N. At that time, the Caribbean hydrography is characterized by enhanced precipitation and fluvial freshwater supply. Also, the North Equatorial Counter Current establishes during northern summer, mainly driven by the combined influence of the southeast trade winds and the diverting Coriolis force. It forces equatorial Atlantic surface waters towards the east and causes strengthened inflow into the Caribbean (Busalacchi and Picaut, 1983; Richardson and McKee, 1984).

Tropical rivers directly or indirectly drain into the Caribbean and, thus, influence the hydrography and chemistry of the Caribbean. The most important Caribbean fresh water sources are the Amazon (mean runoff $V_m = 17.3*10^4\,m^3\,s^{-1}$), the Orinoco ($V_m = 3.9*10^4\,m^3\,s^{-1}$), and the Magdalena ($V_m = 0.8*10^4\,m^3s^{-1}$; Milliman and Meade, 1983). The seasonal change between high and low precipitation propels seasonally varying fluvial supply, which is reflected in seasonally varying salinity, nutrient concentrations (silicate concentrations of 3 to 5 µmol kg^{-1}; Froelich et al., 1978; Morrison and Nowlin, 1982), and portion of terrestrial material in the Caribbean sea sediments (Milliman and

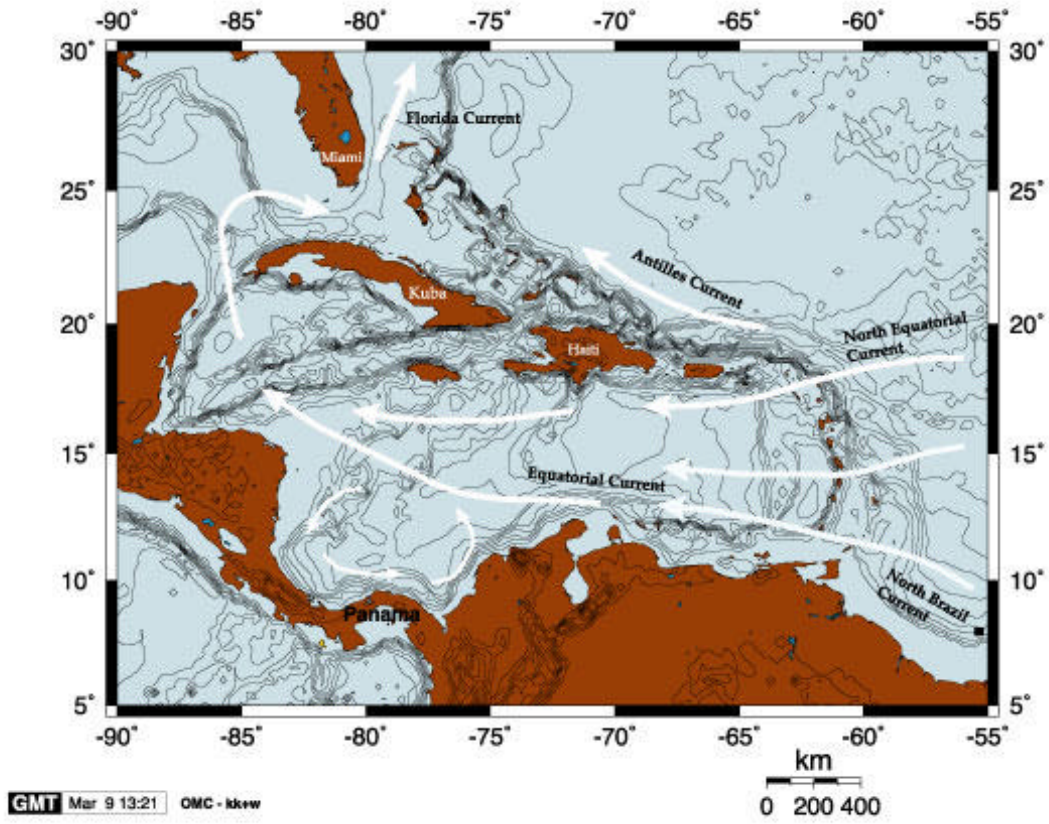

Fig. 5 Bathymetric chart of the Caribbean schematically showing the surface water mass circulation pattern (accordimg to Fisher, 1990; Hogg and Johns, 1995; Stramma and Schott, 1999).

Meade, 1983).

The Caribbean is the source area of warm water masses leaving the low latitudes *via* the Florida Straits, and, thus, effectively promotes the transequatorial heat transfer to the north (Schmitz and McCartney, 1993; Schmitz et al., 1993; Sato and Rossby, 1995). The Gulf Stream System is crucial to the climatic evolution in high northern latitudes and, thus, to the living conditions in NW Europe. The surface water inflow enters the Caribbean through passages within the Lesser Antilles (Wüst, 1964; Stalcup and Metcalf, 1972). The outflow entirely concentrates on the southern Florida Strait between Florida Keys and Cuba, and subsequently to the northern Florida Strait between Bahama Bank and Florida. This outflow builds the starting point of the Gulf Stream (Pickard and Emery, 1982; Hogg and Johns, 1995).

In the framework of the STACS program (**S**ub**t**ropical **A**tlantic **C**limate **S**tudies; Molinari et al., 1985b), the Gulf Stream system in the northern Florida Straits was focus of intensive oceanographic studies since 1982, leading to definite cognition of water volume, heat transport, and its short-term variability. The water volume leaving the northern Florida Straits amounts to an annual average of 29.5 and 32.3 Sv (1Sv = 10^6 m^2 s^{-1}), with a seasonal variability of ±1.4 to ±2.2 Sv (Niiller and Richardson, 1973; Schott and Zantop, 1985; Larsen, 1992). The mean heat flux is 1.13 to 1.25 * 10^{15}W (Lamb, 1981; Hall and Bryden, 1982; Molinari et al., 1985a). Current velocities in the center stream amount to >180 cm s^{-1}, while varying between 10 and 20 cm s^{-1} at the sea floor (Leaman et al., 1987).

Intermediate and deep water masses

The Caribbean deep and intermediate water masses recruit themselves from Atlantic water masses, which enter the Caribbean *via* deep water passages: The northern inflow takes place *via* the Windward Passage (1650 m deep) and *via* the Anegada Passage (ca. 2000 m deep) (Sturges, 1975; Metcalf, 1976). Water masses coming from the south enter the Caribbean *via* the Antilles passages. North Atlantic Inter-mediate Water (NAIW), Upper North Atlantic Deep Water (UNADW), Mediterranean Outflow Water (MOW) and Antarctic Intermediate Water (AAIW) serve as main sources for the Caribbean Deep Water.

AAIW, which is formed at approximately 50°S at the Antarctic Polar Front, flows northward as a cold, low saline, but nutrient-enriched water mass at 800 to 1100 m water depth. UNADW is a young, oxygen-rich and nutrient-poor water mass, which is composed of contributions of MOW, Labrador Sea water masses and overflow from the Norwegian-Greenland Sea. MOW is genereated mainly in the Levantine Basin of the eastern Mediterranean, where salinity is extremely high due to high evaporation rates. MOW crosses the Strait of Gibraltar and enters the North Atlantic as a salty and nutrient-poor water mass (Zenk et al., 1990; Zenk and Armi, 1990; Bryden and Kinder, 1991; Hinrichsen et al., 1989; Price et al., 1993).

UNADW is the major water mass contributing to the deep Caribbean water masses (Kawase and Sarmiento, 1986). Remarkable salinity minima in the deep Caribbean, however, point to the fact that apparently the AAIW contribution is larger than previously assumed. In the southern Caribbean Basin, it may contribute up to 30 % to the Caribbean Intermediate Water (Haddad and Droxler, 1996). From theoretical calculations, Worthington (1971) already postulated an AAIW inflow of 10 Sv into the Caribbean. As the Caribbean is obviously collecting various water masses from the upper western Atlantic, paleoceanographic data sets from the Caribbean may help to document the glacial-interglacial hydrographic and chemical variability of the deep and intermediate Atlantic Ocean.

2.2 Pleistocene to Holocene paleoceanography, a working hypothesis

During Pleistocene to Holocene times, the WAWP remained a dynamic oceanographic feature with implications for the global oceanographic circulation. According to Blunier et al. (1998) and Rühlemann et al. (1999), the Atlantic heat transport into high northern latitudes was closely coupled to northern North Atlantic deep water formation (Keigwin et al., 1991; Driscoll and Haug, 1998) (Fig. 6). During times of enhanced melt water supply into the North Atlantic (e.g. Heinrich events), thermohaline circulation ceased and the transequatorial transfer of warm subtropical waters into the North Atlantic diminished, causing considerable cooling in the North Atlantic (Broecker et al. 1985; Lynch-Stieglitz et al., 1998; Manabe and Stouffer, 1988, 1997; Rahmstorf, 1994; Ganopolski et al., 1998; Bard et al., 2000). The tropical-subtropical Atlantic, instead, heated up (McIntyre and Molfino, 1996; Rühlemann et al., 1999). In the Caribbean (especially in the Gulf of Mexico), the slowed surface water circulation caused considerable piling up of surface waters, which is reflected in both the deepening of the thermocline and the steeping of the ocean surface temperature gradient in this area.

After the re-initiation of the thermohaline circulation in the North Atlantic, the accelerated outflow of warm surface waters through the Florida Straits into the North Atlantic reconstituted (Lynch-Stieglitz et al., 1998), causing a deepening of the thermocline and the steepening of the ocean surface temperature gradient in the Florida Straits, while in the Caribbean, the thermocline shoaled and the temperature gradient was less established. The enhanced outflow induced an increase in heat and moisture transport to the north, which might have favored the rapid and anewed build-up of ice shields and subsequently, the initiation of new melt water events in the North Atlantic (Alley and MacAyeal, 1994).

Indeed, high-resolution paleoceanographic studies in the western tropical Atlantic refer to synchronous changes in sea surface temperatures (SST) and deep-water circulation patterns (Curry and Oppo, 1997). Early reconstruction of SST in the Caribbean only

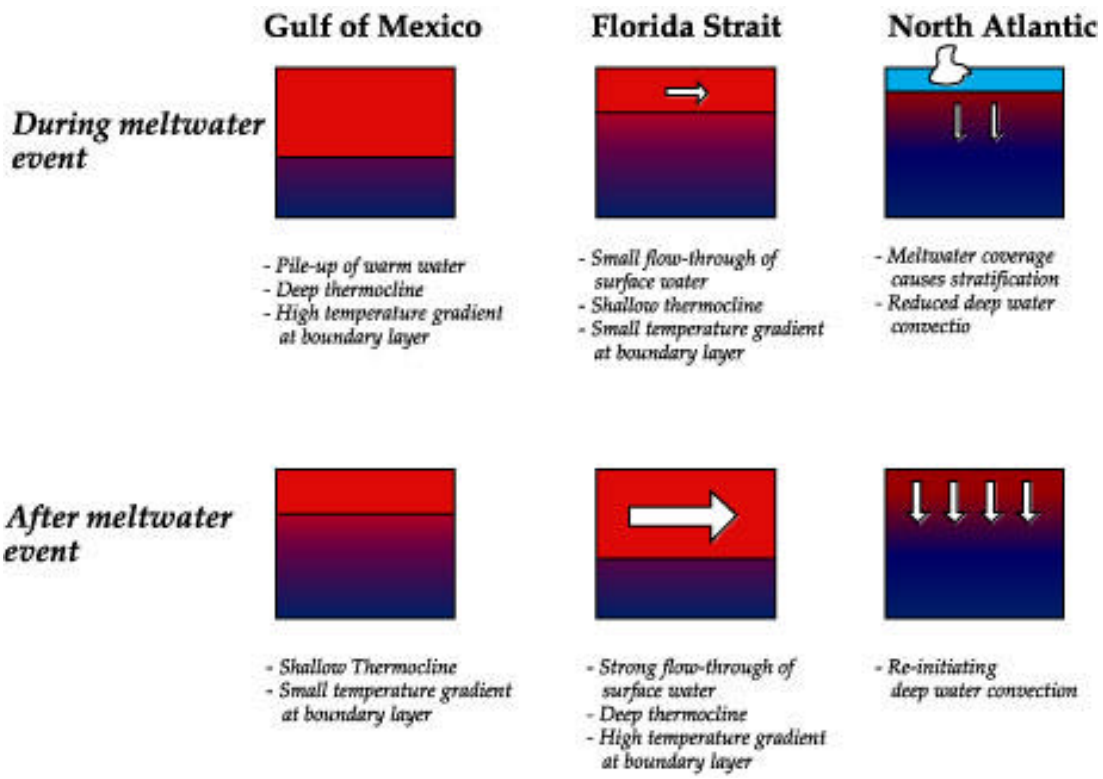

Fig. 6 Schematic diagram illustrating the working hypothesis of the proposed study, which is based on the antiphase-circulation model of Rühlemann et al. (1999) and its feedback-mechanisms on tropical sea surface temperatures.

exhibit small SST changes of ca. 1 to 2°C (Prell and Hays, 1976), while recent studies point to a larger SST amplitude of ca. 2.5 to 3°C during the last glacial-interglacial transition (e.g., Hastings et al., 1998; Rühlemann et al., 1999) (Fig. 7). Even on short-term time scales, variations in SST of about 2 to 4°C were described, which were related to wind-induced upwelling and point to causal connections between tropical climate and Dansgaard-Oeschger oscillations (Hüls and Zahn, 2000). At about 30.000 years BP, Hüls (2000) observed a significant warming in the southern Caribbean, which parallels increasing percentages of the euryhaline planktonic foraminifer *G. ruber* in the Gulf of Mexico, indicative for sea surface warming (Kennett et al., 1985). Contemporaneously, the North Atlantic records a dramatic cooling in response to Heinrich Meltwater Event 3 (Chapman and Shackleton, 1998), which supports the assumption of teleconnections *via* the thermohaline circulation in the Atlantic Ocean.

Based on $\delta^{13}C$ and Cd/Ca studies on benthic foraminifers, Boyle and Keigwin (1987), Cofer-Shabica and Peterson (1986), Oppo and Fairbanks (1987, 1990), Zahn et al. (1987), Curry et al. (1988), Duplessy et al. (1988), Sarnthein et al., (1994), and Oppo et al., (1995) concluded that nutrient concentrations within the North Atlantic Intermediate Water (NAIW) and within the Upper North Atlantic Deep Water (UNADW) were lower during the Last Glacial Maximum than today. This is supported by the benthic $\delta^{13}C$ profile from DSDP Site 502B (central Caribbean) (de Menocal et al., 1992). These data document the good or even improved ventilation of the upper Atlantic and lowered nutrient concentrations during the Last Glacial Maximum. Benthic Cd/Ca data from the Caribbean (KNR64-5-5, 3047 m water depth) also point to glacially reduced nutrient concentrations (Boyle and Keigwin, 1987).

The glacially reduced nutrient concentrations may be related to three processes:

(1) The reduction of high-nutrient Antarctic Intermediate Water (AAIW) flow into the North Atlantic (which generally contradicts to the hydrodynamically more active glacial Southern Ocean).

(2) Enhanced rates of formation of North Atlantic Intermediate Water due to the changed density structure of the glacial subpolar North Atlantic (Boyle and Keigwin, 1987; Duplessy et al., 1988).

(3) Enhanced impact of Mediterranean Outflow (MOW) on the hydrography of the shallow North Atlantic (Zahn et al., 1987; Sarnthein et al., 1994; Jung, 1996).

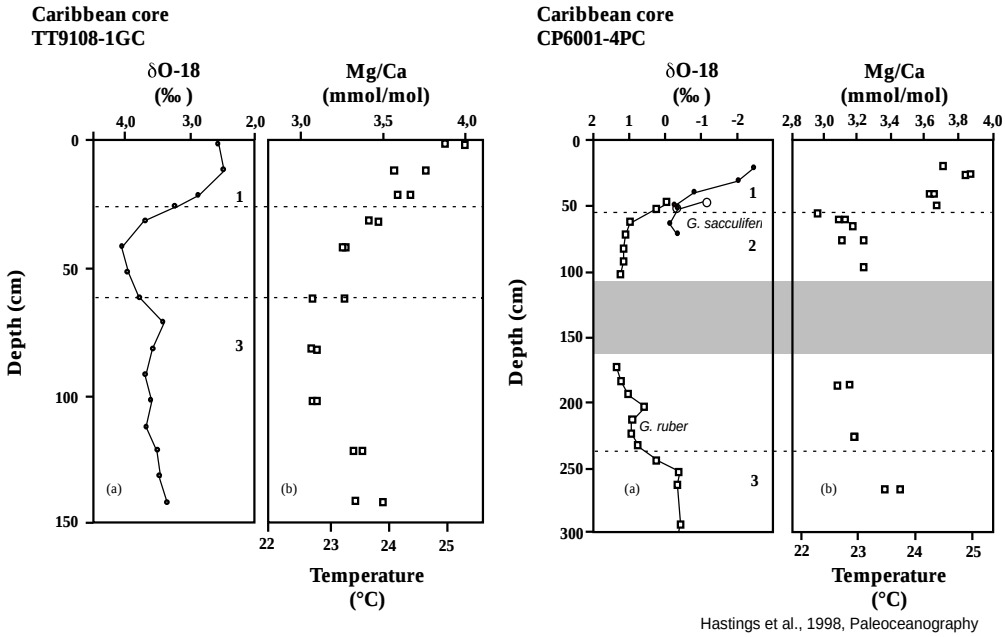

Fig. 7 Mg/Ca ratios of the planktonic foraminifer *G. sacculifer* and the calculated paleo-sea surface temperatures (b) in comparison to oxygen isotopes (a) of two sediment records from the Caribbean (Hastings et al., 1998). Numbers indicate isotope stages. Stage boundaries are indicated by hatched lines. The grey area marks a turbidite.

3. Partipicants

Tab. 1 The R/V SONNE crew.

Rank	Name
Master	Andresen, Hartmut
Ch. Mate	Korte, Detlef
2nd Mate	Aden, Nils Arne
Radio Officer	Göldner, Frank Rüdiger
Surgeon	Walther, Anke
Ch. Eng.	Neumann, Peter-Gerhard
2nd Eng.	Klinder, Klaus-Dieter
2nd Eng.	Lindhorst, Norman
Electrician	Dammann, Thorsten
Ch. Electron.	Angermann, Rudolf
Electron. Eng	Leppin, Jörg
Syst. Manager	Grossmann, Matthias
Fitter	Stenzler, Joachim
Motorman	Zeitz, Holger
Motorman	Kunze, Christian
Motorman	Dorow, Dieter

Rank	Name
Ch. Cook	Prammer, Rudolf
2nd Cook	Falk, Volkhard
Ch. Steward	Wege, Andreas
2nd Steward	Hoppe, Jan
2nd Steward	Baumgärtl, Anja
Auxiliary Boatsman	Schachel, Dirk
Auxiliary Boatsman	Bierstedt, Torsten
Auxiliary Boatsman	Rosin, Peter
Auxiliary Boatsman	Kuhn, Ronald
Auxiliary Boatsman	Etzdorf, Detlef
Stewardess	Droldner, Ellen
Auxiliary Boatsman	Neitzsch, Bernd
Auxiliary Boatsman	Reichmacher, Wolfgang
Auxiliary Boatsman	Etzdorf, Detlef
Auxiliary Boatsman	Lindemann, Erhard

Contact

RF Reedereigemeinschaft Forschungsschifffahrt GmbH,
Haferwende 3, D-28357 Bremen, Germany

Tab. 2 Scientific participants.

Name	Discipline	Institute
Beck, Tim, scientist	Marine Biology	Univ. Tüb.
Brughmans, Natasja, scientist	Marine Geology	GEOMAR
Camoin, Gilbert, Dr., scientist	Sedimentology	Cerege
Castaneda, Julian Jose, Prof. Dr., observer	Oceanography	Inst. Oceano. Venezuela
Dullo, Wolf-Christian, Prof. Dr., chief scientist (Leg II)	Marine Geology	GEOMAR
Fessler, Sebastian, technician	Marine Geology	GEOMAR
Freiwald, André, Prof. Dr., scientist	Palaeontology	Univ. Tüb.
Gaal, Aron, student	Geophysics	GEOMAR
Gussone, Nikolaus, scientist	Geochemistry	GEOMAR
Hansen, Sophie, student	Biology	GEOMAR
Hippler, Dorothee, scientist	Geochemistry	Univ. Bern
Hissmann, Karen, submersible assistant	JAGO-diving	MPI
Kawohl, Helmut, technical advisor	Marine technology	Marinetechnik
Kuhnt, Wolfgang, Prof. Dr., scientist	Palaeontology	Univ. Kiel
Lezius, Jeanette, student	Geology	Univ. Stutt.
LeGrande, Allegra, scientist	Geophysics	Lamont
Martinez-Mendez, Gema, student	Geology	Univ. Kiel
Mills, Matthew, Dr., scientist	Biol. Oceanography	IFM
Mulitza, Stefan, Dr., scientist	Marine Geology	GeoB
Nägler, Thomas, Dr., scientist	Geochemistry	Univ. Bern
Neufeld, Sergej, technician	Marine Geology	KUM
Nürnberg, Dirk, Dr., chief scientist (Leg I)	Marine Geology	GEOMAR
Numberger, Lea, student	Biology	GEOMAR
Petersen, Asmus, technician	Marine Geology	KUM
Rühlemann, Carsten, Dr., chief scientist (Leg III)	Marine Geology	GeoB
Schauer, Jürgen, submersible pilot	JAGO-diving	MPI
Schönfeld, Joachim, Dr., scientist	Marine Geology	GEOMAR
Steingruber, Sandra, Dr., scientist	Environm. Sciences	LRC
Steinmetz, Marc, photographer	Documentation	Freelanced journalist
Steph, Silke, scientist	Marine Geology	GEOMAR
Thiele, Julia, student	Marine Geology	GeoB
Westphal, Hildegard, Dr., scientist	Sedimentology	Univ. Han.

Participating companies and institutes

Cerege – Geosciences de l'environment, Europôle Méditerranéen de l'Arbois, BP 80, 13545 Aix en Provence cedex 04, France

GeoB – Univ.ersität Bremen, Fachbereich Geowissenschaften, Klagenfurterstr., D–28359 Bremen, Germany

GEOMAR – Forschungszentrum für Marine Geowissenschaften der Christian-Albrechts-Univ.ersität zu Kiel, Wischhofstr. 1-3, D–24148 Kiel, Germany

Inst. Oceano. Venezuela – Univ.ersidad de Oriente, Instituto Oceanográfico de Venezuela, Departamento de Oceanografía, Cumaná-Sucre 6101-A, Venezuela

KUM – Umwelt- und Meerestechnik Kiel GmbH, Wischhofstraße 1-3, D–24148 Kiel, Germany

Lamont – Lamont Doherty Observatory, LDEO P.O. Box 1000, 61 Route 9W, Palisades, NY 10964-1000 USA

LRC – Limnological Research Center, CH–6047 Kastanienbaum, Switzerland

Marinetechnik – Am Kreuzkamp 27, D–31311 Uetze, Germany

MPI – Max-Planck-Institut für Verhaltensphysiologie Seewiesen, D–82305 Starnberg, Germany

Univ. Bern – Universität Bern, Institut für Geologie, Baltzerstrasse 1-3, CH–3012 Bern, Sitzerland

Univ. Han. – Universität Hannover, Institut für Geologie und Paläontologie, Callinstraße 30, D–30167 Hannover, Germany

Univ. Kiel – Universität Kiel, Institut für Geowissenschaften, Ludewig-Meyn-Straße 10, D–24098 Kiel, Germany

Univ. Stutt. – Universität Stuttgart, Institut für Geologie und Paläontologie, Herdweg 51, D-70174 Stuttgart, Germany

Univ. Tüb. – Universität Tübingen, Institut für Geowissenschaften, Sigwartstr. 10, D–72076 Tübingen, Germany

Fig. 8 Scientific partipiciants of the SO164 cruise Leg 1 (left) and Leg 3 (right).

4. Narrative of the cruise SO164 (RASTA)

4.1 Leg 1: Balboa – Guadeloupe (RASTA TP2)

D. Nürnberg

During the cruise SO164 (Fig. 9) Leg 1, marine-geological studies were carried out in the Colombian and Venezuelan basins (southern Caribbean), in the Florida Straits, and within the Windward Passage close to the Bahamas. The intention of the studies were to reconstruct ocean surface temperatures and the thermocline depth, and to assess the strength of the West Atlantic Warm Pool through time.

Geological sampling was carried out by piston corer, gravity corer, box corer and multicorer. At most stations, CTD, water sampler, and *in situ* pumping systems were deployed in order to sample the water column.

The cruise started at Balboa (Panama) on May 23rd, 2002, after crew exchange and having loaded three containers with scientific equipment. The entrance into the Panama Canal locks started during late evening of May 23rd, 2002. Due to heavy fog within the Canal, the passage did not commence before early morning of May 24th, 2002. The passage of Panama Canal took 7 hours. The following 430 nm transit to the first station with the Colombian Basin was used to set up the labs and get familiar with the ship´s equipment.

The first station (SO164–01) at ca. 4000 m water depth was reached on May 25th, 2002. During the next days, five stations were positioned at shallower water depths along the Beata Ridge (SO164–02 at ca. 2980 m, SO164–03 at ca. 2740 m, SO164–04 at ca. 1015 m, SO164–05 at ca. 310 m, SO164–06 at ca. 1010 m). Site locations were selected by using the echosounding facilities of R/V SONNE (SIMRAD, PARASOUND). The maximum core recovery of about 13 m on this transect will presumably cover ca.

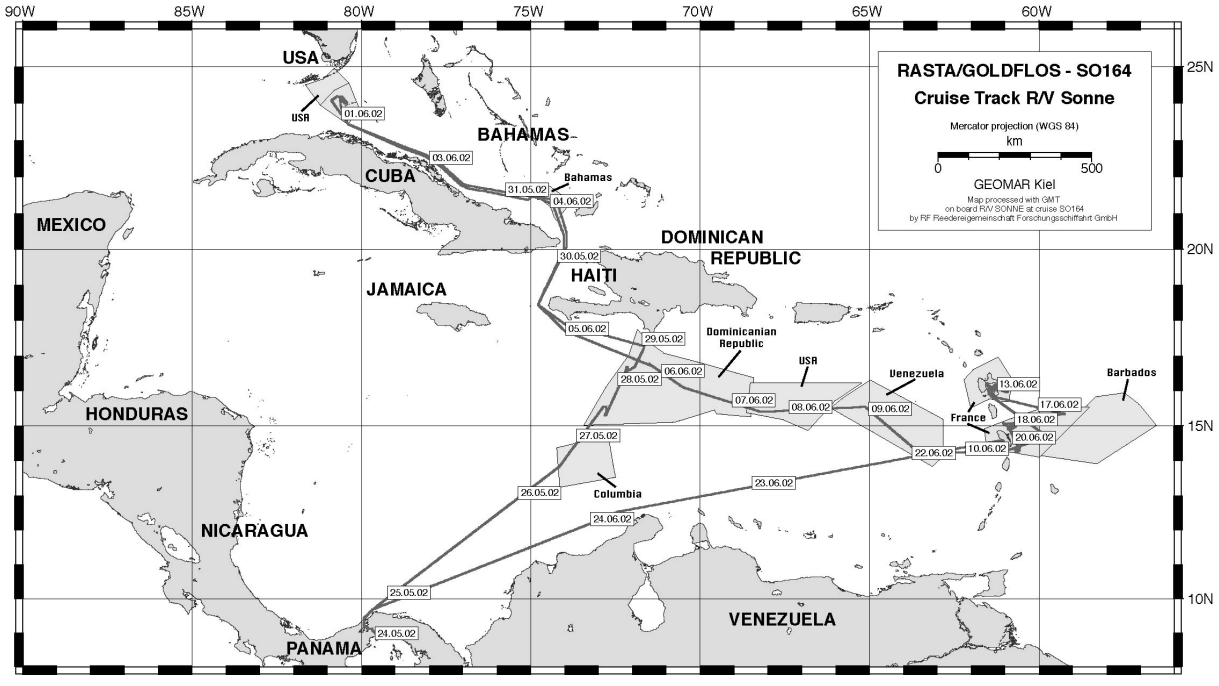

Fig. 9 Cruise track of R/V SONNE during SO164 (RASTA). Stippled areas indicate territorial waters and/or exclusive economic zones of various Caribbean states, where marin-geological studies were performed.

450.000 years of earth history.

After finishing work in the Colombian Basin, R/V SONNE headed towards the Windward Passage. The distance was about 450 nm. The time during transit was used to open, to describe, and to log the sediment cores. On May 30th, 2002, work at station SO164–07 close to the Bahamian island Inagua commenced at a water depth of 2720 m. According to our preliminary stratigraphy, the ca. 13 m long sediment core shows relatively high sedimentation rates and will presumably allow to perform high-resolution studies within Oxygen Isotope Stage 3.

Subsequently, R/V SONNE steamed for about 380 nm and reached the Florida Straits on June 1st, 2002. An intense working program was carried out close to Cay Sal Bank within the framework of GOLDFLOS, a pilot study attached to RASTA (stations SO164–08 to SO164–17). Prior to coring, detailed bathymetric mapping of the study area was carried out. In total, 11 runs of grab sampler and box corer recovered undisturbed surface sediment samples. Four deployments of the gravity corer (3 m length) were unsuccessful due to the sandy sediment and, possibly, hard rock outcrops. Below ca. 800 m water depth, the sediment facies improved and we recoverd 2 piston cores. At a key location within the Florida Straits, piston coring provided a ca. 12 m long sediment core (SO164–17).

The following 380 nm-return trip *via* the Bahama Channel towards the Windward Passage allowed to continue the processing of sample material. On June 3rd, 2002, we started the detailed bathymetric SIMRAD mapping of a submarine plateau within the Windward Passage close to our previous station SO164–07. The echosounding systems aboard R/V SONNE allowed to exactly position our piston corer at the top area of the submarine plateau in ca. 1600 m water depth (SO164–18, SO164–19). Based on first shipboard stratigraphical studies, the longest sediment core approximatly covers 800.000 years of climate and oceanographic history.

After having finished our work within the Windward Passage, R/V SONNE moved to the Venezuelan Basin (480 nm transit). On June 6th, 2002, station work started on Beata Ridge (SO164–20) at ca. 3350 m water depth. Three stations followed on a W-E-trending profile across the Venezuelan Basin in 4000 to 4500 m water depths. Core recovery exceeded 18 m. The last site within the Venezuelan Basin was located on Aves Ridge at ca. 1540 m water depth (SO164–24). Work in the Venezuelan Basin finished on June 9th, 2002.

The last coring site during SO164 Leg 1 was carried out east of Martinique within the central Atlantic at ca. 2720 m water depth (SO164–25), where we recovered a 20 m piston core. The scientific program of Leg 1 was finished on June 11th, 2002, and we subsequently headed towards Guadeloupe (Lesser Antilles), where crew exchange took place on June 2002.

During Leg 1, the ship travelled approximately 3600 nm. Studies were performed within territorial waters or economic zones of 7 states (Bahamas, Barbados, Columbia, Dominican Republic, France, USA, Venezuela). In total, we carried out 13 CTD, 9 fluorometer, 14 multicorer, 1 grab sampler, 10 box core, 8 gravity core, and 14 piston core deployments. The successful accomplishment of our scientific program would not have been possible without the professional help of the captain and the crew of R/V SONNE.

4.2 Leg 2: Guadeloupe – Martinique (RASTA TP1)

W.-Chr. Dullo

The second Leg of RASTA concentrated on sea level changes and the carbonate production on the present shelves of Guadeloupe and Martinique. For this reason we loaded the small submersible JAGO which arrived from Europe in Guadeloupe in time, although there were extreme delays in regard to the container transport in Portuguese harbours. Due to the effort of the JAGOnauts (K. Hissmann and J. Schauer) we achieved a mobilisation of the submersible in time. We left Point à Pitre on June 12th, 2002, at 8:00 a.m., to start our envisaged work on the South-east and shelf of Guadeloupe. We started to perform hydro-acoustic measurements using the PARASOUND and swath bathymetry. We discovered very quickly a prominent shelf break in between 60 and 80 m of present day water depth. This terrace level seems to be characteristical for the entire Caribbean area and presumably it was formed during the Isotopic Stage 3. From this prominent shelf edge the slope deepens down to 650 m and even down to 800 m. We took sediment cores from some of the sediment filled channels, cutting through the margin. The recovery was poor due to the composition of the sediment which was partly lithified. Box cores from the South-east shelf and from the Banc Colombie which represents a drowned plattform recovered a tremendous amount of lithified carbonates and skeletal benthic organisms, including large corals. For this reason, we decided to change our sampling strategy and continued running a series of box cores. During this first week, we performed a first test dive with JAGO on Banc Colombie which showed that there is only a very thin sediment cover of unlithified carbonate silt and ooze. Again, box coring in this area was very, very successful.

On Saturday, June 15th, 2002, we were able to launch the submersible JAGO on the southern shelf margin of Guadeloupe, South-west of the Iles de Petite Terre. Wind regime and swell was moderate. The shelf margin at between 70 to 90 m water depth drops down to 160 m forming an almost vertical cliff. The slope then gently dept down to 250 m having a decreasing inclination wich ended at around 35°. We started with the profile at the sediment slope which showed sporadic carbonate material, derived from shallow water environments. Furthermore, we observed reef out runners which are huge blocks composed of cemented shallow water reef carbonates. These blocks, themselves, form a substratum for deep water biota. The submarine wall

above 150 m of present day water depth exibits distinct karst features. We observed larger caves at around 130 m and they continued up to 100 m of present day water depth. In this depth we discovered sclerosponges which were one of the targets of the cruise. These sponges represent a very interesting and important climate archive which hosts several hundret years of proxydata. The second dive concentrated almost entirely around the bathymetry of the occurrence of these sclerosponges. The third dive was then performed to reveal some details around the Banc Colombie which is located South of Guadeloupe and West of Marie Galante. This dive concentrated on the two terraces which were discovered in PARASOUND tracks. Both terrace systems exibit clear signs of karst features. The coring around the shelf slopes was very difficult. We recovered a lot semi-lithified carbonate sediments and some ash layers. Therefore, the cores were short.

We performed two CTD stations around the area where the dives completed our work around Guadeloupe. In the night of Monday, June 17th, 2002, we started to run the hydro-acoustic mapping on the northern shelf of Martinique in order to check for box coring and gravity coring sites. The recovery of the gravity cores was not very well although the water depth was sufficient to expect soft sediments. Penetration was prohibited due to several ash layers and frequently occuring cemented carbonate pebbles. In the leeward margin of the submerged bank North-west of Martinique we were able to recover longer cores. They showed turbidites or graded beds on the windward margin; we were able to get material by using the box corer. They brought a huge variety of carbonate debris on board. The box coring around the margin and on top of the margin of the submerged bank was very successful. We discovered drowned reefs with corals and a tremendous amount of incrusting coraline algae.

Unfortunately, we were not able to launch the JAGO due to rough weather conditions and an additional forcing of a long and very strong Atlantic swell. Two CTD measurements around the bank completed the program. Although we were a bit disappointed for not having had the chance to deploy JAGO again, the scientific results achieved by using the submersible in connection with the box coring were very successful. For the first time, a submerged bank in the Lower Antilles was completely sampled and we got a tremendous insight into the geometry and architecture of the drowned reefs around the Banc. Due to the perfect effort of the JAGOnauts and the captain of the research vessel SONNE as well as his crew we got the samples we planned to receive and we finished the second Leg with very good results.

4.3 Leg 3: Martinique – Balboa

C. Rühlemann

R/V SONNE departed the port of Fort-de-France on Martinique at 7:00 a.m. on June 22nd, 2002, for the return cruise to Balboa, the starting point of the SO164 expedition. The scientific shipboard party included seven scientists from the GEOMAR, three scientists from the University of Bremen, and one scientist each of the University of Tübingen, the Institut für Meereskunde of Kiel, and the University of Bern. During the five days transit of this last cruise of the RASTA project we opened and sampled nine sediment cores that were retrieved on the preceding legs. Concurrently we started to store the sampling devices, working material, and sediment and water samples as well as to save electronic data. The last days were dedicated to document the scientific results of the SO164 expedition in a preliminary cruise report. At 7.00 a.m. on June 25th, 2002, R/V SONNE reached Cristobal and started the transit through the Panama Canal on 6.00 p.m. Shortly after midnight on June 26th, 2002, we arrived in Balboa where cruise SO164 ended as scheduled.

5. Operations and preliminary results

5.1 Coring site selection

D. Nürnberg

SIMRAD EM120 Multibeam-System

EM 120 is a high performance Multibeam echosounder for deep water mapping (up to 11.000 m), with up to 191 simultaneous beams. The sounding accuracy satisfies the requirements for IHO S-44 order 2 surveys. The system is designed in order to produce a regular pattern of soundings on the bottom, and to obtain the optimum quality of the resulting terrain model or map (www.kongsberg-simrad.com):

- Active electronic pitch and roll compensation is applied.
- For each sounding profile, it is possible to select between equiangular and equidistant spacing between the soundings on the bottom.
- For the typical water depths where EM 120 is used, gaps in the sounding coverage will be experienced when the ship is yawing in heavy seas. The system has therefore active yaw compensation of the transmission pattern.

Two transducer arrays are fixed on the hull of the ship, which send successive frequency coded acoustic signals (11.25 to 12.6 kHz). The 12 kHz operating frequency is the optimum choice in order to achieve efficient mapping of larger ocean areas. Still the system can be applied to mapping of shallower water areas, and it is then the most efficient tool which is available, covering a swath of 6 times the water depth. Data aquisition is based on successive emission-reception cycles of the acoustic signal. The emission beam is 150° wide across the track (75° per port/starbordside), and 2° along track direction. One ping is sent and the reception of the acoustic signals is obtained by 191 overlapping beams by the transducer unit through the hydrophones in the receiver unit. Beam widths are 2° across and 20° along the track. The echoes from the intersection area (2° * 2°) between transmission and reception patterns produce a signal from which depth and reflectivity are extracted. The ping-rate is dependant on water depth and the running time of the signal through the water column. In order to optimize the usable beams, the variation of angular coverage sector and beam pointing angles was set automatically.

Data processing was done aboard R/V SONNE by the WTD (Wissenschaftlich-Technischer Dienst) during the cruise by applying the coverage software EM120 and the accessory software NEPTUNE and CFLOOR (Roxa, Smedvig Tech., Oslo, Norway). After processing, the bathymetric data were exported in ASCII x,y,z format. Further information on the SIMRAD EM120 Multibeam echosounder can be derived from GEOMAR Reports 102, 103, 104, and 106.

During R/V SONNE cruise SO164, the SIMRAD EM120 Multibeam echosounder was used continuously, except in territorial waters and economic zones of countries which did not provided research permissions. An example of the resulting 3D-seafloor topography is shown in Fig. 10.

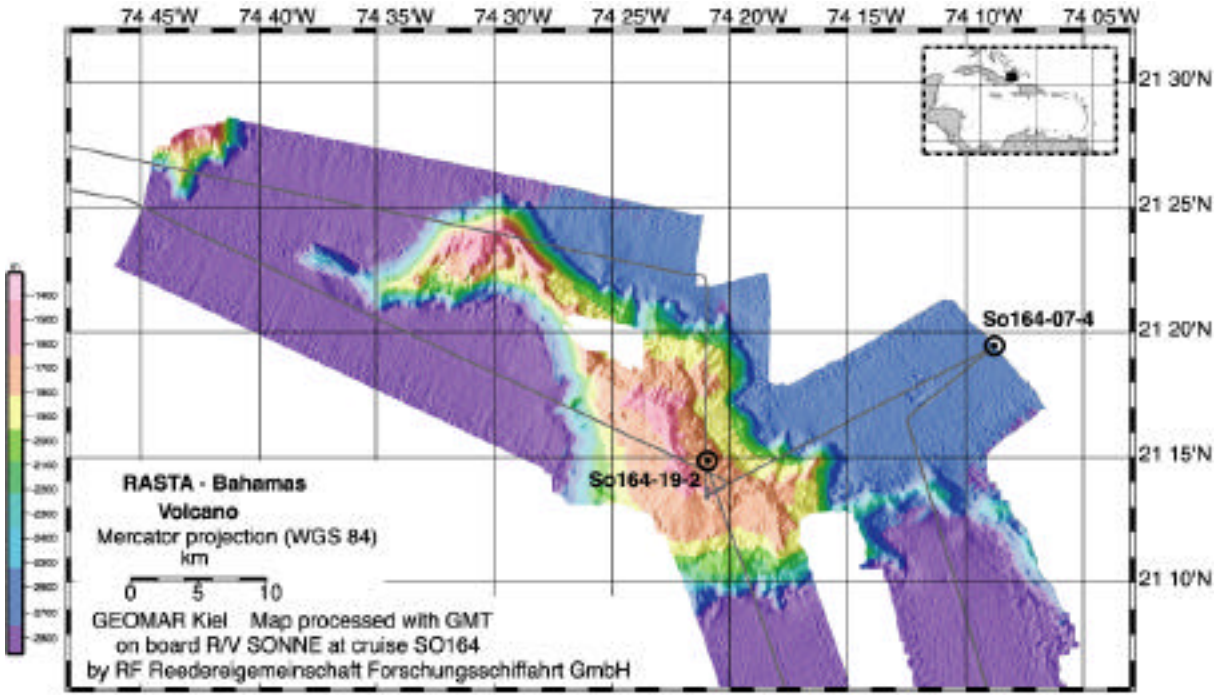

Fig. 10 Volcanic structure at the Bahamas mapped with the SIMRAD EM120 Multibeam echosounder.

PARASOUND

Detailed decriptions of the PARASOUND sediment echosounding system can be derived from GEOMAR Reports 102, 103, 104, and 106. The PARASOUND system operates as a high-frequency narrow beam sounder to determine the water depth, and as a low-frequency sediment echosounder. It makes use of the parametric effect, which produces additional frequencies through non-linear acoustic interaction of finite amplitude waves. If two sound waves of similar freqeuncies (here: 18 kHz and e.g. 22 kHz) are emitted simultaneously, a new signal from the difference between both freqencies is generated (e.g. 4 kHz) for sufficiently high primary amplitudes. The new component travels within the emision cone of the original high frequency waves, which are limited to an angle of only 4° for the equipment used. The footprint size, consequently, amounts to 7 % of the water depth and is much smaller than for conventional systems. Both vertical and lateral resolution are strongly improved.

The PARASOUND hull-mounted transducer array possesses 128 elements within an area of 1 m^2. An electric power of 70 kW is needed to run the equipment, due to the low degree of efficiency of the parametric effect. Beam formation, signal generation, and separation of the primary (18.22 kHz) and secondary frequencies (4 kHz) are obtained in 2 elctronic units. The third electronic unit is located in the echosounder control room of the ship and allows continuous operation of the system.

Due to the fact that the two-way travel time in the deep-sea is long compared to the length of the reception window of up to 266 ms, the PARASOUND system generates a burst of pulses at 400 ms intervals, until the first echo returns. The coverage in this discontinuous mode is dependant on the water depth and also produces non-equidistant shot distances between bursts.

Analogue signal recording is done with the b/w DESO 25 device. In addition, the PARASOUND system is equipped with the digital data acquisition system ParaDigMA. The data are stored on removable hard disks using the SEGY format.

During the SO164 cruise, the combined PARASOUND/ParaDigMA system ran continuously, except in territorial waters and economic zones of countries which did not provided research permissions. Only selected seismic profiles used for selecting coring locations were recorded digitally.

CTD / Velocity Probe data

To obtain accurate sound velocity profiles needed for bathymetric swathmapping, we used the SIMARD Sound Velovity Probe several times. The SIMRAD Sound Velovity Probe was attached to the CTD/water sampling device and lowered down to water depths of 2000 m and 1000 m at a speed of 1 m s^{-1} while measuring the *in situ* sound velocity continuously.

5.2 Water and plankton investigations

5.2.1 CTD-profiling and Rosette

N. Gussone, D. Hippler, S. Mulitza, L. Numberger, C. Rühlemann, S. Steingruber, S. Steph

CTD and Rosette

A SBE 911 plus CTD profiler was used at 19 stations in conjunction with a Sea Bird SBE 32 carrousel water sampler (Fig. 11) to study the vertical variability of temperature, salinity, and oxygen, and to obtain water samples over the water profile. The system consists of a CTD sensor unit (temperature, conductivity, pressure), an oxygen sensor, and a Rosette with twenty-four 10 l Niskin-bottles. Further, a mobile fluoroprobe was installed to monitor the chlorophyll a content in the upper water column.

Fig. 11 The Sea Bird SBE 32 carrousel water sampler.

The registration of the hydrographic parameters was performed from sea surface down to sea bottom and vice versa. Depending on the regional hydrography, sea water samples were taken between the surface and at maximum water depth of 4500 m immediately after recovery for the following purposes:

- 1 glass bottle (25 ml) for the analyses of stable carbon isotopes of total dissolved CO_2
- 1 glass bottle (25 ml) for the analyses of stable oxygen isotopes of seawater
- 1 PE bottle (100 ml) for the analyses of trace elements and calcium isotopes
- 1 glass vial (5 to 7.5 ml) for the analyses of stable nitrogen isotopes
- 1 glass bottles (250 ml) for the analyses of $^{15}NO_3^-$ and $^{15}NH_4^+$

To prevent any biological activity, the water samples for $\delta^{13}C$ and total CO_2 were poisoned with 1 ml saturated HgCl solution and stored at 4°C.

5.2.2 Preliminary results of hydrographic measurements

J. Castañeda

Introduction

Hydrographic measurements of temperature, salinity, and oxygen collected during the SO164 cruise in the Caribbean Sea are used to characterize the distribution of temperature, salinity, typical water masses, and their variability in the region. The position of the stations responds to the original aim of the project, and some valuable information on the water column can be extracted. The locations of hydrographic stations span three regions: Caribbean, Lesser Antilles, and South Florida. However, most of the deep CTD stations belong to the Caribbean, so the first result presented herein correspond to that area (Fig. 12).

Very briefly, we can say that the Caribbean is a semi-enclosed sea adjacent to the landmasses of Central and South America. The closely spaced chain of islands, banks, and sills of the Lesser Antilles Islands Arc separate the Caribbean from the Atlantic Ocean and act as a sieve for the inflow of Atlantic water. The Caribbean region is important from the oceanographic view point because it is thought that it plays a key role in latitudinal exchange of near-surface water form the South Atlantic into the North Atlantic circulation system.

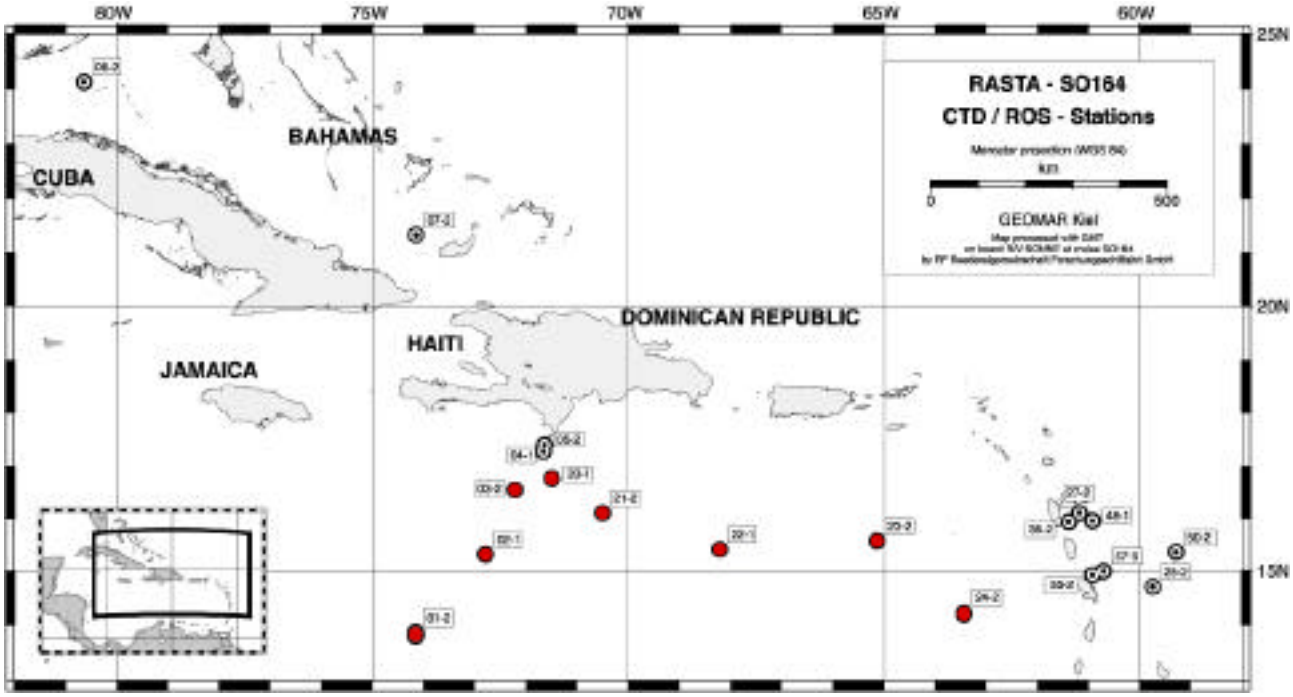

Fig. 12 Location of hydrographic stations during R/V SONNE cruise SO164. Filled dot indicates deep CTD station in the Caribbean.

Preliminary results

At all stations sampled during the cruise, it is apparent that the Caribbean Sea is highly stratified in the upper 1200 m of the water column, weakly stratified between 1200 and 2000 m, and nearly homogeneous below 2000 m (Fig. 13, 14). This water structure is directly related to the sill depths of the Lesser Antilles Islands Arc which impedes the flow of deep water into the Caribbean (Gordon, 1967).

There is some historical evidence based on hydrographic surveys (Wüst, 1964; Gordon, 1967) and new outcomes from numerical models (Johns et al., 2002), sustaining that water flows into the Caribbean Sea mainly through the Grenada, St. Vincent, and St. Lucia Passages in the South-east.

In the upper layer (<60 m), the Caribbean Sea shows the presence of relatively fresh water with salinities values less than 35.5. This water mass is named Caribbean Water (CW; Wüst, 1964), and it is believed to be a mixture of the Amazon and Orinoco River outflow, and North Atlantic surface water. A salinity maximum between 150 to 160 m is also noticeable (Fig. 15). This is the signature of the Subtropical Under Water (SUW), which is characterized by a salinity maximum of 37. It is believed that this water mass is formed in the central tropical Atlantic, where the evaporation rate exceeds precipitation. So it sinks along the isopycnal $s_\Theta = 25.4$ kg m^{-3} (Hernandez-Guerra and Joyce, 2000) (Fig. 16). This water mass was found almost in the entire Caribbean region. Down in the water column around 800 m, a salinity minimum of 34.8 is found. It is attributed to the Antarctic Intermediate Water (AAIW) that is characterized by its low salinity and high oxygen-content (Wüst, 1964). The lower depth limit at approximately 1200 m is due to the sill depths in the passages between the Less Antilles where the AAIW protrudes into the Caribbean.

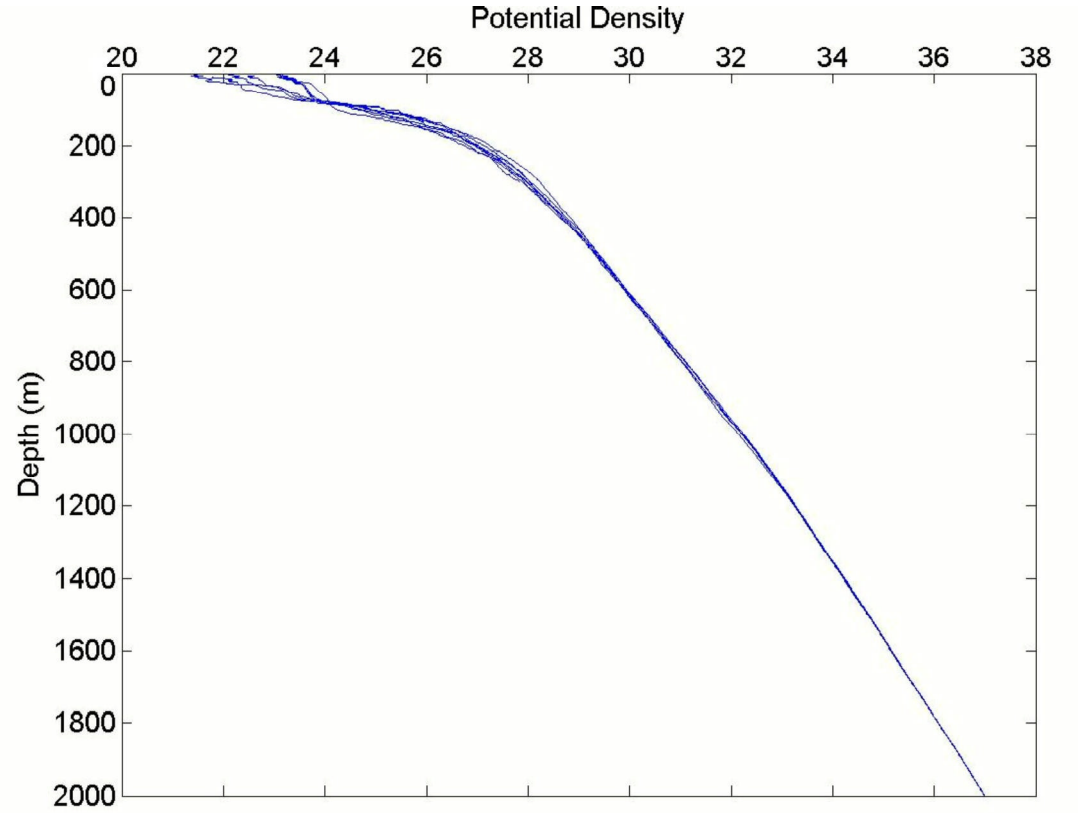

Fig. 13 Composite of density profiles versus depth of CTD stations within the Caribbean Sea (SO164–01, –02, –03, –20, –21, –22 and –24).

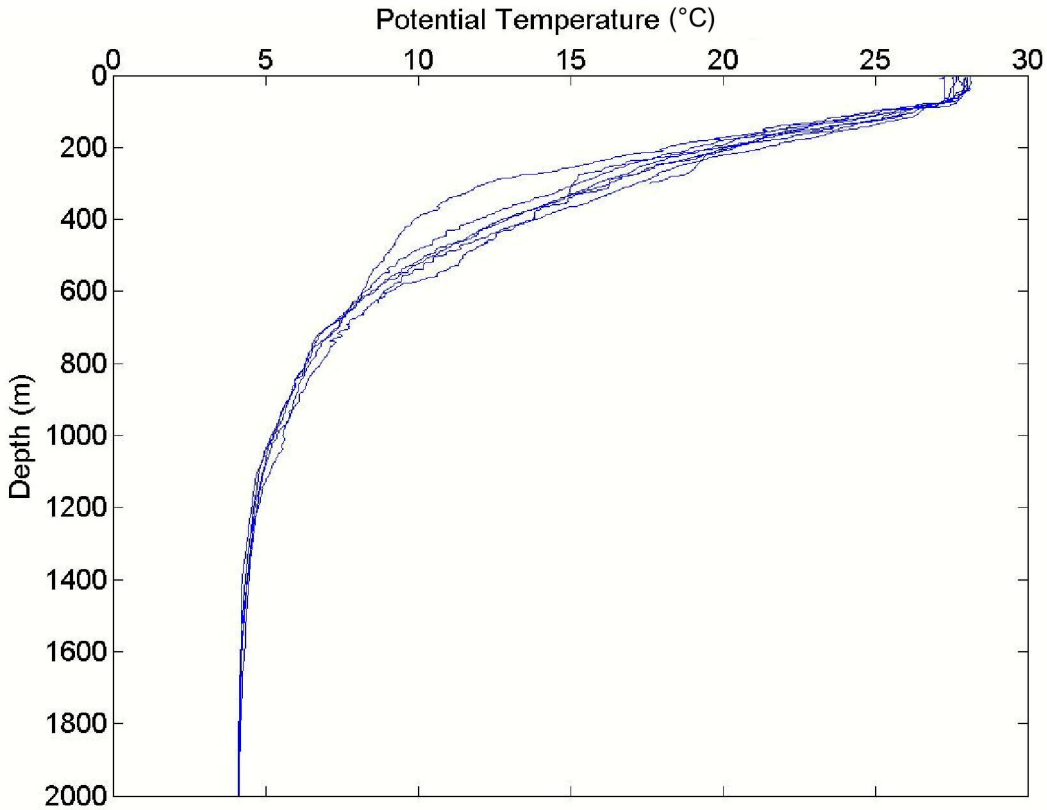

Fig. 14 Composite of potential temperature (Θ, °C) profiles of CTD stations within the Caribbean Sea (SO164–01, –02, –03, –20, –21, –22 and –24).

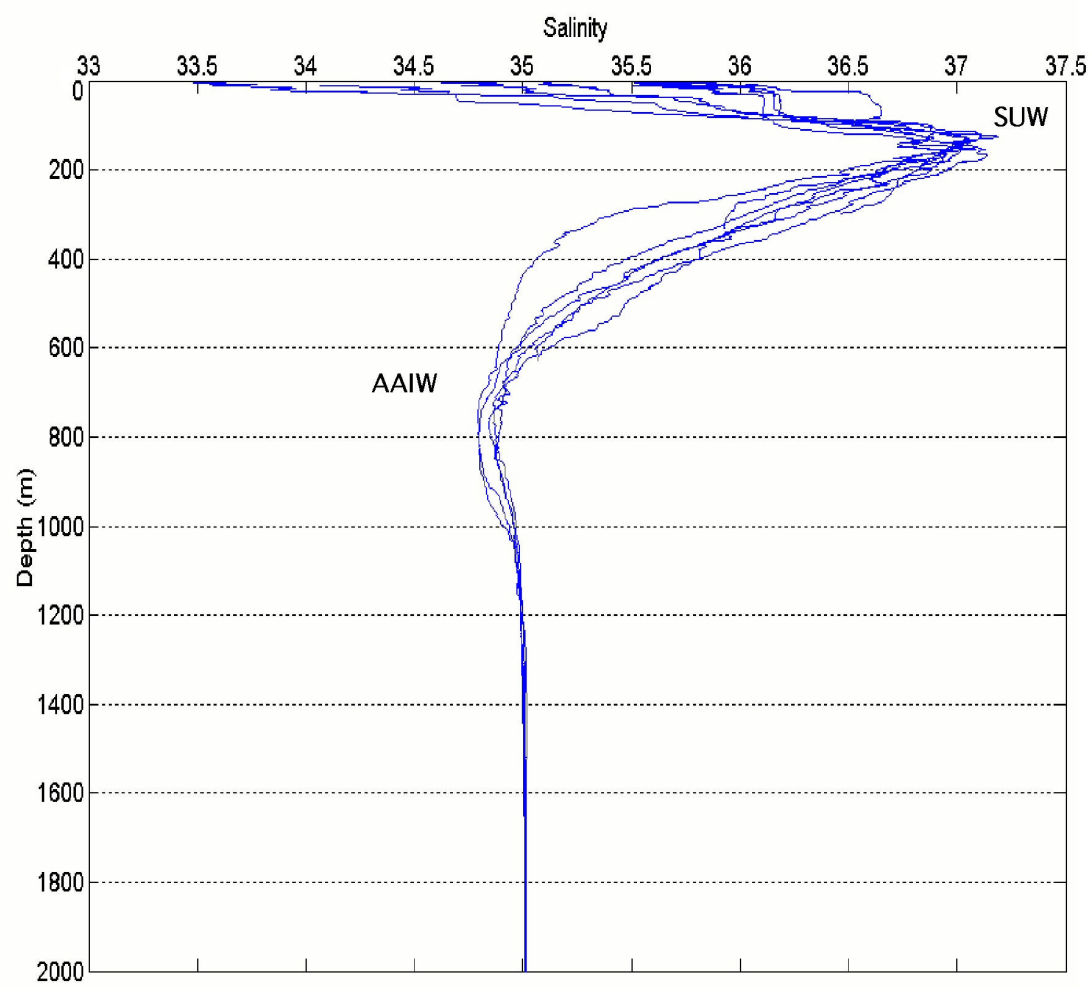

Fig. 15 Composite salinity profile of CTD station within the Caribbean Sea (SO164–01, –02, –03, –20, –21, –22 and –24).

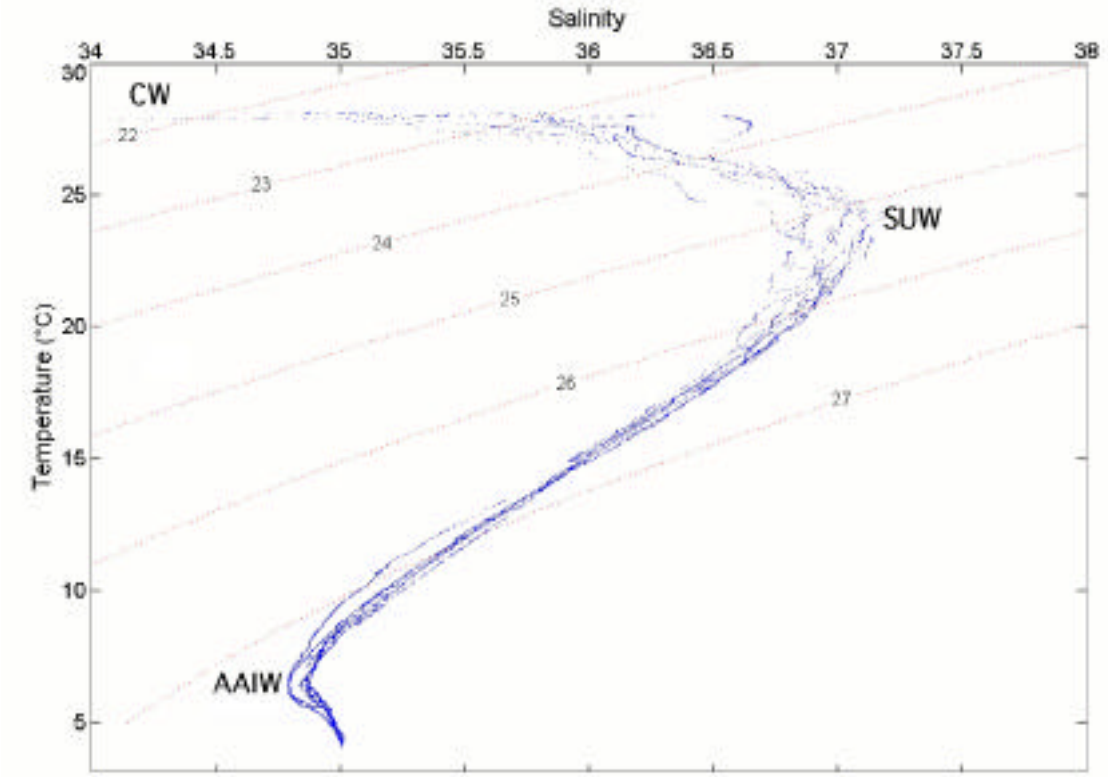

Fig. 16 T-S diagram for the Caribbean Water (SO164–01, –02, –03, –20, –21, –22 and –24).

5.2.3 Fluorometer

L. Numberger

Due to the fact that algae of the same division contain similar quantities of photosynthetic pigments their fluorescence excitation spectrum (with a fixed emission wavelength at 680 nm) is significant for each division. Thus, it is possible to differentiate divisions of algae by their fluorescence excitation spectrum. The bbe FluoroProbe for algae differentiation uses 5 LEDs for fluorescence excitation. The LEDs emit light at 5 selected wavelengths (450 nm, 525 nm, 570 nm, 590 nm, 610 nm). The FluoroProbe can be used to distinguish five groups of Algae: *Chlorophyceae, Cyanophyceae, Dinophyceae, Bacillariophyceae,* and *Cryptophyceae* (differentiation of *Bacillariophyceae* and *Dinophyceae* is not possible). Although the phycocyanin content per cell in *Cyanophyceae* varies, the average fingerprint can be used to differentiate this division. For the measurement, first the different divisions of algae are measured separately to calibrate the instrument. The measured spectra, or fingerprints, are stored in the FluoroProbe. During the measurement, the spectrum of the samples is loaded in the storage device of the instrument or sent to an external computer. The computer calculates the content of the separately measured algae divisions. The concentration of every algae division is given in µg chlorophyll a/l.

The fluorometer was deployed at chosen stations covering the entire working area (Columbia Basin, Beata Ridge, Bahamas, Florida Straits, Venezuela Basin, Eastern Central Atlantic traverse, Guadeloupe, Martinique; see Fig. 17, Tab. 3). The intension is to get an idea of chlorophyll distribution patterns in the Caribbean Sea and adjacent regions. The maximum penetration depth was 150 m, but due to the restricted calibration efficiency of the equipment, further runs were performed only down to 120 m.

At CTD runs, which were combined with fluorometer measurements, water samples of one litre were taken from the Rosette sampler in defined depths of 150, 120, 90, 60, 30, 5 and 1 m. The subsequent determination of the chlorophyll maximum was done online. On the basis of these preliminary results further water samples were deployed in the chlorophyll maximum zone in a second sampling run. Afterwards, the water samples were filtered. The shore-based analysis of the filters for the concentration of *Chloropyceae, Dinophyceae,* and the total concentration of algae is thought to improve the FluoroProbe measurements.

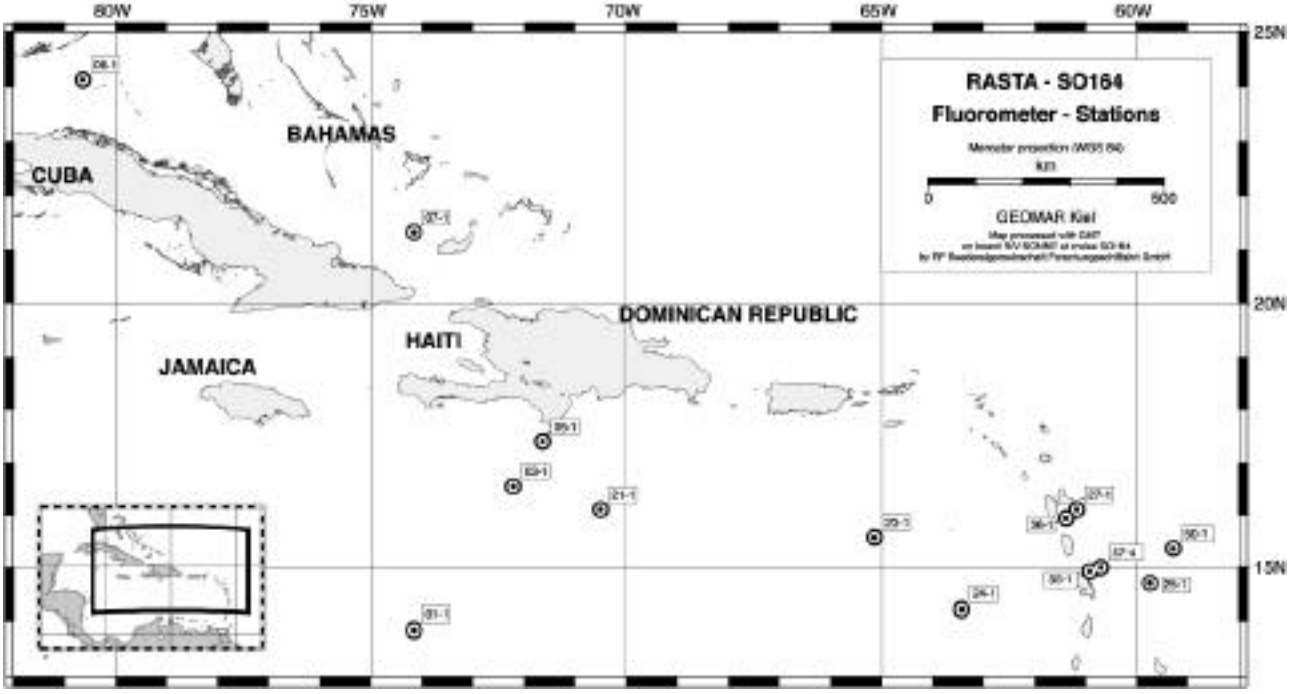

Fig. 17 Location of the Fluorometer stations.

Tab. 3 List of samples of suspended particulate matter for analyses chlorophyll concentration

No	Station No. SO164 -	Region	Date 2002	Water depth [m]	Longitude N/ latitude W	Time UTC	Weather conditions	Sample depth [m]	Pressure [bar]	Depth of max. Chloroph. [m]
1	01-1	Columbia Basin	26.05.	4025	13°50,145/ 74°09,006	08:25	Night, windy	120, 88, 60, 30, 0	124, 93, 65, 35, 4	89
2	03-1	Beata Ridge I	27.05.	2740	16°32,39/ 72°12,34	03:28	Night, calm	150, 120, 90, 60, 30, 5, 1	152, 123, 91, 62, 33, 8, 4	122

No	Station No. SO164 -	Region	Date 2002	Water depth [m]	Longi-tude N/ latitude W	Time UTC	Weather conditions	Sample depth [m]	Pressure [bar]	Depth of max. Chloroph. [m]
3	05-1	Beata Ridge II	28.05.	306	17°23,52/ 71°38,01	22:33	Day, calm	150, 120, 100, 60, 30, 5, 1	153, 122, 101, 62, 32, 7, 3	98
4	07-1	Bahamas	30.05.	2723	21°19,47/ 74°08,78	08:30	Night, calm	125, 98, 60, 30, 5, 1	127, 101, 62, 32, 7, 3	81
5	08-1	Florida Straits	01.06.	1027	24°07,8/ 80°38,33	02:30	Night, calm	120, 101, 60, 30, 5, 1	120, 101, 61, 33, 8, 4	102
6	21-1	Venezuela Basin I	07.06.	4000	16°06,03/ 70°30,03	03:36	Night, windy	120, 90, 60, 30, 5, 1	/ , 95, 62, 32, 7, 3	100
7	23-1	Venezuela Basin II	08.06.	4323	15°34,01/ 65°08,09	10:33	Day, windy	120, 90, 67, 60, 30, 5, 1	123, 93, 72, 62, 33, 8, 4	65
8	24-1	Venezuela Basin III	09.02.	1540	14°12,06/ 63°25,67	10:53	Day, calm	120, 90, 67, 60, 30, 5, 1	122, 92, 68, 62, 33, 8, 3	60
9	25-1	East Traverse	10.06.	2688	14°41,25 / 59°44,48	13:13	Day, calm	120, 110, 90, 60, 30, 5, 1	123, 113, 93, 63, 34, 8, 4	59
10	27-1	Guadeloupe I	12.06.	628	16°05,99/ 61°10,21	21:20	Day, windy	120, 90, 60, 30, 5, 1	/ , 92, 63, 33, 8, 3	49
11	36-1	Guadeloupe II	14.06.	206	15°56,02/ 61°22,98	18:01	Day, windy	120, 90, 60, 30, 5, 1	122, 92, 63, 33, 8, 4	85
12	50-1	Atlantic	17.06.	3782	15°21,21/ 59°16,96	04:27	Night, windy	120, 90, 60, 30, 5, 1	125, 95, 65, 35, 10, 6	92
13	55-1	Martinique I	18.06.	343	14°55,12/ 60°54,81	23:23	Night, windy	120, 90, 60, 30, 5, 1	122, 92, 61, 32, 7, 3	61
14	57-4	Martinique II	19.06.	1007	14°59,33/ 60°41,72	15:32	Day, windy	120, 90, 60, 30, 5, 1	123, 93, 62, 33, 8, 4	32

5.2.4 First results on fluorometer deployments: Comparison of optical measurements of algae concentrations with High Pressure Liquid Chromatograph (HPLC) measurements.

Filter samples from water samples taken at fluorometer stations were kept frozen, brought to the Institut für Meereskunde, Kiel, and were analyzed for their concentrations of organic pigments, i.e. chlorophyll a, divinylchlorophyll a (reported herein), and related substances by using the HPLC (Barlow et al., 1997). The aim of the study was to compare optical measurements of algae concentrations from the fluorometer probe with HPLC data. The probe should be tested in a natural enviroment, and we took water samples for the HPLC measurement in order to verify the data produced with the fluorometer deployments. Altogether, we took fourteen stations, but only four stations were considered for this comparison (Fig. 18). If these data are compared, one has to be aware of the different entities and proportions. The data from the probe mirrors the concentration of phytoplankton particles in the water column, whereas the HPLC returns the concentration of different pigments.

The shipboard data display a marked chlorophyll maximum between 60 m and 100 m water depth. That was much deeper than we initially supposed. The comparison of different pigment concentrations from the phytoplankton cultures revealed that the HPLC measurements generally confirm the fluorometer probe results. The depth location and magnitude of the shipboard measured maxima is in good agreement with Cla-concentrations in the water samples. Hence, the probe works properly and produces reliable results.

SO164–23–1

The probe indicates a near-surface peak of high phytoplankton concentrations between 0 m and 10 m. The HPLC measurements also display a near-surface maximum, but at slightly greater depth. Provided the maxima are related, this offset could be due to wave action or turbulences. This was a problem during the on-board measurements. There are often differences in the results between 5 m and 10 m. Near 70 m water depth, there is a marked maximum in all measured values. Shipboard and HPLC measurements are highly coincident.

SO164–36–1

The algal concentrations show two peaks, one at 40 m and one at 90 m. Unfortunately, the second peak was not recognized by the HPLC data, even though a water sample is available from 90 m depth. Maybe this is due to the confined area and/or the drift of the probe and water sampling unit.

SO164–50–1

These data are indistinct, there is no profound maximum visible as at the other stations. But nevertheless a broad maximum is recognized between 90 m and 100 m in both datasets. At the pigment concentrations, chlorophyll a and divinyl chloropohyll a were differentiated.

SO164–57–4

Fluorometer and HPLC data display a maximum between 0 m and 10 m, and a second peak near 30 m. In the probe data, this peak is dominated by brown algae. Within the pigments, the maximum is made of chlorophyll a and divinyl chlorophyll a.

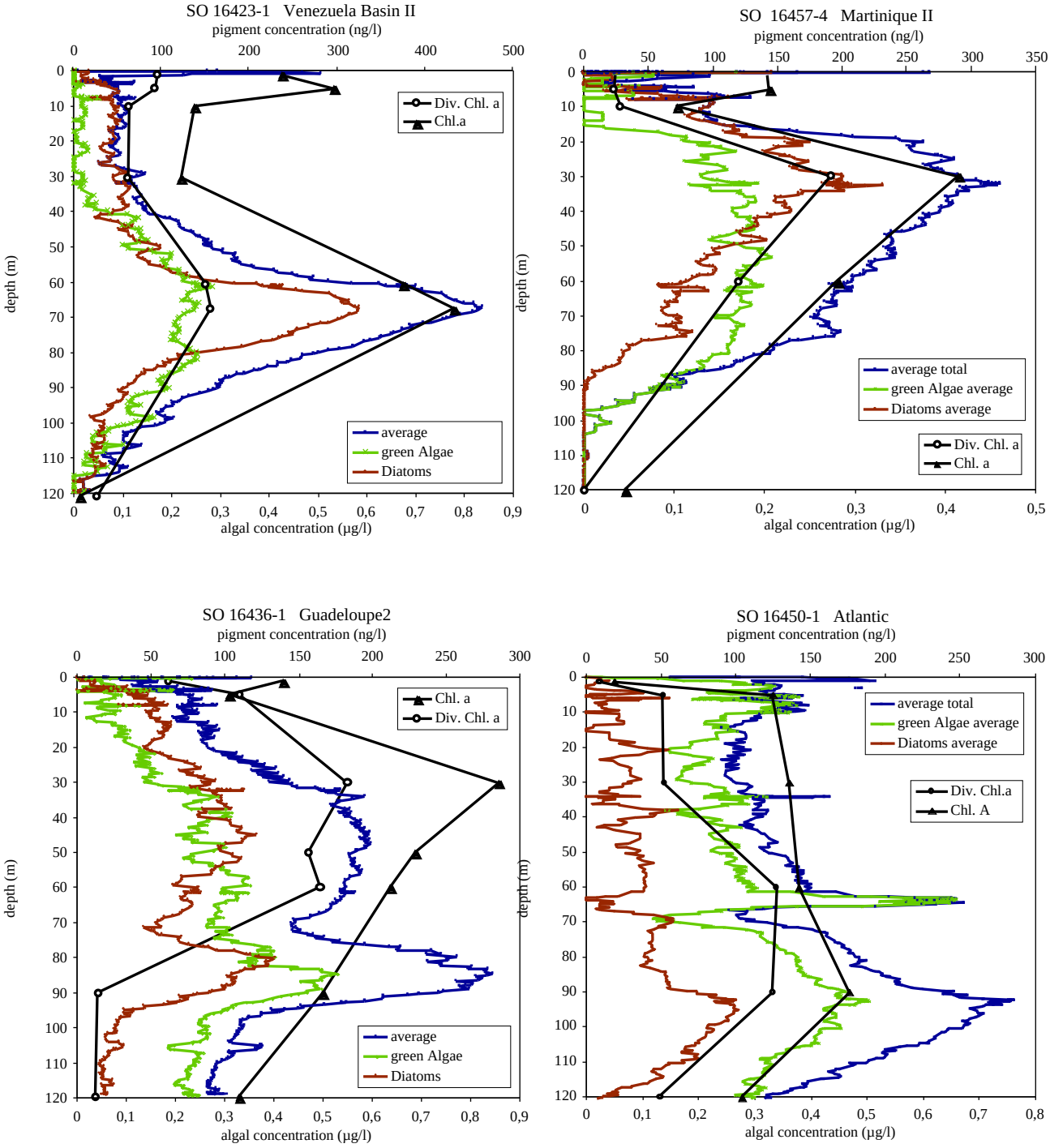

Fig. 18 Concentration of major algal groups vs. water depth from four selected SO164 fluorometer stations in comparison with pigment concentrations from filtered water samples.

5.2.5 Sampling of planktonic foraminifers

S. Mulitza

Planktonic foraminifers were collected using a 150 µm-mesh size plankton net (HYDRO-BIOS). Sea surface water (3.5 m water depth) was constantly pumped for several hours with the help of the vessel's "fire extinguishing pump". Samples were rinsed several times with freshwater. Planktonic foraminifers were then separated from other particles, aggregates, and organisms, then dried up and put in storage-cells for future isotope analysis. Salinity and temperature (Tab. 4) were measured continously with the onboard CTD. The existing data set - accomplished with the results from this cruise – will be used to calibrate the $\delta^{18}O$ composition of shallow-dwelling planktonic foraminifers from surface waters against the present-day surface water hydrography.

Fig. 19 displays the absolute amount of shells collected on each transect (A), temperature, and salinity (B) as well as percentage of the dominant species (C). The number of foraminifers caught per sampling interval varied from day to day. Highest amounts were obtained shortly before new moon (Fig. 19A), and increased again towards full moon at the end of the cruise. This pattern might be due to a beweekly or lunar triggered reproduction cycle of *G. ruber*, which dominats the assemblage at least in the southern parts of the working area. It has to be be noted, however, that the total amount of foraminifera is only a qualitative indicator of the total standing stock, because the volume of water pumped through the net was not measured and seems to be not constant.

Water temperature was relatively stable during pumping and varied between about 27.3 and 28.8°C (Fig. 19B), wheras sea surface salinity decreased continously from values well above 36 in the northern Caribbean to values below 32 in the South. In the northern Caribbean, the assemblage was dominated by *G calida* (Fig. 19C). Further south *G. ruber* (pink) was the most abundant species. This change in species composition is associated with a major drop in sea surface salinity, and a change to a generally shallower thermocline. Presumably, *G. ruber*, *G. calida*, *G. menardii*, and *N. dutertrei* provide enough carbonate for isotope analyses, which will allow calibration against SST and $\delta^{18}O$ of seawater.

Tab. 4 Location, temperature, salinity, and water depth at the beginning and at the end of each pumping transect for planktonic foraminifers.

No	Date 2002	Start (UTC)	Latitude N	Longitude W	SST °C	SSS	Water depth	Stop (UTC)	Latitude N	Longitude W	SST °C	SSS	Water depth
1	26.05.	14:35	13°50, 150’	74°09, 063’	27.6	36.2	4025	18:35	13°50, 177’	74°08, 908’	27.6	36.2	4025
2	27.05.	14:19	15°18, 304’	72°47, 077’	27.6	36.2	2979	06:16	16°32, 396’	72°12, 334’	27.3	36.1	2743
3	31.05	17:30	23°00, 021’	79°12, 756’	27.6	36.1	---	20:19	23°14, 063’	79°50, 277’	27.5	36.1	---
4	31.05	20:19	23°14, 063’	79°50, 277’	27.5	36.1	---	01:08	23°51, 891’	80°35, 545’	28.5	36.1	---
5	01.06	11:16	24°01, 212’	80°25, 250’	28.0	36.1	527	16:09	24°00, 757’	80°26, 156’	28.2	36.1	572
6	01.06	22:47	24°05, 141’	80°31, 156’	28.8	36.1	963	13:25	23°23, 244’	80°15, 604’	28.1	36.1	---
7	03.03	16:00	21°23, 416’	74°27, 227’	27.9	36.3	2696	20:40	21°14, 716’	74°21, 017’	27.5	36.4	1695
8	05.06	12:05	16°45, 774’	71°29, 202’	28.1	36.2	3356	20:04	16°45, 491’	71°29, 222’	28.3	36.2	3358
9	05.06	20:05	16°45, 491’	71°29, 222’	28.3	36.2	3358	13:51	16°06, 004’	70°29, 999’	27.9	36.1	3995
10	07.06	04.24	15°24, 003’	68°12, 004’	27.9	36.2	4509	17:52	15°23, 993’	68°12, 001’	28.0	36.2	4508
11	08.06	12:29	15°33, 030’	65°08, 112’	28.1	35.5	4324	21:00	15°33, 030’	65°08, 112’	28.3	35.8	4327
12	09.06	12:13	14°11, 964’	63°25, 650’	27.9	34.8	1539	16:59	14°12, 151’	63°23, 829’	28.1	34.8	1520
13	10.06	14:21	14°41, 250’	59°44, 530’	27.9	35.0	2716	21:16	14°41, 248’	59°44, 529’	28.0	35.0	2721
14	12.06	23:17	16°05, 999’	61°10, 212’	28.2	35.2	655	04:21	16°01, 680’	61°19, 190’	28.2	35.3	604

No	Date 2002	Start (UTC)	Lati-tude N	Longi-tude W	SST °C	SSS	Water depth	Stop (UTC)	Lati-tude N	Longi-tude W	SST °C	SSS	Water depth
15	13.06	18:55	15°54, 366’	61°23, 134’	28.2	35.0	---	00:47	16°03, 235’	61°20, 587’	28.1	35.2	568
16	14.06	16:48	15°59, 462’	61°23, 739’	28.2	35.0	167	23:29	15°59, 285’	61°24, 402’	28.2	34.9	94
17	15.06	12:44	16°08, 964’	61°09, 967’	28.0	35.1	---	23:52	16°02, 854’	61°11, 775’	28.1	35.0	995
18	16.06	14:13	15°59, 364’	61°24, 094’	28.0	35.1	---	20:43	15°38, 826’	60°32, 295’	28.0	32.1	---
19	17.06	09:33	15°21, 195’	59°16, 891’	27.8	32.4	3999	---	15°21, 195’	59°16, 891’	27.8	32.4	3999
20	19.06	12:41	15°00, 314’	60°41, 677’	27.6	31.7	1005	---	14°49, 177’	60°49, 403’	28.1	31.7	54

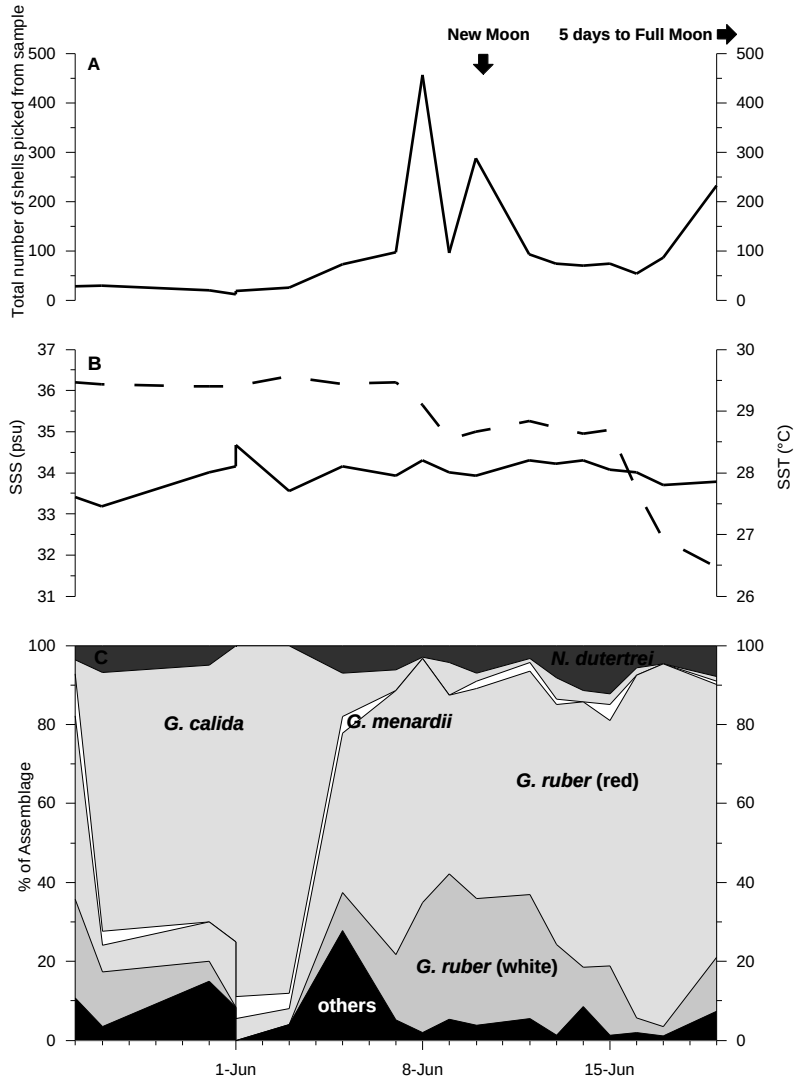

Fig. 19 (A) Absolute amount of shells collected on each transect, (B) temperature and salinity, and (C) percentage of the dominant species.

5.2.6 Sampling of suspended particulate matter

C. Rühlemann

Sampling of particulate organic matter for alkenone analysis

At each location 500 to 2000 litres of surface water were sampled with the vessel's membrane pump for the shorebased analyses of alkenones (Tab. 5). The water was passed through glass fibre filters (GMF 5, Sartorius AG) to obtain the suspended particulate matter. The pumping was done with a commercial GARDENA garden pump. After filtering, all samples were dried immediately in an oven at 40°C.

Tab. 5 List of samples of suspended organic matter for alkenone analysis. Temperature and salinity are from the shipboard thermosalinograph which was switched off after leaving Martinique (after sample No. 21)

No	Date 2002	Start (Local time)	Latitude North START	Longitude West START	SST [°C]	SSS	Stop (Local time)	Latitude North STOP	Longitude West STOP	SST [°C]	SSS	Volume filtered [L]	Comments
1	25.05.	10:27	11°57.6’	76°39.0’	28.76	36.1	12:20	12°10.8’	76°21.6’	27.69	36.60	643	
2	26.05.	04:25	13°50.2’	74°09.0’	27.58	36.17	06:45	13°50.2’	74°09.0’	27.61	36.19	860	Site SO164-01
3	27.05.	10:45	15°18.3’	72°47.1’	27.57	36.16	12:41	15°18.3’	72°47.1’	27.63	36.16	801	Site SO164-02
4	28.05.	06:30	16°32.4’	72°12.3’	27.29	36.14	08:40	16°32.4’	72°12.3’	27,29	36.14	837	Site SO164-03
5	28.05.	13:45	17°16.4’	71°39.1’	27.60	36.16	16:00	17°16.4’	71°39.1’	27.60	36.16	860	Site SO164-04
6	29.05.	05:00	21°19.5’	74°08.8’	27.01	36.29	09:22	21°19.5’	74°08.8’	27.01	36.29	1291	Site SO164-07
7	31.05.	13:30	23°00.0’	79°12.6’	27.61	36.06	14:45	23°06.6’	79°30.2’	27.63	36.20	560	
8	01.06.	09:00	24°01.0’	80°25.5’	28.03	36.11	12:35	24°01.6’	80°26.1’	28.29	36.15	1479	Site SO164-09-11
9	01.06.	20:20	24°08.0’	80°34.1’	28.83	36.12	21:45	24°07.9’	80°34.2’	28.74	36.12	580	Site SO164-15
10	05.06.	08:40	16°45.5’	71°29.2’	28.14	36.17	10:47	16°45.5’	71°29.2’	28.21	36.17	750	Site SO164-20
11	06.06.	10:20	16°06.0’	70°30.0’	27.87	36.09	14:33	15°56.6’	69°59.1’	27.98	36.49	2001	Site SO164-21
12	07.06.	02.05	15°24.0’	68°12.0’	27.90	36.15	05:30	15°24.0’	68°12.0’	27.88	36.15	501	Site SO164-22
13	08.06.	09:25	15°33.0’	65°08.1’	28.08	35.52	13:20	15°33.0’	65°08.1’	28.28	35.72	1082	Site SO164-23
14	09.06.	09:00	14°12.0’	63°25.7’	27.95	34.75	13:00	14°12.0’	63°25.7’	28.07	34.78	1026	Site SO164-24
15	10.06.	13:24	14°41.3’	59°44.5’	27.99	35.05	16:30	14°41.3’	59°44.5’	28.01	35.06	871	Site SO164-25
16	12.06.	17:55	16°06.0’	61°10.2’	28.23	35.19	20:00	16°06.0’	61°10.2’	28.18	35.21	647	Site SO164-27
17	16.06.	10:26	15°59.4’	61°24.1’	28.02	35.13	15:45	15°40.9’	60°41.3’	28.14	32.79	902	
18	16.06.	17:35	15°36.5’	60°22.4’	28.07	31.74	20:00	15°30.2’	59°55.7’	28.14	31.75	430	
19	17.06.	00:51	15°21.2’	59°17.0	27.90	32.38	05:50	15°21.2’	59°16.9’	27.79	32.42	926	Site SO164-50
20	18.06.	13:35	15°05.0’	61°04.92	27.86	33.60	17:23	15°01.1’	60°58.5’	27.80	34.36	854	Site SO164-??
21	19.06.	08:30	15°00.3’	60°41.7’	27.63	31.67	10:25	15°00.3’	60°41.7’	27.70	31.63	724	Site SO164-57
22	21.06.	11:35	14°26.2’	61°56.8’	---	---	14:50	14°18.8’	62°37.1’	---	---	793	No SST and SSS data available
23	22.06.	10:03	13°36.3’	66°31.1’	---	---	13:19	13°29.1’	67°10.4’	---	---	1000	
24	23.06.	10:21	12°46.4’	71°05.0’	---	---	11:42	12°41.2’	71°33.3’	---	---	635	
25	23.06.	19:21	12°15.9’	73°02.1’	---	---	23:10	12°02.0’	73°38.2’	---	---	827	
26	24.06.	08:36	11°13.0’	75°44.1’	---	---	11:00	11°02.0’	76°12.4’	---	---	707	

The alkenone method provides a tool for reconstructing past sea surface temperatures (SSTs). Certain *Haptophyte* algae, especially coccolithophores of the species *Emiliania huxleyi*, synthesize long-chain (C_{37}-C_{39}) unsaturated ketones (alkenones) in different proportions, depending on the temperature of ambient seawater during growth of the algae. Brassell et al. (1986) introduced the temperature-dependent alkenone unsaturation index U^{K}_{37} which, in a simplified form ($U^{K'}_{37}$), uses the di- and triunsaturated C_{37} alkenones only (Prahl and Wakeham, 1987):

$$U^{K'}_{37} = [C_{37:2}]/[C_{37:2} + C_{37:3}]$$

The use of alkenones as paleotemperature proxy relies on a linear correlation between $U^{K'}_{37}$ and growth temperature of the alkenone-producing algae (Prahl et al., 1988; Müller et al. 1998). Culture studies, however, have reported significant deviation of $U^{K'}_{37}$ from the values predicted by the Prahl et al. (1988) calibration and suggest that the temperature response of $U^{K'}_{37}$ may differ significantly between species, and also within the same species isolated from widely different oceanographic environments (Conte et al., 1998). This finding is reinforced by several regional studies derived from suspended particulate organic matter of surface waters suggesting that a single calibration may not be applicable in all oceanographic regions (see review of Sicre et al., 2002). Part of the deviation from the Prahl et al. (1988) calibration may be attributed to the fact that most of the studies are restricted to certain oceanic regions and/or that only small data sets covering a limited temperature range are used to establish each calibration. Especially for the warm surface waters of the tropical to subtropical ocean only very few ground-truth $U^{K'}_{37}$ data from particulate organic matter exist. Our sampling program was aimed to fill this gap.

5.2.7 Sampling of surface waters for oxygen isotopes

S. Mulitza

Samples for the analyses of oxygen isotope composition of seawater were taken with the ships pump at 25 positions from about 4 m water depth (Tab. 6). 25 ml of sea water have been siphoned into brown glass bottles. Temperature and salinity were measured continously with the ships thermosalinograph (Thermosalinometer (OTS-Sonde/VDT) by ME-Meerestechnik Elektronik GmbH, Sea & Sun). The data derived from the samples will be used to derive local $\delta^{18}O$ salinity relationships in the Caribbean, and will also contribute to global databases of the oxygen isotope composition of sea water.

Tab. 6 List of surface water samples for analysis of stable oxygen isotopes. Temperature and salinity are from the shipboard thermosalinograph.

No.	Date 2002	Local Time (UTC)	Latitude N	Longitude W	SST [°C]	SSS	Remarks
1	26.05	14:42	13°50,133’	74°09,064’	27.6	36.2	Strong rainfall
2	28.05	19:27	17°16,373’	71°39,106’	27.7	36.2	-
3	29.05	18:51	18°42,509’	79°38,725’	27.3	35.5	-
4	30.05	10:03	21°19,474’	74°08,755’	27.0	36.3	-
5	31.05	17:13	23°00,021’	79°12,756’	27.6	36.1	-
6	31.05	22:21	23°23,831’	80°16,493’	28.1	36.1	-
7	01.06	11:20	24°01,212’	80°25,250’	28.0	36.1	-
8	01.06	19:39	24°02,810’	80°27,655’	28.5	36.2	-
9	03.06	20:12	21°13,620’	74°21,038’	27.4	36.3	Site SO164-18
10	05.06	13:36	16°45,496’	71°29,225’	28.1	36.2	Site SO164-20
11	07.06	21:16	15°25,050’	67°49,566’	28.0	36.1	-
12	08.06	12:32	15°33,030’	65°08,112’	28.1	35.5	Site SO164-23, strong rain
13	09.06	17:03	14°12,226’	63°23,114’	28.1	34.8	Site SO164-24
14	12.06	20:02	16°11,488’	61°09,347’	28.2	35.1	Site SO164-26
15	13.06	22:32	15°57,502’	61°26,025’	28.1	35.0	-
16	16.06	20:55	15°38,311’	60°30,095’	28.1	32.1	-
17	17.06	05:47	15°21,215’	59°16,903’	27.9	32.4	Site SO164-50
18	19.06	12:49	15°00,314’	60°41,677’	27.6	31.7	-
19	23.06	19:31	12°32,600’	72°18,999’	-	-	no TS data available
20	24.06	01:23	12°07,077’	73°24,979’	-	-	no TS data available
21	24.06	13:02	11°15,509’	75°37,731’	-	-	no TS data available
22	24.06	16:17	11°01,277’	76°14,334’	-	-	no TS data available
23	24.06	20:48	10°41,607’	77°04,783’	-	-	no TS data available
24	25.06	06:04	10°00,944’	78°48,998’	-	-	no TS data available
25	25.06	13:26	9°23,095’	79°55,170’	-	-	no TS data available

Sampling of coccoliths for analysis of Strontium/ Calcium ratios

At each location 20 to 100 l of surface water were sampled with the vessel's membrane pump for the shore-based analyses of coccolith Sr/Ca ratios (Fig. 20, Tab. 7). To obtain mainly coccoliths the water was passed through polycarbonate filters and a 22 µm gaze used as a pre-filter. After sampling the filters were stored in petridishes at 4°C. The pumping was done with a commercial GARDENA garden pump.

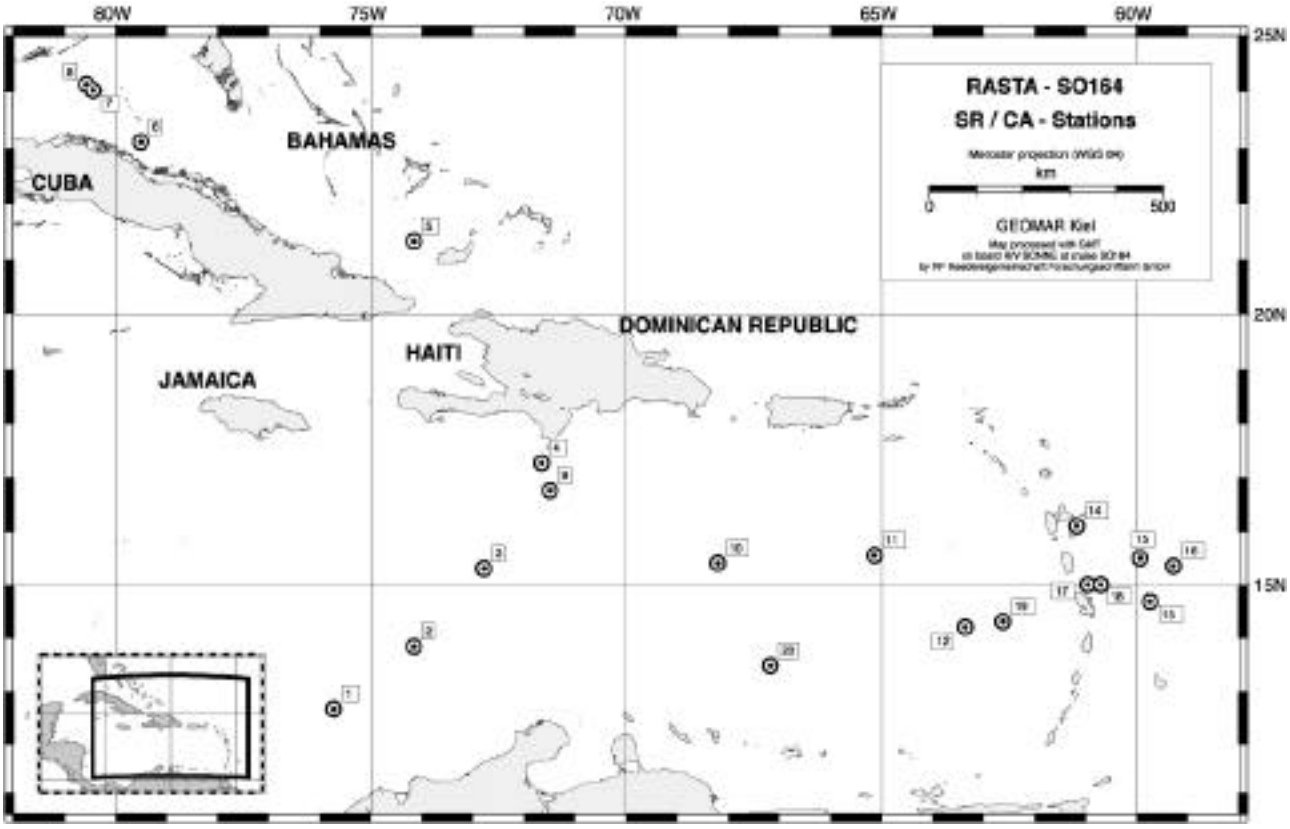

Fig. 20 Location of the Sr/Ca stations.

Tab. 7 List of samples of suspended particulate matter for coccolith Sr/Ca analysis. Temperature and salinity are from the shipboard thermosalinograph which was switched off after leaving Martinique (after saple No. 18).

No	Date 2002	Start (Local time)	Latitude North START	Longi-tude West START	SST [°C]	SSS [‰]	Stop (Local time)	Latitude North STOP	Longi-tude West STOP	SST [°C]	SSS [‰]	Volume filtered [L]	Com-ments
1	25.05.	17:00	12°39.7'	75°43.1'	27.8	36.22	18:50	12°51.8'	75°27.0'	27.80	36.18	74	
2	26.05.	06:52	13°50.2'	74°09.0'	27.60	36.17	08:00	13°50.2'	74°09.0'	27.57	36.16	106	Site SO164-01
3	27.05.	12:45	15°18.3'	72°47.1'	27.63	36.17	13:50	15°18.3'	72°47.1'	27.66	36.17	106	Site SO164-02
4	28.05.	21:30	17°16.3'	71°39.1'	27.62	36.18	22:30	17°16.3'	71°39.1'	27,6	36.20	---	Site SO164-04
5	29.05.	09:30	21°19.5'	74°08.8'	27.10	36.32	11:21	21°19.5'	74°08.8'	27.10	36.32	77	Site SO164-07
6	31.05.	14:45	23°06.6'	79°30.2'	27.63	36.20	17:45	23°21.09'	80°09.0'	27.63	36.20	116	
7	01.06.	12:45	24°01.6'	80°26.1'	28.25	36.16	14:30	24°01.2'	80°27.2'	28.68	36.17	101	Site So 164-11
8	01.06.	21:52	24°07.9'	80°34.2'	28.74	36.12	23:45	24°07.9'	80°34.2'	28.74	36.12	99	Site SO164-15
9	05.06.	10:50	16°45.5'	71°29.2'	28.21	36.17	---	16°45.5'	71°29.2'	28.21	36.17	---	Site SO164-20

No	Date 2002	Start (Local time)	Latitude North START	Longitude West START	SST [°C]	SSS [‰]	Stop (Local time)	Latitude North STOP	Longitude West STOP	SST [°C]	SSS [‰]	Volume filtered [L]	Comments
10	07.06.	00.35	15°24.0'	68°12.0'	27.91	36.15	02:20	15°24.0'	68°12.0'	27.91	36.15	100	Site SO164-22
11	08.06.	13:25	15°33.0'	65°08.1'	28.29	35.73	17:54	15°33.0'	65°08.1'	28.30	35.73	80	Site SO164-23
12	09.06.	01:10	14°12.3'	63°21.4'	28.08	34.78	15:55	14°13.3'	62°50.2'	28.21	34.48	86	Site SO164-24
13	10.06.	16:30	14°41.3'	59°44.5'	28.01	35.06	19:02	14°45.9'	59°51.2'	27.93	34.86	68	Site SO164-25
14	12.06.	20:00	16°06.0'	61°10.2'	28.18	35.21	22:03	16°02.8'	61°11.3'	28.04	35.09	60	Site SO164-27
15	16.06.	20:10	15°30.2'	59°55.7'	28.14	31.75	23:12	15°22.9'	59°24.2'	27.93	31.93	43	
16	17.06.	09:57	15°21.2'	59°16.9	27.85	32.60	13:40	15°21.2'	59°16.9'	27.85	32.60	32	
17	18.06.	17:31	15°00.4'	60°57.3	27.80	34.40	19:15	14°55.1'	60°54.8'	27.78	34.01	21	
18	19.06.	10:30	15°00.3'	60°41.7'	27.70	31.63	---	15°00.3'	60°41.7'	27.70	31.63	---	
19	21.06.	14:50	14°18.8'	62°37.1'	---	---	17:07	14°13.8'	62°04.0'	---	---	50	No SST and SSS data available
20	22.06.	13:19	13°29.1'	67°10.4'	---	---	15:22	13°24.6'	67°35.4'	---	---	84	

5.3 Sediment sampling and processing

D. Nürnberg, J. Schönfeld, T. Beck, S. Hansen, D. Hippler, A. Freiwald, A. LeGrande, J. Lezius, G. Martinez-Mendez, M. Mills, S. Mulitza, T. Nägler, L. Numberger, C. Rühlemann, S. Steingruber, S. Steph, J. Thiele, H. Westphal

Sea floor sediments at 400 to 4500 m water depth were sampled at 100 stations in the Caribbean Sea and the Atlantic Ocean east of the Lesser Antilles arc. For this purpose, multicorer (MUC), box corer (BC), piston corer (PC), and gravity corer (GC) were used. In total 17 multicorers, 45 box cores, 15 piston cores, and 23 gravity cores were retrieved. Details concerning region, position, time, and retrieval can be seen in the station list and on detailed bathymetrical charts in the appendix.

5.3.1 Multicorer

The coring device suited best for the sampling of undisturbed surface sediments including overlying bottom water is the multicorer (MUC). The MUC used on this cruise (Fig. 21) was equipped with eight plastic tubes, each of 60 cm length and 10 cm in diameter, respectively.

Fig. 21 The shipboard used multicorer.

Depending on the sediment composition, the recovery of the multicorer varied between 11 and 41 cm (Tab. 8, Fig. 22).

Tab. 8 Multicorer sampling.

Station SO164-	Position Latitude N / Longitude W	Water depth [m]	Core length [cm]	Benthic Foraminifera	Planktic Foraminifera	Chlorophyll
01-3	13°50,195N/74°09,028W	4025.7	25	X	X	X
02-2	15°18,290N/72°47,07W	2979.6	/			
02-3	15°18,290N/72°47,06W	2977	41	X	X	X
03-3	16°32,400N/72°12,31W	2744	38	X	X	X
04-2	17°16,380N/71°39,09W	1013	19	X	X	X

Station SO164-	Position Latitude N / Longitude W	Water depth [m]	Core length [cm]	Benthic Foraminifera	Planktic Foraminifera	Chlorophyll
05-3	17°23,000N/71°37,980W	313.4	/			
07-3	21°19,460N/74°08,760W	2722	34	X	X	X
18-1	21°13,61N/74°21,00W	1629	11	X	X	X
20-2	16°45,49N/71°29,22W	3357	37	X	X	X
21-3	16°06,00N/70°30,00W	3995	/			
22-2	15°24,00N/68°12,00W	4506	39	X	X	X
23-3	15°34,01N/65°08,09W	4328	35	X	X	X
24-3	14°11,89N/63°25,43W	1545	34			
25-3	14°41,25N/59°44,48W	2720	/			
48-2	15°57,02N/60°55,00W	1286	19	X	X	X
50-3	15°21,25N/59°16,94W	4002	33	X	X	X
61-1	14°21,49N/60°35,72W	1879	/			

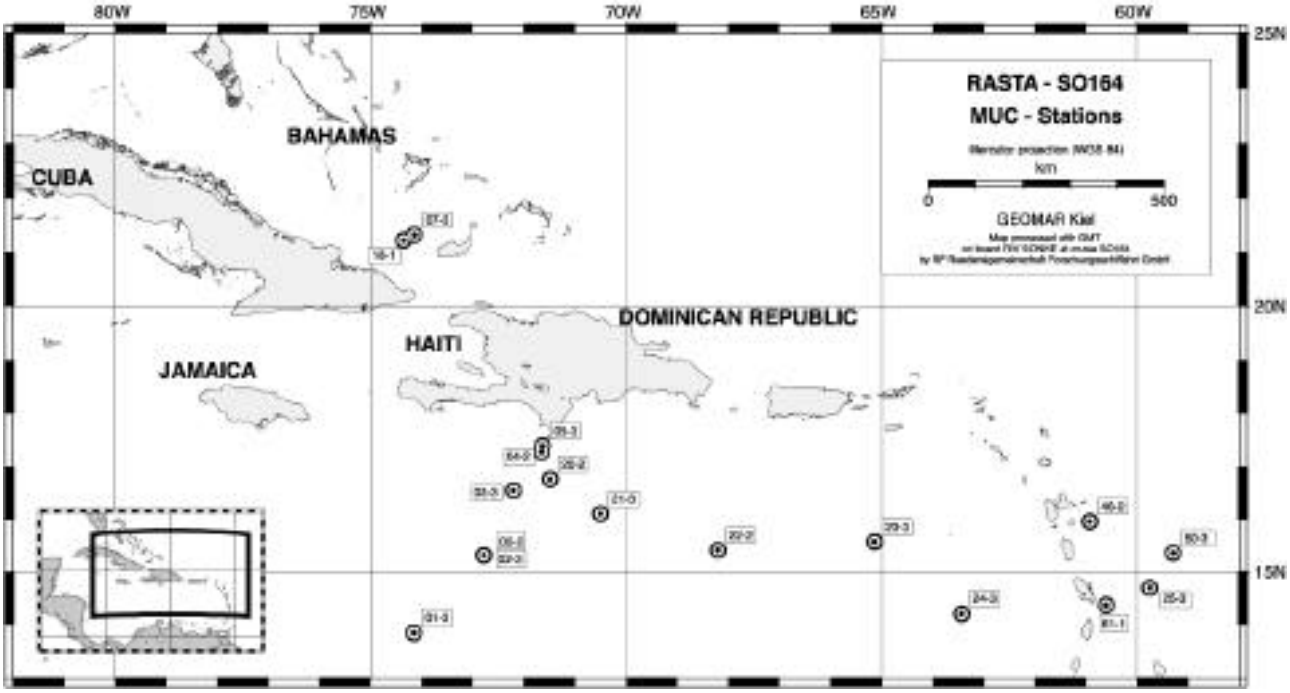

Fig. 22 Location of the MUC stations.

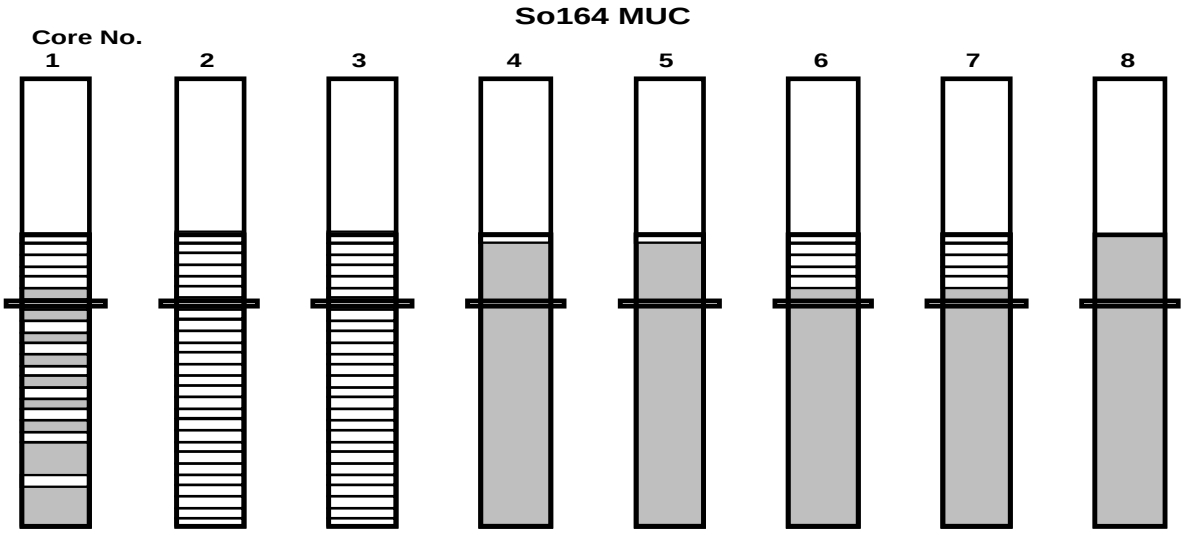

Fig. 23 Sampling scheme for the maximal available 8 multicorer tubes.

If possible, the MUCs were sampled as follows (Fig. 23):

Core 1 (LRC)

0 to 5 cm: every cm
5 to 20 cm: everey other cm
>20 cm: every fifth cm

Core 2 (GeoB)

core top sample and 1 core in cm slices

Core 3 (GEOMAR)

core top sample and 1 core in cm slices

Core 4 to 7 (Uni Kiel)

2 x 1 core top samples 0 to1 cm
2 x 1 cm slices, down to 5 cm

5.3.2 Box corer

The box cores were used to map the sedimentary environment, even in shallow water regions, and to select the coring positions of gravity cores or piston cores.

The box corer used on this cruise (Fig. 24) is able to recover maximal sediment depths of 50 cm.

Depending on the sediment composition, the recovery of the box cores varied between 5 and 45 cm (Fig. 25, Tab. 9).

A van Veen Grab sampler was used only once an sta-tion SO164–09–1, but had no substantial recovery.

Fig. 24 The shipboard used box corer.

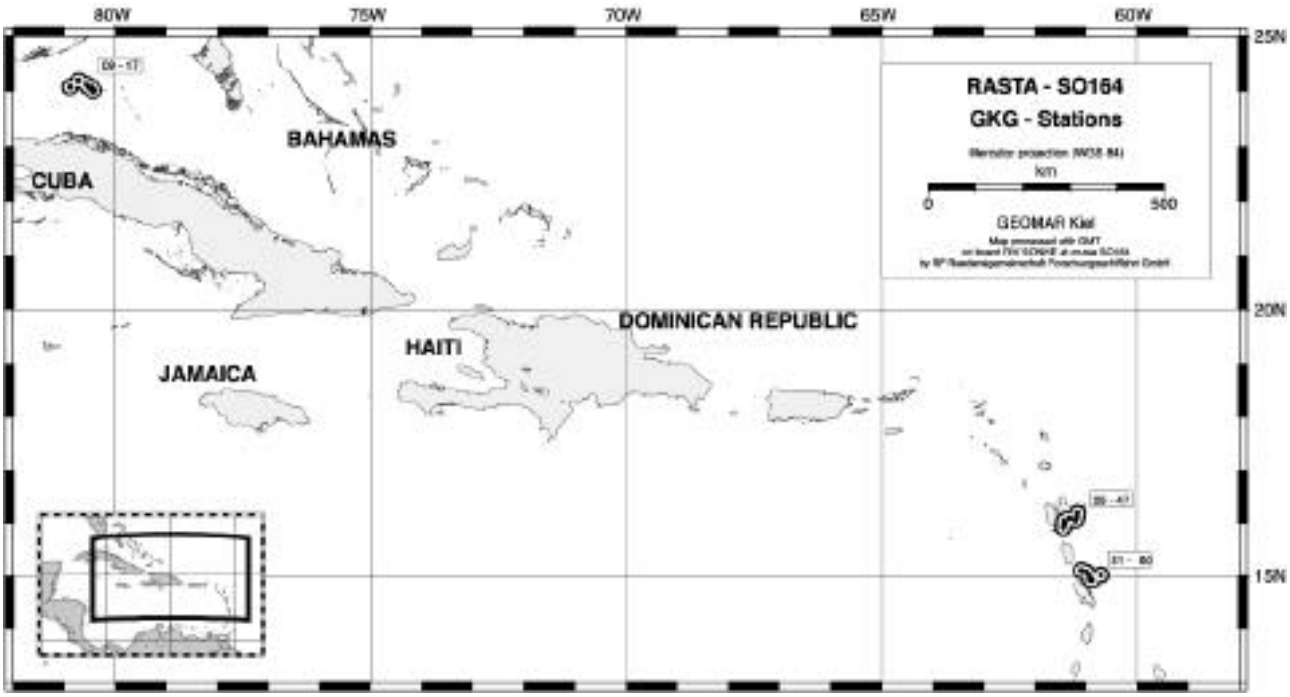

Fig. 25 Location of the box core stations.

Tab. 9 Box corer sampling.

Station SO164-	Position Latitude N / Longitude W	Water depth [m]	Core length [cm]	Benthic Foraminifera	Planktonic Foraminifera	Chlorophyll
09-1	24°01,20N/ 80°25,33W	527	/			
09-2	24°01,13N/ 80°25,31W	522	/			
09-3	24°01,02N/ 80°25,50W	525	/			
10-1	24°00,75N/ 80°26,19W	567	16	X	X	X
11-1	24°01,60N/ 80°26,13W	661	/			

Station SO164-	Position Latitude N / Longitude W	Water depth [m]	Core length [cm]	Benthic Foraminifera	Planktonic Foraminifera	Chlorophyll
12-1	24°01,23N/ 80°27,06W	706	14,5	X	X	X
13-1	24°02,90N/ 80°27,42W	796	12	X	X	X
14-1	24°04,98N/ 80°31,45W	968	14	X	X	X
15-1	24°07,81N/ 80°34,43W	1059	14	X	X	X
16-1	24°11,89N/ 80°42,93W	826	29	X	X	X
17-1	24°04,93N/ 80°52,89W	952	31			
26-1	16°11,49N/ 61°09,43W	32.1	22	X	X	X
27-3	16°06,00N/ 61°10,21W	667	/			
27-4	16°06,00N/ 61°10,21W	658	/			
28-1	16°28,3N/ 61°11,27W	993	14			
29-1	16°05,16N/ 61°18,97W	829	25	X	X	X
30-1	16°01,754N/ 61°25,926W	380	35			
32-1	15°57,51N/ 61°26,02W	73.0	20			
33-1	15°58,01N/ 61°25,49W	55	10			
33-2	15°58,00N/ 61°25,50W	55	15			
37-1	15°54,14N/ 61°26,21W	226	10	X	X	X
38-1	15°55,46N/ 61°26,27W	185	8	X	X	X
39-1	15°55,61N/ 61°26,27W	178	/			
39-2	15°55,60N/ 61°26,26W	179	/			
40-1	15°59,29N/ 61°24,40W	93	10			
40-2	15°59,28N/ 61°24,41W	93	10			
41-1	15°58,97N/ 61°24,43W	77	10			
41-2	15°58,98N/ 61°24,43W	77	15			
42-1	15°59,39N/ 61°63,91W	149	/			
43-1	15°59,23N/ 61°24,16W	117	8			
43-2	15°59,24N/ 61°24,14W	118	/			
44-1	15°59,11N/ 61°24,28W	94	10			
44-2	15°59,12N/ 61°24,28W	95	5			
47-1	16°02,87N/ 61°11,80W	995	13			
51-1	15°00,26N/ 60°56,07W	465	20			
52-1	15°03,27N/60°58,93W	813	14			
53-1	15°04,97N/61°04,89W	1328	45			
54-1	14°59,07N/ 60°54,95W	80.2	12			
54-2	14°59,07N/ 60°54,93W	80.2	10			
55-3	14°55,12N/ 60°54,80W	343	12			
56-1	14°54,61N/ 60°52,03W	82	/			
57-1	15°00,31N/ 60°41,68W	1009	38			
59-1	14°54,66N/ 60°52,04W	90	18			
59-2	14°54,64N/ 60°52,04W	86.3	21			
60-1	14°54,30N/ 60°52,03W	70.5	15			

After description of the surface, the box cores, if possible, were sampled routinely as follows (see Fig. 26).

Surface

- 1 PVC-bottle 500 ml for two 0 to 1 cm samples „J“; sample stained with Methanol/Rose Bengal.
- 4 PVC-bottles 500 ml, each one for 0 to 1 cm sample „W“; sample stained with Methanol/ Rose Bengal.
- 100 ml PVC-bottles and PS-boxes for hard substrates; conservation with Methanol/Rose Bengal.
- 10 cc syringes for surface sediment: Syringes capped, sealed, put in plastic bag with some water, and stored cold and dark.
- Radiographie-Box: X-ray slab preparation.
- MUC-Tube: slice as MUC cores (see above).

Section

- 2 x 8 10 cc syringes for section series: Syringes capped, sealed, each series put in a separate plastic bag with some water, stored cold and dark.
- Archive-Box: stabilized, and stored cold.

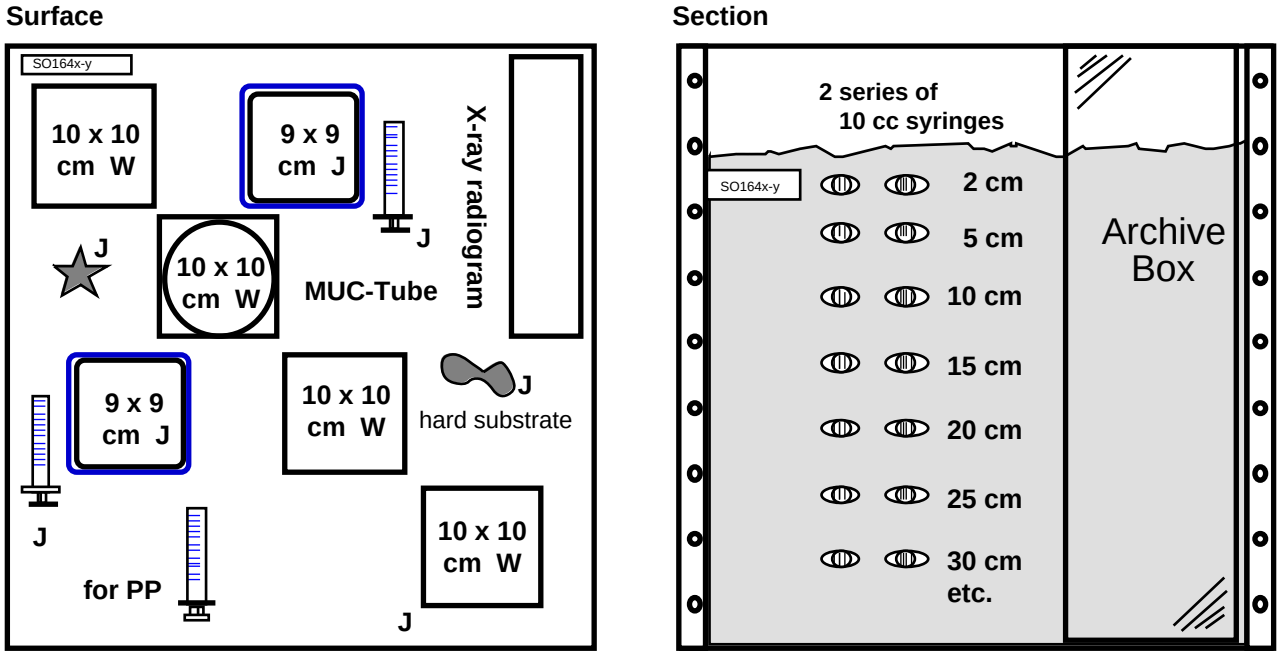

Fig. 26 Sampling scheme for the Florida Straits' box cores.

5.3.3 Sediments and benthic communities from the southern Florida Straits

J. Schönfeld

On Saturday, June 1st, 2002, we commenced with a CTD station in the core of the Florida Current to achieve a sound-velocity calibration data set. We proceeded with an extended SIMRAD and Parasound survey on a section to the northwest of Cay Sal Bank. We needed a detailed bathymetric map to define box-core sampling locations, and to explore sediments with a stratified echo signature that may be prospective for coring. By the end of the survey we recognized that water depths were with at least 500 m far higher than expected. The Captain did not proceed into shallower waters for safety reasons as we were considerably close to the Islands of Cay Sal group. We decided to perform a scattered but dense succession of box core deployments downslope into the centre of the Florida Trough, and upslope on the American side again (see Fig. 27).

Box core and Van Veen grab sampler deployments on the shallowest stations recovered small amouts of foraminiferal sand with pebbles of reef debris. Gravity cores were empty but had limestone chips in the core catcher and the cutting shoe was damaged. Seemingly, only a thin veneer of sand on hard-rock outcrops prevails in this area. Below 580 m depth, however, box core recovery improved. Coarse sand with reef debris and pebbles of up to 10 cm in diameter were found at one station. The pebbles were stocked with epizoans as hydroids and chrinoids, which again were densely populated with epibenthic foraminifers. *Discanomalina semipunctata, Cibicides lobatulus* and *Planulina ariminensis* were observed. The surface sediments pass into fine sand with ripples at 700 m depth, and into flaser-bedded fine and medium sands at 800 m. In the centre of the Florida Channel, we even retrieved a 0.89 m long sediment core with a 5 m piston corer. The core shows two fining upwards sequences from bioclastic coarse sand to silty fine sand with large shell fragments. The sedimentary facies was completely different on the opposit, American slope of the Florida Channel trough. Sandy spiculitic clays with undulated or flat surfaces were recovered at 800 and 900 m depth.

5.3.4 Description of box cores from the southern Florida Straits

The coordinates and water depths of the sample locations (ground contact) are given in Tab. 9. Photographs of sediment surfaces and sections are given in Plate 1.

SO164–09–2

The box was washed out, but a small amount of medium sand and a few pebbles of reef debris with attached hydroids were recovered. The hydroids are densely stocked with epibenthic foraminifers, in particular *Aggerostramen rusticum*, *Planulina ariminensis* and *Discanomalina semipunctata*. Polychaets and a monopod were also observed.

SO164–10–1

Surface

The box core surface was smooth and showed only irregular, shallow undulations of 2 to 3 cm amplitude. The surface was washed in places, in particular in a 10 cm wide strip at the frontal lid. The sediment was a pebbly medium to coarse sand. The colour was pale cream. The surface showed aligned patches of finer sand. They alternated with elongated areas of coarse

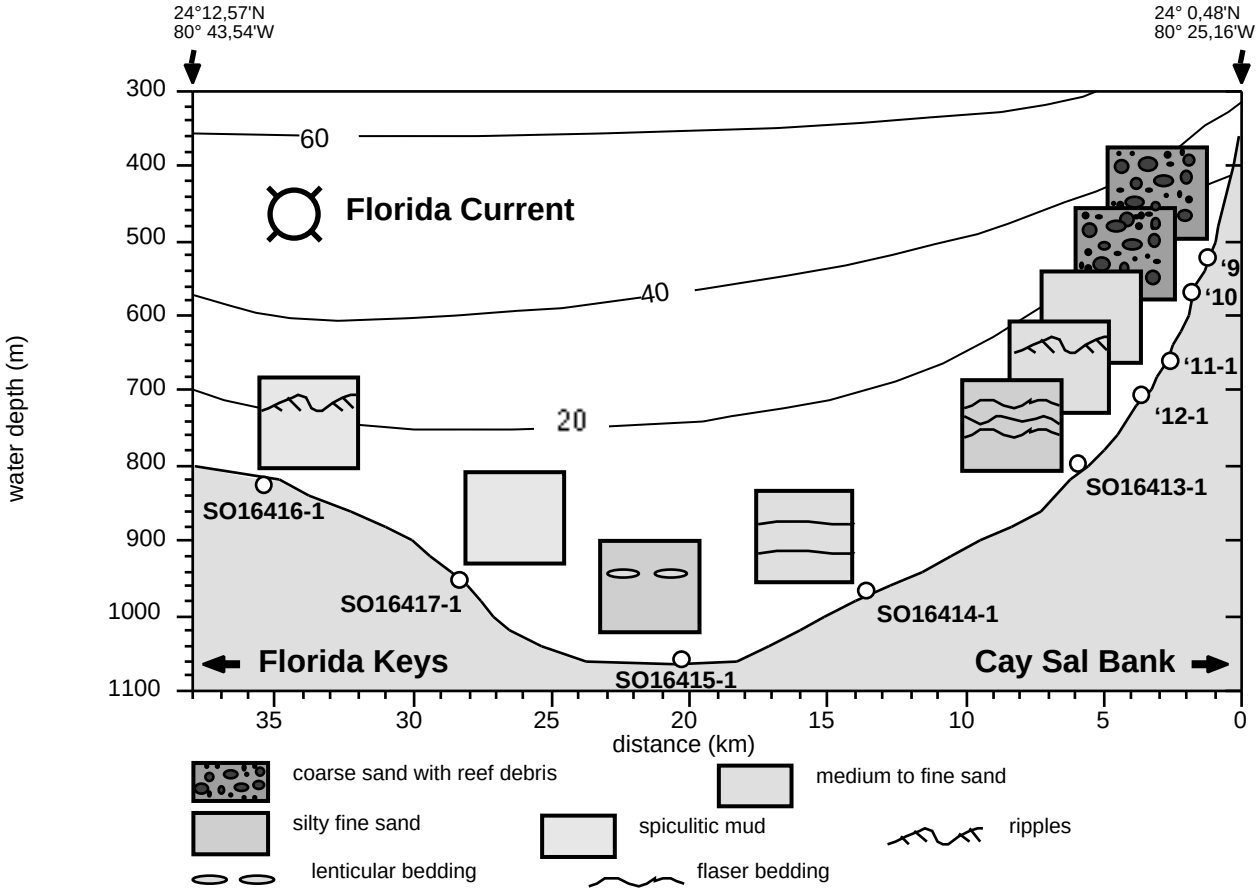

Fig. 27 Near-surface sediments on the GOLDFLOS transect at the northern slope of Cay Sal Bank, Bahamas. The sediments at depths above 660 m are mainly composed of shallow-water carbonate debris which derives from Cay Sal Bank. The structures depict the decrease in current intensity with depth, where the lower limit of recent sediment transport may be recognised between 830 and 950 m. Thin contour lines: average northeastern current velocity in cm per second (Section I, Richardson et al., 1969).

sand where pebbles and bioclasts were more abundant. The pebbles were mostly well-rounded limestone fragments, i.e. reef debris. Bivalve shells and fragments, echinoid fragments (tests and large spines), and coral fragments were abundant. Pteropods, gastropods, and bryozoans were also recorded. Hydroids were frequent, and they were mostly attached to larger limestone pebbles, but a few solitary specimens were also found. They were stocked with epibenthic foraminifers; *Discanomalina semipunctata* and *Planulina ariminensis* were frequent. Other benthic organisms were a couple of polychaet tubes standing close to a pebble with attached hydroids.

Sediment succession
An archive box revealed no change in colour, sediment composition or texture over a depth of 16 cm.

SO164–11–1

The box was washed out. Only a small amount of medium foraminiferal sand with dark-brown claystone chips of a few mm in size was recovered.

SO164–12–1

Surface
The box core surface was undulated with irregular smooth ripples. The width was 15 to 16 cm, the amplitude was mostly 2 to 3 cm, but increased to 8 cm in the frontal part. The surface was slightly washed, in particular in a 13 cm wide strip at the frontal lid. The sediment was a sharp, well sorted fine sand with pteropods. The colour was greyish cream. The surface showed patches where pteropod shells, dark-brown claystone chips, and crustacean fragments of several millimetres in size were concentrated predominantly at the lee side of the ripples. Among benthic organisms, only a few solitary polychaet tubes and a nematode were found.

Sediment succession

0 to 0.5 cm	fine sand, greyish cream, homogenous.
0.5 to 1.5 cm	pteropod hash, yellowish cream.
1.5 to 14.5 cm	fine sand, greyish cream, homogenous.

SO164–13–1

Surface
The box-core surface was inclined in the frontal part but otherwise almost flat. Only an irregular roughness of 1 cm amplitude at maximum was recognised. The

sediment was a soft, silty fine to medium sand. The colour was yellowish cream. The surface showed patches where pteropod shells and other coarser components of millimetres in size were concentrated. The patches were either 3 to 5 cm in diameter and aligned, or elongated, 4 cm in width and 40 cm in length. The lines of patches run parallel and were 10 to 15 cm apart. Pebble-sized debris consists of a few limestone pebbles of 1 to 2 cm in diameter, large echinoid spines, up to 5 cm long, a coral fragment of the same dimensions and large pteropod shells of 0.5 cm in diameter. Hydroids were abundant. They were either attached to limestone pebbles or recorded as solitary specimens that gathered in line at patches with shell concentrations.

Sediment succession

0 to 0.2 cm	pteropod hash in places, yellowish cream.
0 to 5 cm	silty fine to medium sand, less sorted, greyish cream with darker spots, homogenous.
5 to 8 cm	silty fine to medium sand, less sorted, yellowish cream, homogenous, with mm-sized coral and bryozoan fragments. Bed thickness varies with shallow undulations over the 50 cm section examined.
8 to 10 cm	(in places 11 cm) silty fine to medium sand, less sorted, greyish cream, homogenous.
10 to 12 cm	silty fine to medium sand, greyish cream.

SO164–14–1

Surface

The box core surface was almost flat. Only very shallow undulations with a width of 22 cm and an amplitude of 1 cm were recognised in the section. The sediment was a silty fine to medium sand. The colour was reddish to greyish cream. The surface showed a marked meandering groove of 2 cm width and 1 cm depth with walls of excavated material to both sides. This groove is regarded as a feeding trace, possibly made by a sea cucumber. Other biogenic structures were a cluster of burrow openings of 0.5 cm in diameter, and circular heaps of 2 cm in diameter made of excrement around polychaet burrows. Pteropod shells and other coarser components as thin, black echinoid spines and solitary corals of a few centimetres in size were distributed irregularly over the sediment surface. Only the pteropods were concentrated in a patch of about 10 cm in size.

Sediment succession

0 to 10 cm	silty fine to medium sand, greyish cream.
10 to 10.5 cm	dashed lentil of fine sand in depressions on top of the lower bed.
10 to 14 cm	medium to coarse sand, sharp and with less silt than above, brownish to greyish cream, darker than above, pteropods common. Top undulated.

SO164–15–1

Surface

The box core surface was flat. The sediment was a silty fine to medium sand. The colour was yellowish cream. Biogenic structures were a funnel-shaped burrow opening of 5 cm in diameter and circular heaps of up to 4 cm in diameter made of excrement around burrows. The openings were not visible, however. Among living organisms, polychaet tubes were common. They tend to form closer together with hydroids and bryozoans, and a *Pheronema* sponge. A few tubular arenaceous foraminifers, *Rhabdammina abyssorum*, were also observed. They were lying flat on the sediment surface. Coarser components as pteropod shells and thin, black echinoid spines were also common, and they were distributed irregularly all over the sediment surface.

Sediment succession

0 to 7 cm	silty fine to medium sand, greenish to greyish cream. Pteropod shells are concentrated in a millimetre-thick veneer at the sediment surface. Two silt-rich lenses of 2 cm thickness and 8 and 10 cm in length were recorded close to the base of the unit.
7 to 14 cm	medium to coarse sand, brownish cream, with abundant pteropods and fragments. Two silt-rich lenses of 2 cm thickness and 7 cm length were found near the top of the unit. An oblique lens of pteropod hash with 6 cm length and 3 cm thickness occurred at the bottom of the unit between 7.5 and 14 cm.

SO164–16–1

Surface

The box core surface was humpy with irregular, smooth undulations, probably mud ripples. The width was 20 to 30 cm, the maximum amplitude was 4 cm. The sediment was a sandy spiculitic clay, very soft at the surface. The colour was greenish light-brown. Biogenic structures were not recognised. Among living organisms, a few polychaet tubes were observed. They tended to form a cluster together with tubular arenaceous foraminifers (recorded as ”greenish flocs”). Two small hydroids were also found. Coarser components were rare, only a few pteropod shells and some droplets of crude oil were found.

Sediment succession

0 to 2 cm	sandy clay, soft, yellowish light-brown, homogenous.
2 to 7 cm	sandy clay, yellowish brown, mottled. An indistinct, dashed seam of dark brown manganese oxide staining is recognised at 3 cm.
7 to 9 cm	sandy clay, light grey, mottled, but distinct burrows become visible near the base of the unit.
9 to 29 cm	sandy clay, light greenish grey, homogenous, sand-sized components enriched in mottles.

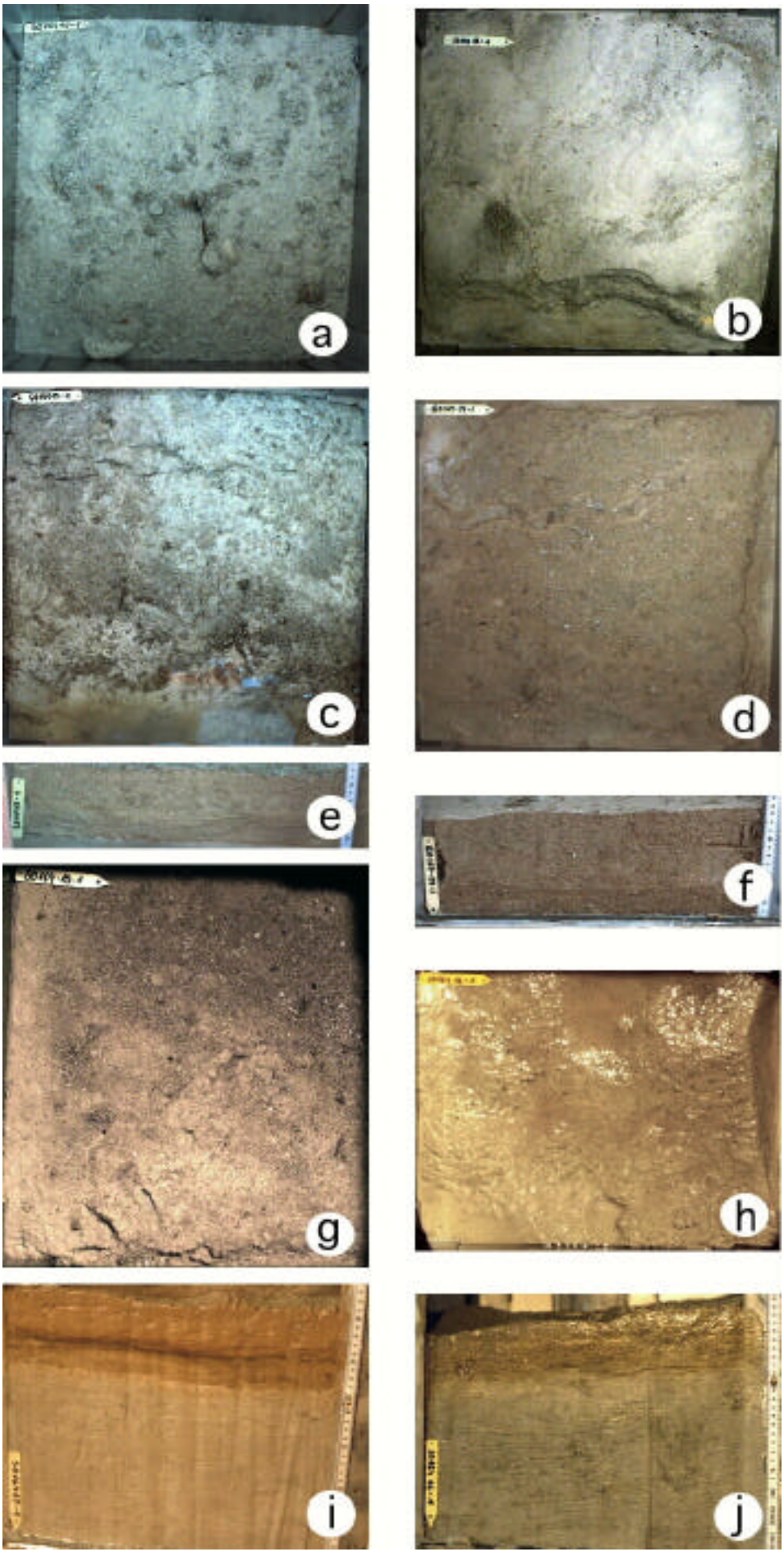

Plate 1:
Box core photographs from the southern Florida Straits off Cay Sal, Bahamas. Note: The tag with station number is 10.0 cm long. The width of the box corer is 50 x 50 cm.
SO164–10–1: a) surface. Note the large pebbles of reef debris.
SO164–12–1: b) surface.
SO164–13–1: c) surface, e) section.
SO164–14–1: d) surface, f) section. Note the undulated top of the lowermost medium sand bed.
SO164–15–1: g) surface. Note that the photograph covers only 80 % of the surface area.
SO164–16–1: h) surface, j) section. Note that the image covers only 80 % of the surface area. The groove in the lower part of the photograph corresponds to the depression in the central part of the sediment surface in figure j).
SO164–17–1: i) section.

SO164–17–1

Surface
The box core surface shows irregular, smooth undulations of 20 to 30 cm width and 2 cm amplitude at maximum. The sediment was a light sandy spiculitic clay, the texture was crumbly. The colour was brownish to greenish grey. Biogenic structures were funnel-shaped and plain, circular burrow openings of 0.5 cm in diameter and circular heaps of 2 cm in diameter made of excrement around burrows. Among living organisms, hydroids and polychaet tubes were common. They were standing in clusters or as solitary organisms. Coarser components were rare, only a few large miliolid foraminifers were found.

Sediment succession

0 to 5 cm	light sandy, spiculitic clay, light-brown, homogenous.
5 to 6 cm	seam of dark brown manganese oxide staining
6 to 10 cm	light sandy, spiculitic clay, brownish grey, mottled.
10 to 31 cm	light sandy, spiculitic clay, light grey, mottled, distinct larger burrows visible.

5.3.5 Piston corer and gravity corer

D. Nürnberg, J. Schönfeld, T. Beck, S. Hansen, D. Hippler, A. Freiwald, A. LeGrande, J. Lezius, G. Martinez-Mendez, M. Mills, S. Mulitza, T. Nägler, L. Numberger, C. Rühlemann, S. Steingruber, S. Steph, J. Thiele, H. Westphal

To recover deeper and older sediment sequences, a piston corer (PC) with pipe lengths of 5, 10, 15, or 20 m and a weight of 2.5 tons, and a gravity corer (GC) with pipe lengths of 6, 9, or 12 m and a weight of 1.5 tons was used at 38 stations (Fig. 28 and 29).

To retain the relative orientation of the core, all liners used have been marked lengthwise with a straight line. On board, the sediment core was cut into 1-meter sections, closed up with caps on both ends and labeled according to a standard scheme (Fig. 30). A total of 26 cores were retrieved with recoveries between 383 and 4508 m (Tab. 10). At 12 deployments the core tube returned empty.

Core segments were cut into "archive" and "work" halves. The "archive" half was used for core description, smear slide sampling for initial biostratigraphic investigations, and scanning of light reflectance. The "work" half was sampled with two series of 10 ml syringes for geochemical and foraminiferal analysis at 5 cm intervals and at 2 cm intervals.

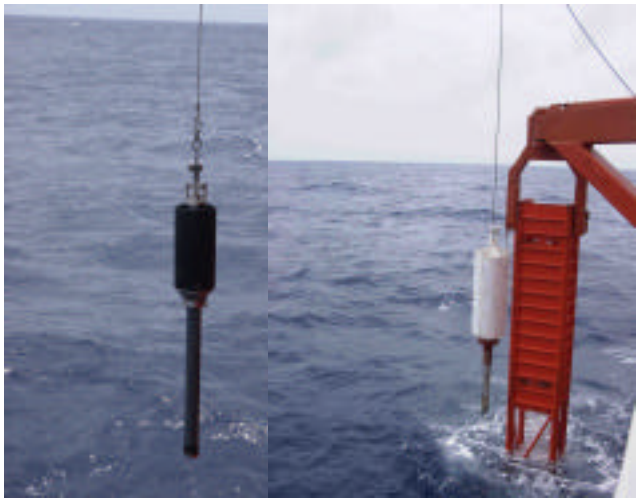

Fig. 28 The shipboard used gravity corer (left) and the piston corer (right).

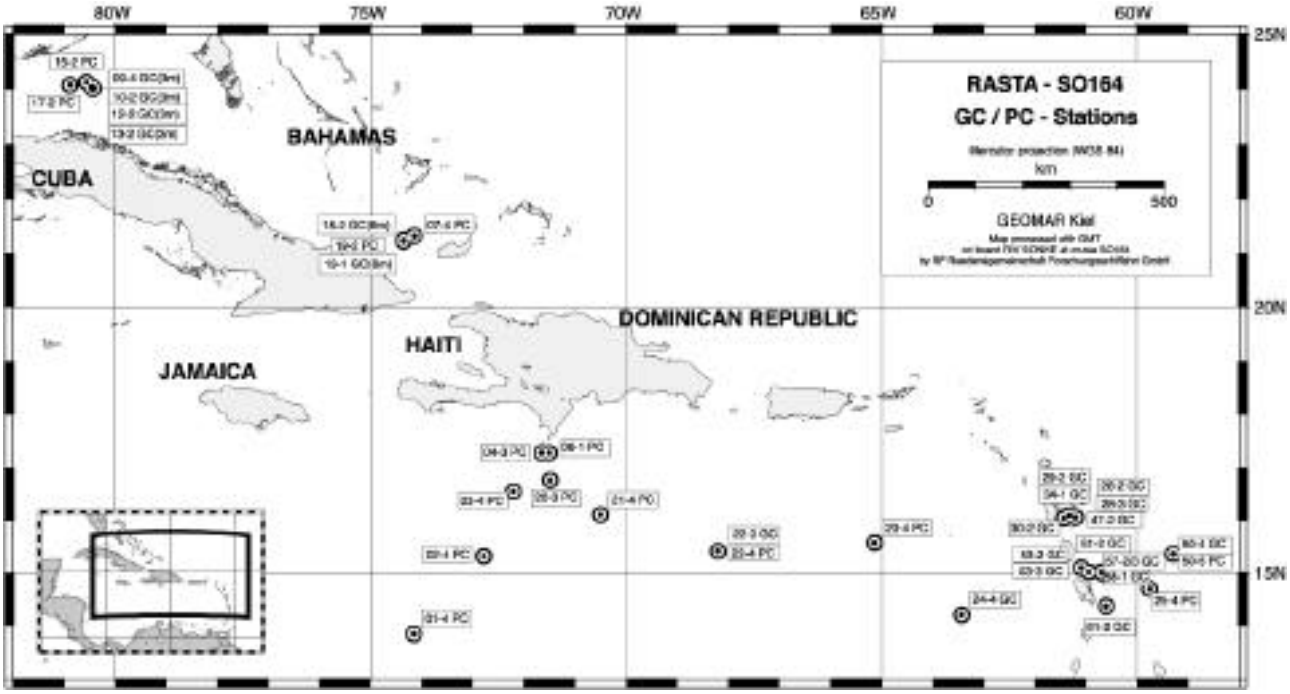

Fig. 29 Location of the GC and PC stations.

Tab. 10 Piston corer and gravity core sampling.

Station SO164-	Device	Position Longitude N/ Latitude W	Water depth [m]	Core length [cm]	Geomar Forams 10 ml	GeoB Forams 10 ml	PP	Smear slides
01-4	PC	13°50,140N/ 74°09,02W	4033	7,1	X	X	X	X
02-4	PC	15°18,290N/ 72°47,05W	2985	8.37	X	X	X	X
03-4	PC	16°32,370N/ 72°12,31W	2744.7	13.16	X	X	X	X
04-3	PC	17°16,390N/ 71°39,07W	1017	/				
06-1	PC	17°16,330N/ 71°30,070W	1017	0.42	X	X	X	X
07-4	PC	21°19,460N/ 74°08,770W	2722	12.6	X	X	X	X
09-4	GC	24°01,04N/ 80°25,47W	514	/				
10-2	GC	24°00,71N/ 80°26,33W	588	/				
12-2	GC	24°01,29N/ 80°27,60W	698	/				
13-2	GC	24°02,88N/ 80°27,51W	801	/				
15-2	PC	24°08,01N/ 80°33,89W	1055	0.89	X	X	X	X
17-2	PC	24°04,99N/ 80°53,00W	954	11.76	X	X	X	X
18-2	GC	21°13,61N/ 74°21,00W	1623	/				
19-1	GC	21°14,72N/ 74°21,00W	1702	0.35				
19-2	PC	21°14,71N/ 74°20,99W	1704	6.93	X	X	X	X
20-3	PC	16°45,49N/ 71°29,22W	3358	9.68	X	X	X	X
21-4	PC	16°06,00N/ 70°30,00W	3996	18.96	X	X	X	X
22-3	GC	15°24,00N/ 68°12,00W	4508	8.99	X	X	X	X
22-4	PC	15°24,00N/ 68°12,00W	4508	9.26	X	X	X	X
23-4	PC	15°34,01N/ 65°08,09W	4331	6.39	X	X	X	X
24-4	GC	14°11,92N/ 63°25,55W	1542	8.56	X	X	X	X
25-4	PC	14°41,25N/ 59°44,43W	2721	15.01	X	X	X	X
28-2	GC	16°28,20N/ 61°11,27W	994	/				
28-3	GC	16°28,20N/ 61°11,27W	996	/				
29-2	GC	16°05,16N/ 61°18,97W	826	1.24	X	X	X	X
30-2	GC	16°01,73N/ 61°25,89W	383	1	X	X	X	X
34-1	GC	16°50,00N/ 61°18,90W	836	1.36	X	X	X	X

Station SO164-	Device	Position Longitude N/ Latitude W	Water depth [m]	Core length [cm]	Geomar Forams 10 ml	GeoB Forams 10 ml	PP	Smear slides
47-2	GC	16°02,85N/ 61°11,77W	995	/				
48-3	GC	15°57,01N/ 60°54,99W	1287	1.28	X	X	X	X
50-4	GC	15°21,20N/ 59°16,91W	3999	4.3	X	X	X	X
50-5	PC	15°21,19N/ 59°16,90W	3993	/				
51-2	GC	15°00,27N/ 60°56,08W	466	0.52	X	X	X	X
53-2	GC	15°05,00N/ 61°04,91W	1335	0.78	X	X	X	X
53-3	GC	15°05,00N/ 61°04,91W	1335	0.81	X	X	X	X
57-2	GC	15°00,32N/ 60°41,70W	1008	/				
57-3	GC	15°00,31N/ 60°41,69W	1009	/				
58-1	GC	14°59,34N/ 60°41,00W	1038	0.25	X	X	X	X
61-2	GC	14°21,38N/ 60°35,70W	1884	1.06	X	X	X	X

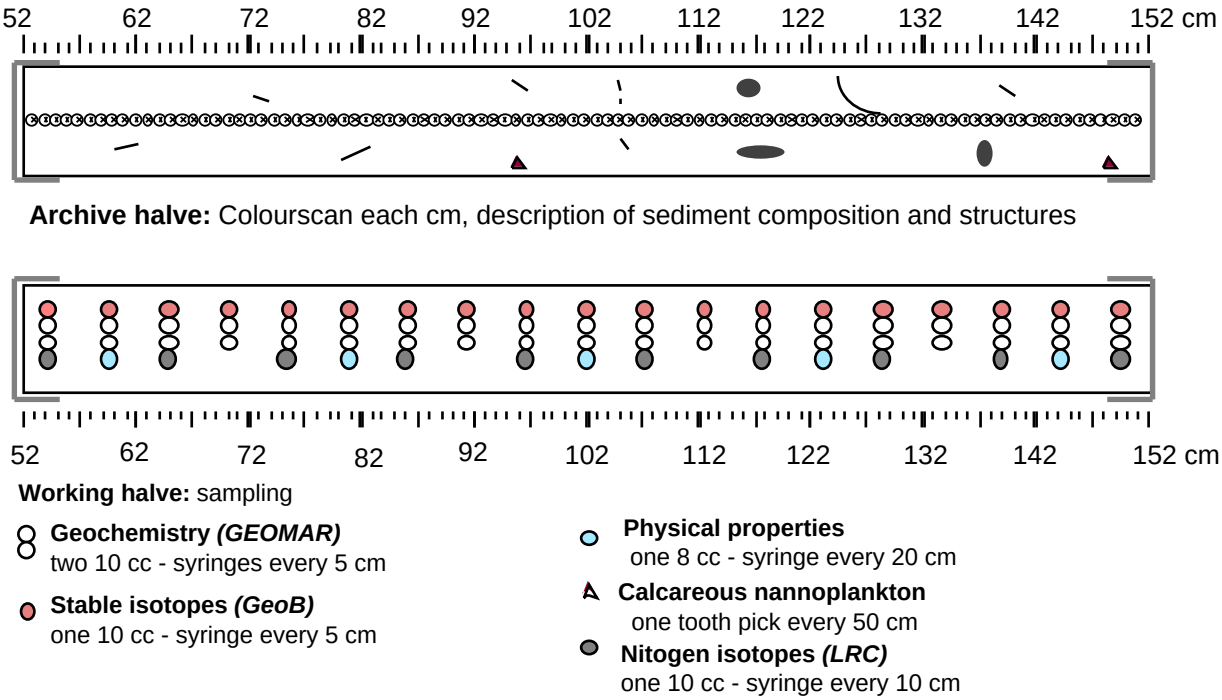

Fig. 30 Sampling scheme for the treatment of piston core and gravity core segments.

Columbia Basin

Five sediment cores were retrieved from water depths ranging from 2977 to 4033 m. The location of the core stations is shown in Fig. 31. Core recoveries were between 0.25 and 8.37 m. All sediment cores were opened and described on board.

Bahamas

Six sediment cores were retrieved from water depths ranging from 1623 to 2722 m. The location of the core stations is shown in Fig. 31. Core recoveries were between 0.11 and 12.6 m. All sediment cores were opened and described on board.

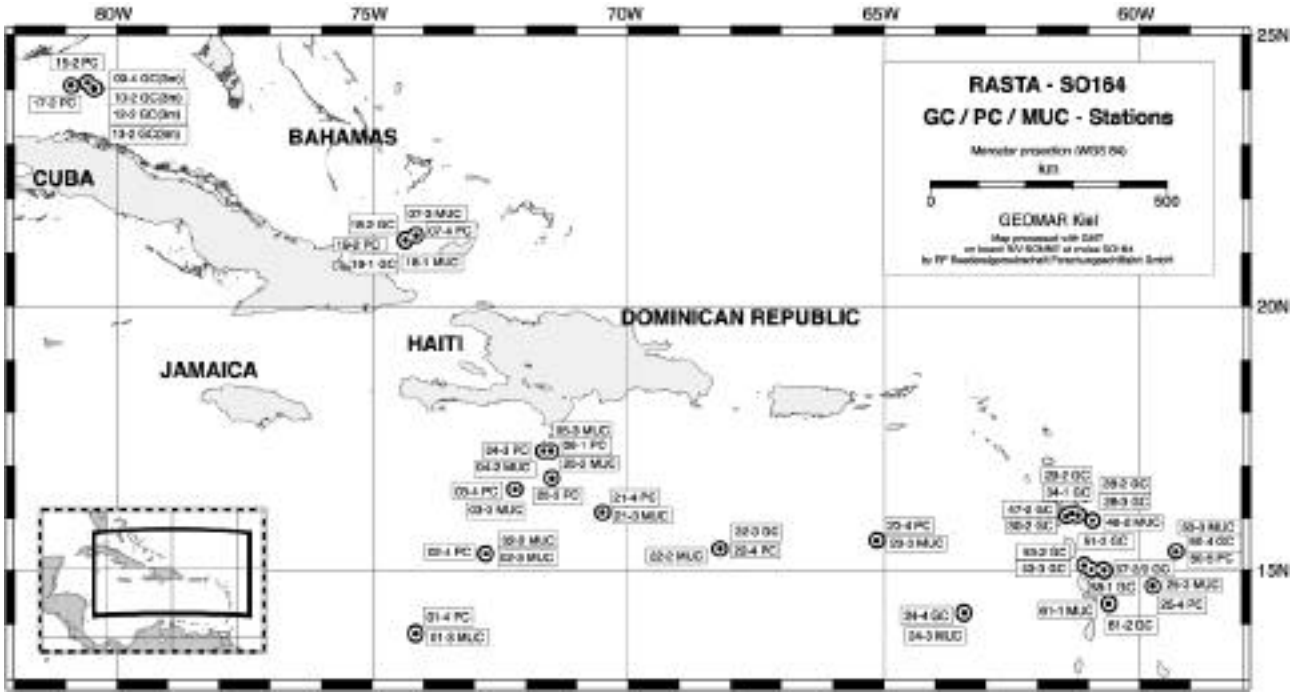

Fig. 31 Location of the sediment cores (GC, PC, and MUC stations).

Florida Straits

Two sediment cores were retrieved from water depths ranging from 954 to 1055 m. The location of the core stations is shown in Fig. 31. Core recoveries were between 0.89 and 11.76 m. All sediment cores were opened and described on board.

Beata Ridge

Six sediment cores were retrieved from water depths ranging from 313.4 to 2744.7 m. The location of the core stations is shown in Fig. 31. Core recoveries were between 0.19 and 13.16 m. All sediment cores were opened and described on board.

Venezuela Basin

Eleven sediment cores were retrieved from water depths ranging from 1542 to 4331 m. The location of the core stations is shown in Fig. 31. Core recoveries were between 0.34 and 18.96 m. All sediment cores were opened and described on board.

Atlantic East of the Lesser Antilles Arc

21 cores have been taken east of the Lesser Antilles Arc from water depths between 383 and 3999 m. Core lengths varied between 0.19 and 15.01 m. The location of the core stations is shown in Fig. 31.

5.3.6 Visual core description

W. Kuhnt

The sediment core graphical descriptions, carried out on the archive half of all piston core and gravity core segments, summarise data obtained during shipboard visual inspection of each core. The ODP conventions were used for the compilation of the core description forms and the exceptions to these procedures adopted by the SO164 shipboard scientific party are described below.

All sediment core descriptions were documented with the software package AppleCORE, using a lithology custom file containing patterns for the standard ODP sediment classification scheme, a modified version of the lithologic classification of Mazzullo et al. (1988) (see core graphics in the appendix). Sediments were named on the basis of composition and texture using a principal name together with major and minor modifiers. Principal names define the degree of consolidation (induration) and granular sediment class. Composition and texture of cored sediments and rocks were determined aboard ship by visual observation of the core, and visual estimates in smear slides, and coarse fractions. Calcium carbonate content was qualitatively estimated in smear slides, and quantitatively by carbonate bomb analysis for core SO164–17–2 (see chapter 5.3.10). Brightness (L*) and green/red reflected light component values (a*) are collected from the Minolta spectro-photometer. Brightness (L*) is shown in the column to the left of the graphic lithology.

The location and nature of sedimentary structures, the occurrence of ichnofossil genera and major groups of macro- and microfossils, as well as accessories such as pyrite, iron sulphides, lamina, and shell fragments are shown in the third column of the core description sheet. The symbols used to designate structures found in each core are shown in the legend to each core description.

The positions of smear slides taken from each core for analysis are indicated by the letters SS (smear slide) in the “Sample” column of the core description sheet. Colour was visually estimated using comparison to a

Munsell colour chart and the Minolta spectrophotometer readings.

The text description for each core consists of a list of major lithologies followed by a more detailed description of the composition (as determined from smear slides), sedimentary structures, and other notable features. Descriptions and locations of thin, interbedded, or minor lithologies are also included in the text.

Colour Spectrophotometry

A Minolta CM-508d hand-held spectrophotometer was used to measure light reflectance on sediment cores opened on board R/V SONNE. These measurements were determined on the damp core surface, and clear plastic film was used to cover the core. The spectrum of the reflected light is measured by a multi-segment light sensor. The spectral reflectance is measured at a 10 nm pitch over the wavelength from 400 to 700 nm, and a double-beam feedback system automatically compensates for variation in the illumination from the CM 508d's pulsed xenon arc lamp. Routine measurements were made at 1 cm spaced intervals, and automatically recorded on a Toshiba Satellite 2060 DS laptop computer using Minolta's software Spectramagic v.2. 11 (release 1998).

The spectrophotometer was calibrated for white color reflectance and "zero calibrated" at least twice a day, at the beginning of each work shift. This color calibration was made to avoid variation in color readings due to the laboratory environment (temperature, humidity, and background light) and instrument variations.

From the reflectance data, the standard color-values X, Y, and Z were automatically calculated by the software Spectramagic, which are displayed in the L*, a* and b* CIELAB color coordinates. The L* value represents brightness and can be directly correlated to greyvalue measurements (i.e. from video-systems).

5.3.7 Shipboard core logging

N. Brughmans, N. Gussone, D. Hippler, G. Martinez-Mendez, S. Steph

Magnetic susceptibility and reflectance were used as the primary parameters for a preliminary age model and a correlation between sedimentation cores from different sites.

Multi sensor core logging-tool

High resolution magnetic susceptibility and P-wave velocity measurements were performed using a Multi-Sensor-Core-Logger (GEOTEK). The sediment cores were logged in one meter sections and in one centimeter steps. A standard liner filled with distilled water was measured at the beginning and at the end of each core. Additional standard measurements within the core allows to apply a drift correction if necessary. Two additional parameters, core temperature and core thickness, were determined.

P-wave velocity

Ultrasonic transducers measure the velocity of compressional waves in the core. The P-wave velocity sensor system is composed of two transducers with a characteristic frequency of 500 kHz. The ultrasonic wave, produced in the sender, travels through the sediment core and reaches the receiver. The time difference between sending and receiving is the P-wave travel time. The simultaneously measured temperature and core thickness allow for P-wave travel time corrections.

5.3.8 Processing of magnetic susceptibility data

J. Schönfeld

The raw data of magnetic susceptibility were first checked for consistency, and obvious outliers were removed. The measured sections were brought into stratigraphic succession, and a composite, "true" depth scale was created according to the logs of actual and inscribed core section lengths. They were often different. A standard seawater filled section was measured at the beginning and end of each core, and some times in between. The measured susceptibilities mostly showed an offset to the assigned zero, which also varies during the logging. Offset and a linear trend of standard section measurements were removed from the original susceptibility values. As each core section was logged individually, the magnetic susceptibility shows a marked decrease towards the beginning and end of each section. This is due to the fact that the amount of material detected by the loop diminishes once the core is shifted to one side of it. This denominated "end effect" could substantially interfere with any variability in susceptibility. We therefore developed a dynamic equalization factor as revealed from a polynominal regression of core section records with rather uniform material and susceptibility (Fig. 32). This factor allows to shift the lowered susceptibility values near the ends of the core sections to more realistic levels. The internal variability is unaffected, though may be slightly amplified at the very ends. We therefore skipped susceptibility values from the first 3 to 5 cm at the top and bottom of each section.

5.3.9 Shipboard physical properties measurements

A. LeGrande

Water content and density are basic sediment properties that are measured most accurately through mass and volume determinations (Blum, 1997). Wet bulk density and porosity as calculated from these determinations are index parameters defining the geotechnical properties, and their record along a sediment core provides insight in the successive physical compaction. The dry bulk density is an important variable for the calculation of accumulation rates (van Andel et al., 1975). It is known, however, that structural alterations take place due to desiccation and mechanical perturbances during core handling and transportation. These can result in a loss of pore water, compaction, and

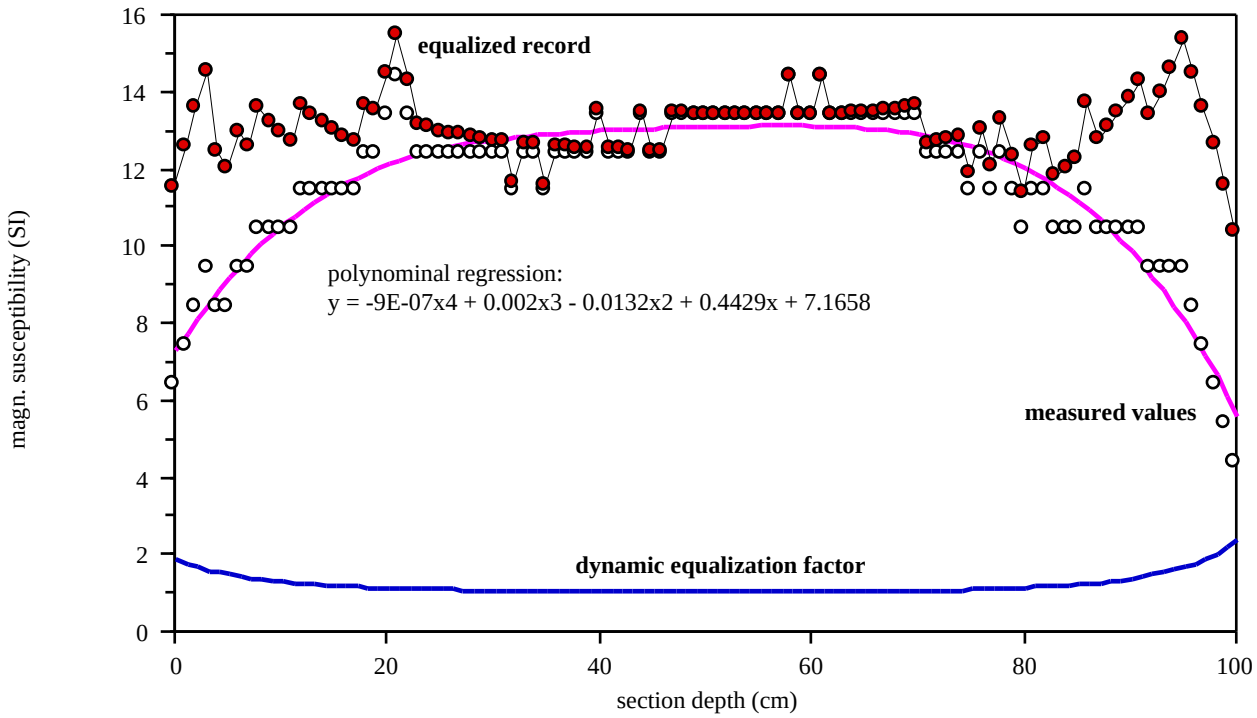

Fig. 32 Application of the dynamic equalization factor by example of core SO164–02–4, section 2. The factor is created by the polynominal regression residuals normalized to the mid-section level. Multiplying the measured values with the equalization factor shifts the lowered susceptibility values near the section ends to more realistic levels. The internal variability is preserved though slightly amplified.

shrinkage of the sediment. Hence, the most reliable density and porosity measurements are to be done as soon as possible after core retrieval and opening.

Density and porosity measurements were taken on cores collected during the R/V SONNE cruise SO164. No radioactive source was available to conduct near-continuous density measurements during core logging by gamma-ray attenuation. Discrete measurement were made from samples extracted and analysed aboard ship.

Several 10 cm^3 syringes are plunged into the working half of the cores to collect samples for physical properties analysis. Sample volumes range between 4.5 cm^3 and 11.75 cm^3. The sampling interval for most cores is 20 cm. Cores with ample unused material are sampled at a higher resolution of 8 cm. Cores that have disturbed sedimentation stratigraphy or cannot be sampled regularly are sampled at intervals larger than 20 cm; for example, cores with broken up sediment sections within the core tube or hard turbidite sequences were sampled at intervals as great as 84 cm.

The masses of small aluminium trays (55 mm in diameter) are taken beforehand and inscribed on each tray; these range from 1.27 g to 1.33 g. Each wet sample is expunged from the syringe into a tray and any excess remaining in the syringe is removed using a metal spatula. The tray and sample are weighed, and the wet mass is recorded. Each tray is placed into an oven at 105°C for a minimum of 12 hours to dry. After the samples are completely dry, they are reweighted, and their dry mass is recorded. Samples from core SO164–17–2 are crushed and motared for subsequent carbonate analysis, while samples from all other cores are stored as they are.

Ship pitch and roll create additional forces on weights measured aboard; this movement results in weight measurements that are either greater or smaller than the measured mass. To adjust for ship movement, each sample is weighed on a sea going balance ("Seegangswaage", Geomar Technologie GmbH, Kiel). This device is tuned so that it takes the average of 400 instantaneous measurements, the maximum possible for this machine. This average eliminates a significant portion of the apparent mass change due to ship movements.

In addition, the software accompanying this device provides a plot of the instantaneous measurements used in its average. This plot is used subjectively to assign a ”Variation,” or deviation about the mean, to each weight measurement. Each day standards (5 g, 10 g, and 20 g) are weighed on the device to test for drift in the machine (Fig. 33). Also, weight measurements are only taken if ship movement is small, with the threshold of variation about the mean of less than 0.1 g.

The relative error of the density and porosity determinations owing to laboratory procedures is considered to be in the range of ±2.5 % (Boyce, 1976). Parallel determinations, which would help to constrain the reproducibility of the data, and a volumetric calibration of the syringes were not made. The precision of the balance is only half to a third of conventional laboratory equipment (±0.1 %). This strongly suggests that

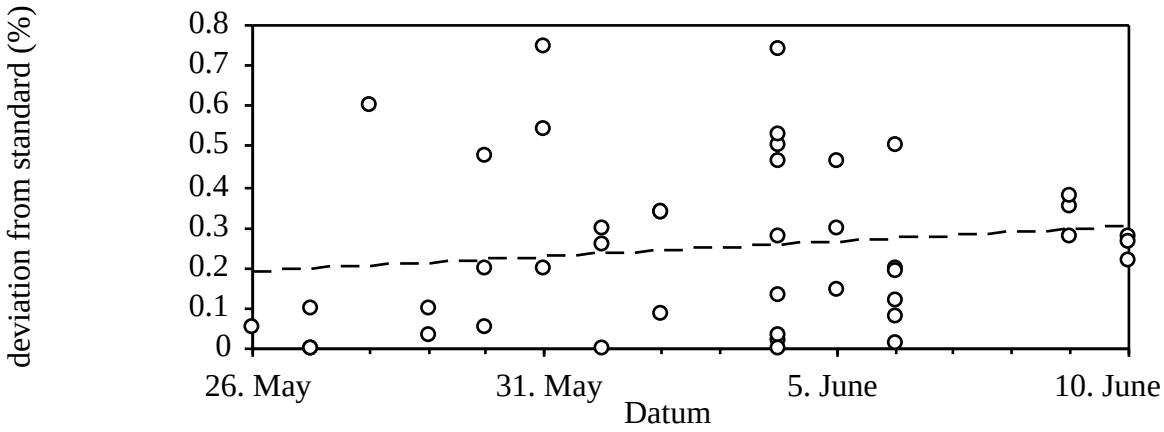

Fig. 33 Deviation of standard weight measurements given in percent of the assigned value vs. time of balance operation. The linear regression (dashed line) infers a negligible drift and an average deviation of the balance, i.e. precision, in the order of ±0.2 to 0.3 %.

our determinations are well within the limits of the above error estimate.

Data from the laboratory journal are transposed into Excel, and data entry is double checked. Physical properties are calculated from the masses and volumes recorded as such:

WBD = (WW – TW) / SV
DBD = (DW – TW – ((WW – DW) * (PWD – 1))) / SV
WC = (WW – DW) / (WW – TW) * 100
PO = (WW – DW) / SV * 100

WW : wet sample weight including aluminium tray (g)
DW : wet sample weight including aluminium tray (g)
TW : tray weight (g)
SV : sample volume (cm^3)
PWD : porewater density at laboratory conditions =1.024 g/cm^3
WC : water content (% of wet bulk sediment)
PO : porosity (volume %)
WBD : wet bulk density (g/cm^3)
DBD : dry bulk density, salinity corrected (g/cm^3)

5.3.10 Shipboard carbonate measurements

J. Schönfeld

Piston core SO164–17–2 was sampled continuously every 20 cm for carbonate measurements (Fig. 34). A total of 94 samples has been analyzed on board. Carbonate concentrations were determined using the "carbonate bomb" described by Müller and Gastner (1977). This device is designed to measure the CO_2 pressure that is generated after dissolving all carbonate in a sediment sample with HCl.

The CO_2 pressure is a function of the sample's carbonate content for each measure 750 mg of dry and ground-up sediment were taken and leached with HCl to dissolve the carbonate. As the volume of generated CO_2 depends on temperature and atmospheric pressure the measured values have to be corrected. The correction was done with a standard carbonate sample of 750 mg pure $CaCO_3$ at a 10 sample interval. The $CaCO_3$ weight percentages (see appendix) were calculated using equation:

wt.% $CaCO_3$ (spl) = $CaCO_3$ (man) x (100/$CaCO_3$ (man)) x (weight(std) / weight (spl))

man = value read from the manometer
spl = sample
std = standard

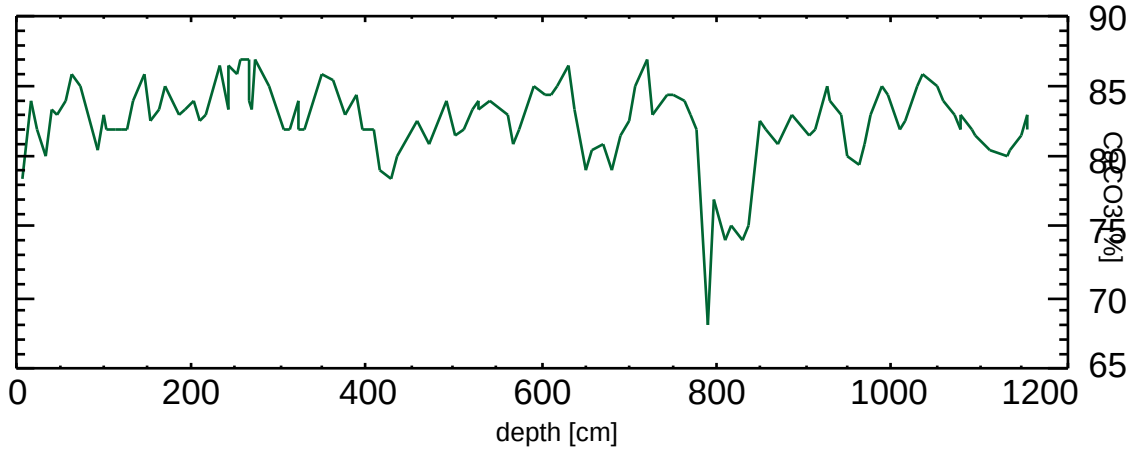

Fig. 34 The $CaCO_3$ content of the sediments of core SO164–17–2.

5.4 JAGO

5.4.1 Underwater navigation and communication

K. Hissmann

Our two men submersible JAGO (Fig. 35) is a completely autonomous underwater vehicle which means that once it is launched and released from the crane hook and lines there is no physical connection to the mothership. However, it is not completely left alone. In order to stay in contact with the submersible crew and to track JAGO´s movements when submerged we use two independent systems: An underwater telephone and a special underwater navigation system. The telephone consists of two identical units, one mounted on board the mothership and one inside JAGO. Each unit includes a hydrophone which functions both as receiver and transmitter (a „transceiver“), and an electronic unit that converts the ultrasonic signals into audible sound. It has a range of more than 1 kilometer, and under normal sea conditions communication is surprisingly clear, even from 400 m water depth. In heavy sea or if JAGO submerges into a canyon while the mothership stays above shallower water communication is less clear. It then requires a little bit of practise to understand what the voice from the deep is trying to tell the operator and everybody else who gathered around the telephone at the surface.

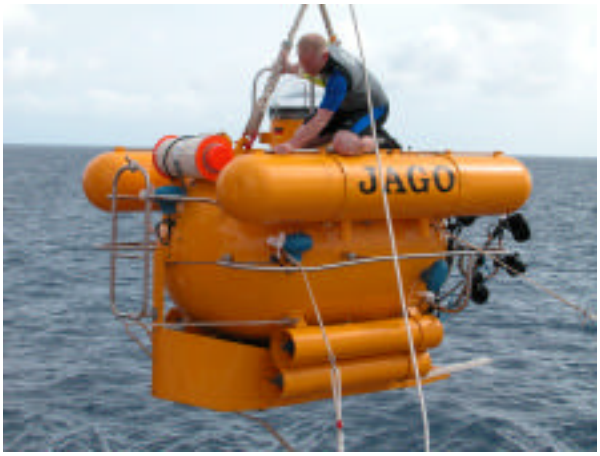

Fig. 35 The two men submersible JAGO.

It helps if the two people at both ends of the „line“ are familiar with each other – like Juergen, JAGO’s pilot, and myself, Karen. If communication gets really bad, people might find me in a strange position – leaning with one ear on the loudspeaker of the telephone unit and tuning the volume and gain controls with one hand while I slowly shout at Juergen through the microphone in my other hand. Since we know each other quite well, this „technique“ is usually successful, and I can translate Juergen’s answer to everybody waiting impatiently for news. „What do they see on the sea floor ?“ „How they are doing ?“ Well, often I cannot satisfy expectations and have to confess that I don’t know. Time runs differently under water and it has to be used most efficiently for the objectives of the dive. I usually state to the disappointed audience that we are not diving in order to chat with the surface and that we should restrict our short verbal contacts to the most important information, which is the actual diving depth and interesting positions. These I mark as special waypoints on JAGO’s dive track in the underwater navigation system. This system enables us to follow JAGO’s move close to the sea floor from the surface and to guide the submersible to certain positions we would like it to inspect (for the SO164 cruise see Tab. 11).

The following sounds simple but is in reality complicated hi-tech, manufactured in the USA: An acoustic sound source is mounted on JAGO; its signal is received by a special hydrophone below the ship’s keel. It gives us a bearing relative to the ship and JAGO’s straight line distance, and together with the known diving depth of JAGO these data are converted by a computer programme into an actual latitude/longitude position. Positions are graphically displayed on a PC monitor. The display is also a great help for the ship’s master (captain) and mates to keep the ship in range for communication and tracking if the ship drifts off; at any time they can see where the ship is in relation to JAGO. So JAGO effectively cannot get lost underwater. Juergen sometimes wishes that he was less controlled and observed by the operator on the surface when he steers the submersible through interesting terrain but shouldn’t stop since he still has to reach a certain waypoint!

5.4.2 Diving operation

J. Schauer

What is it like to drive a submersible?

Isn’t it the dream of many Scuba Divers to go deeper and stay longer in the sea?

Well, if you are the lucky one who drives a submersible this dream becomes reality.

A submersible is an underwater vehicle in which the crew is not exposed to the pressure and the coldness of the ocean, you don’t even get wet.

Our submersible Jago is a relatively small craft, it weighs three tons and it can take two people, a pilot and an observer, to a depth of 400 m.

In principle Jago functions exactly like one of the big Navy submarines. Underwater it works on batteries and has two big floatation tanks which makes it buoyant at the surface. When these tanks are flooded it is still not completely submerged, however, most of the positive buoyancy is lost. The descent is initialized when the air inside another buoyancy tank in JAGO’s keel is replaced by sea water. JAGO then becomes negatively buoyant and starts to sink. We observe the scenery through two large acrylic windows. One is a top dome which also functions as the hatch (entrance into the submersible), the other is a large acrylic glass bow window 70 centimeters in diameter at the front of Jago.

Floating at the surface is usually the most uncomfortable part of the dive. JAGO dances like a cork in the waves when the sea is rough. People sometimes get seasick inside under such conditions. The most exciting

part of the dive starts when JAGO submerges. Then the motions of the sea and the noise of breaking waves are left behind. Light slowly starts fading out, colours disappear, only a bluish dim light remains, similar to the dim light of a full moon night. JAGO slowly sinks down at 10 meters per minute. Every 10 minutes, however, the silence is harshly interrupted by a loud buzzer, the „deadman“. It has to be cancelled by pressing a button within 30 seconds; otherwise a ballast plate of 60 kg is automatically dropped and JAGO inevitably rises to the surface. This emergency device is set up so that in the unlikely case that both crew members lose consciousness at the same time the submersible will still rise to the surface and the crew can be rescued. Oxygen is constantly added to the air inside the pressure chamber and a filter absorbs the exhaled carbon dioxide, in a device called the “scrubber”. The breathing air is permanently analysed by an oxygen sensor. During descent I activate JAGO’s vertical echosounder which gives us an idea how far we are from the bottom. I reduce the descent rate about 10 m above the sea floor which slowly becomes visible below the keel. This very first view on the sea bed is always an exciting moment. It is like the first step into a completely unknown landscape. Then I send a short call to the surface ship: "JAGO has landed at 400 m, everthing ok! We are facing a slight current from the North, over.“ The answer through the underwater telephone follows promptly: „Ok JAGO, copy that, your course to the first target position is 240 degree, I repeat: 240 degrees, over.“

The water pressure now on each square centimeter of JAGO’s hull is 40 kg - that means the entire surface of our little steel-coated air bubble is exposed to more than 3.000 tons of pressure. It may sound like a lot of weight resting on JAGO, but we have 100 % confidence in JAGO’s 20 cm thick hull.

Then the first drops of condensation water on the cold walls appear. The first time I saw these drops was 22 years ago. On my very first dive I thought the submersible was leaking until I tasted them and found out that they were not salty. It is the exhaled breathing air of the two people inside the submersible condensing on the steel hull which is cooled down to the temperature of the ambient sea water.

The exciting exploration of the unknown landscape starts when we are hovering at about half a meter above the sea floor. JAGO is battery powered. I usually steer the submersible with a small control panel which has 5 switches, three for the thrusters at the stern, and two for the rotatable thrusters on the starboard and port sides. This arrangement of thrusters makes JAGO a highly and very precisely manoeuverable vehicle.

Where should we go now? Usually we follow the dive plan which was set up before the dive. The operator at the surface guides us to the positions which were chosen on the bathymetrical map and plotted into the underwater navigation system. We either follow the bottom contour or slowly cruise up or down slope. If it is not completely dark, like in the Indian Ocean at 100 or even 200 m, we can drive without using JAGO’s strong lights. In the bluish dim light we can search a larger distance in front, above, and below us that with the lights on. The lights are only switched on if we want to have a careful look on the sea floor and when we are using the colour video or still cameras. In this manner we move along the sometime very steep canyon slopes for several hours, some dives last more than 5 hours. We either look out through the front window or through the top dome which is a bit more uncomfortable since we cannot stand straight in the dome but have to bend a bit. From the top we have a wide overview on the under-water scenery.

Tab. 11 Details on submersible "JAGO" dives off Guadeloupe, June 2002, R/V SONNE SO164.

Dive No.	Location	Duration (min)	Touch down Lat/Long	Lift off Lat/Long	Min/Max. depth (m)	Pilot	Observer	Comments / Observations
784	GP, Marie-Gal. Banc Colombie SE	76			200/ 225	Schauer	Dullo	sandy plain, no structures, dive abundant
785	GP, Iles de Petite Terre	185	16°08.97N/ 61°10.01W	16°08.97N/ 61°10.11W	73/ 250	Schauer	Dullo	reef edge at 110 m, steep slope 250 m sandy, 120 m sclerosponges
786	GP, Iles de Petite Terre	197	16°08.94N/ 61°09.99W	16°08.97N/ 61°10.07W	81/ 140	Schauer	Freiwald	karstic slope with caves, sclerosponges in caves
787	GP, Marie-Gal. Banc Colombie NE	149	15°59.32N/ 61°24.16W	15°59.21N/ 61°24.20W	97/ 150	Schauer	Camoin	gentle carbonate slope, collection of carbonate crusts + soft sponges
Total: 4 dives		607 (10h)						

6. Sediment records from cruise SO164 relevant for paleoceanographic studies

J. Schönfeld, D. Nürnberg

During cruise SO164 with R/V SONNE, various valuable paleoceanographic records were recovered. Most important for the onboard procedures is the development of an initial stratigraphy. It provides supporting evidence to assess the quality of the sediment cores and helps to define the scheme for subsequent sampling and analyses. The stratigraphical approach primarily relied on both the magnetic susceptibility and the reflectivity (Lightness, L-value) records.

The basis for developing a chronostratigraphic model from the magnetic susceptibility and reflectivity records is the fact that the observed structures of both curves resemble those of the well-known global climatic record as revealed by the stacked isotope records (Imbrie et al., 1984; Martinson et al., 1987). Such downcore-patterns seen in our sediment cores are mainly caused by climatically controlled changes in the flux of riverine suspension or windblown dust into the ocean basins. During glacials, i.e. times of lowered sea level, estuaries or shallow shelf seas did not retain the fluvial suspension input, and let the discharge pass directly on the continental slopes and into the deep sea. The abundance of terrigenous material (i.e. magnetic minerals) is, thus, enhanced in glacial core sections. The higher aridity in Africa during glacial times and the concomittant stronger dust supply even amplifies the riverine-based effect in the Carribean region. The glacial intervals appear to be darker or more intense coloured and, hence, yield lower optical reflectivity values.

In the case that the sedimentary successions were entirely pelagic and undisturbed, the magnetic susceptibility and reflectivity records could be tied to the global climatic record. Turbidites create a pattern that adulterates the climatic signal. For example, terrigenous mud turbidites may create distinct positive excursions deviating largely from the ambient pelagic magnetic susceptibility signal. Instead, calcareous turbidites or foraminiferal sand layers induce exceptional low values. Once these odd data were removed from the records by defining their levels with the core descriptions, the original climatically induced signal emerged.

In the following, a few sediment records from different regions of the study area are presented, for which we established preliminary age models.

6.1 Columbia Basin

Piston core SO164–02–4 (15°18.29N, 72°47.05W) was recovered from the deep part of Beata Ridge within the Columbia Basin at 2985 m water depth. Core length is 8.37 m. The core shows a monotonous sequence of homogenous, bioturbated clayey sand to sandy clay with varying abundances of planktonic foraminifers. Pteropods appear throughout the entire sediment section providing evidence for an excellent carbonate preservation. Turbidites were not recognized. The magnetic susceptibility record exhibits distinct downcore variations (ca. 5 to 25 SI-units) which inversely correspond to the reflectivity variations (ca. 50 to 67 %). The preliminary correlation of the reflectivity record to the SPECMAP stacked isotope record (Imbrie et al., 1984) suggests that core SO164–02–4 presumably covers various glacial-interglacial cycles back to Marine Isotope Stage 13 (ca. 480 kyrs, Fig. 36). The according depth/age diagram suggests a low, but linear and continuous sedimentation of about 1.5 cm kyr^{-1}.

6.2 Windward Passage

Within the Windward Passage, two sediment records were recovered during cruise SO164. Piston core SO164–07–4 (21°19.46N, 74°08.77W) was taken from 2722 m water depth from an abyssal plain adjacant to the Bahamian island Inagua. Core recovery was 12.6 m. The core mainly consists of monotonous, bioturbated sandy clay. Pteropods are abundant throughout the entire core and prove excellent carbonate preservation. Turbidite sequences of graded clayey silt sequences are commonly intercalated, mostly with sharp bases. Also, intercalations of graded, clayey foraminiferal sand beds of varying thicknesses are present throughout the core. The magnetic susceptibility record shows low values of ca. 5 to 50 SI-units, and generally is anticorrelated to the reflectivity record. The reflectivity record reveals distinct downcore variations, with highest values within either the foraminiferal sands or the clayey silt turbidites. When removing the turbiditic sequences from the data record, we produce a typical magnetic susceptibility pattern, which resembles the global climate record with glacial and interglacial changes (Fig. 37).

Adjacant to core SO164–07–4, but from much shallower water depths (1704 m), we recovered a piston core from a submarine (volcanic?) plateau. Piston core SO164–19–2 (21°14.7N, 74°20.9W) shows a sediment recovery of 6.93 m. The uppermost ca. 2 m consist of a homogenous, medium to light creamy brown clayey foraminifer sand with abundant pteropods. Below, the facies changes into a soft and homogenous sandy clay lacking pteropods. Thin layers of turbiditic foraminiferal sand are commonly intercalated between ca. 2 m and 3.2 m core depth. From 3.2 m downcore, these thin foraminiferal turbidites are missing. Magnetic susceptibility values (5 to 25 SI-units) of core SO164–19–2 are even lower than at Site SO164–07–4 from the adjacant abyssal plain, nevertheless, the downcore variations compare to those of core SO164–07–4. The reflectivity record is anticorrelated to the magnetic susceptibility record, and exhibits distinct downcore variations resembling glacial-interglacial variations (Fig. 38).

The turbidite-corrected magnetic susceptibility records of both cores, SO164–07–4 from the abyssal plain and SO164–19–2 from the adjacant submarine plateau, exhibit resembling downcore variations, and allow the detailed inter-site correlation (Fig. 38). The close correspondance to the SPECMAP climate record

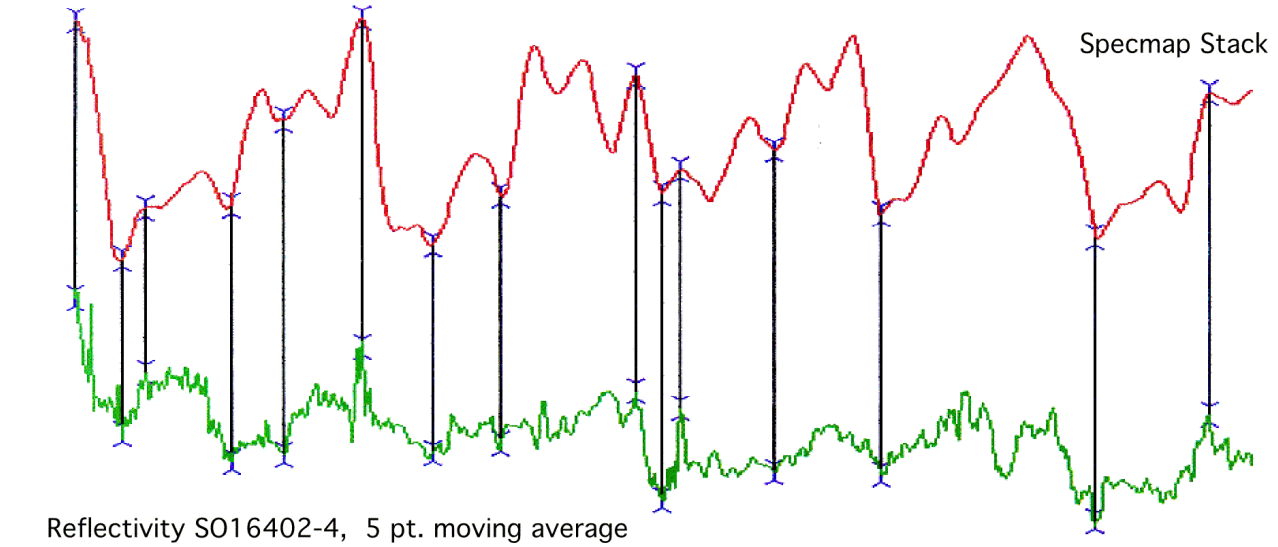

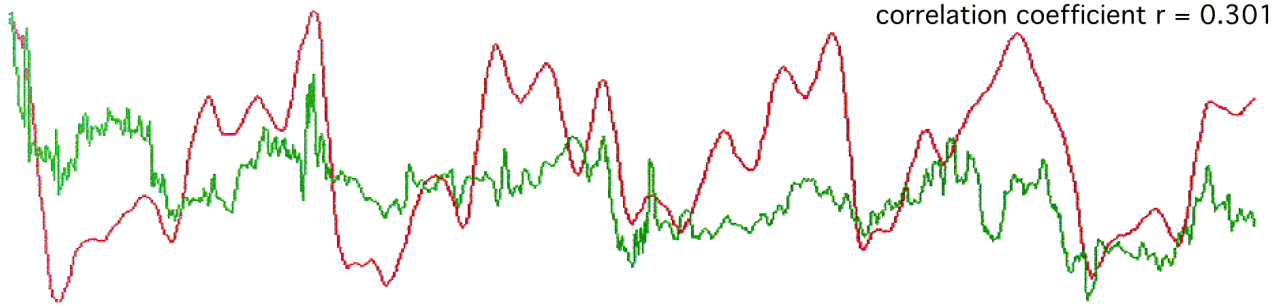

age model:

depth (cm)	time (ka)
1	0
40	20
62	30
141	66
180	89
239	122
279	152
326	181
379	238
409	250
426	257
458	297
522	343
668	434
731	482

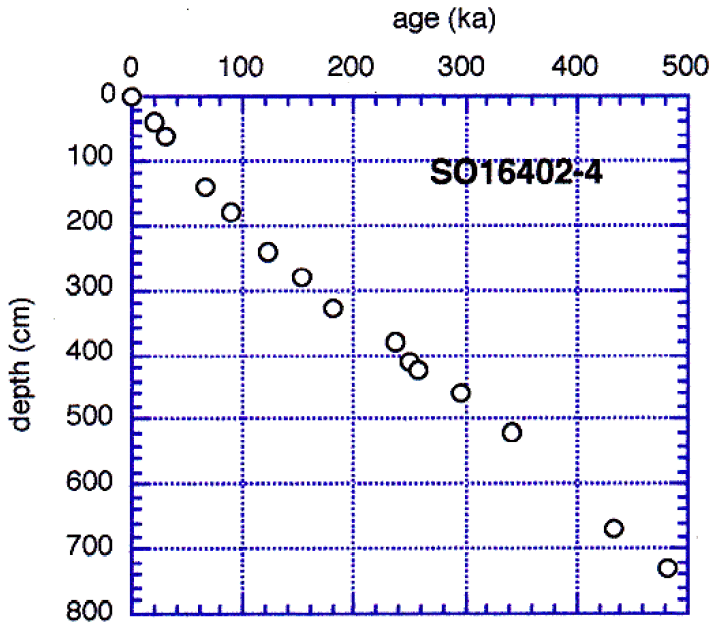

Fig. 36 Age model for core SO164–02–4. a) Reflectivity record vs. SPECMAP showing the tie points used for core correlation. b) Reflectivity record in comparison to the SPECMAP climate record of Imbrie et al. (1984). c) Age/depth diagram for core SO164–02–4.

allows to establish a tentative age model. According to this preliminary stratigraphical approach, the ca. 10 m long core SO164–07–4 from the abyssal plain covers several glacial/interglacial changes back to Marine Isotope Stages 9/10, while the shallow core SO164–19–2 probably reaches far beyond the Brunhes/Matuyama boundary. Sedimentation rates range between ca.

3 cm kyr^{-1} and 0.6 cm kyr^{-1} for cores SO164–07–4 and SO164–19–2, respectively.

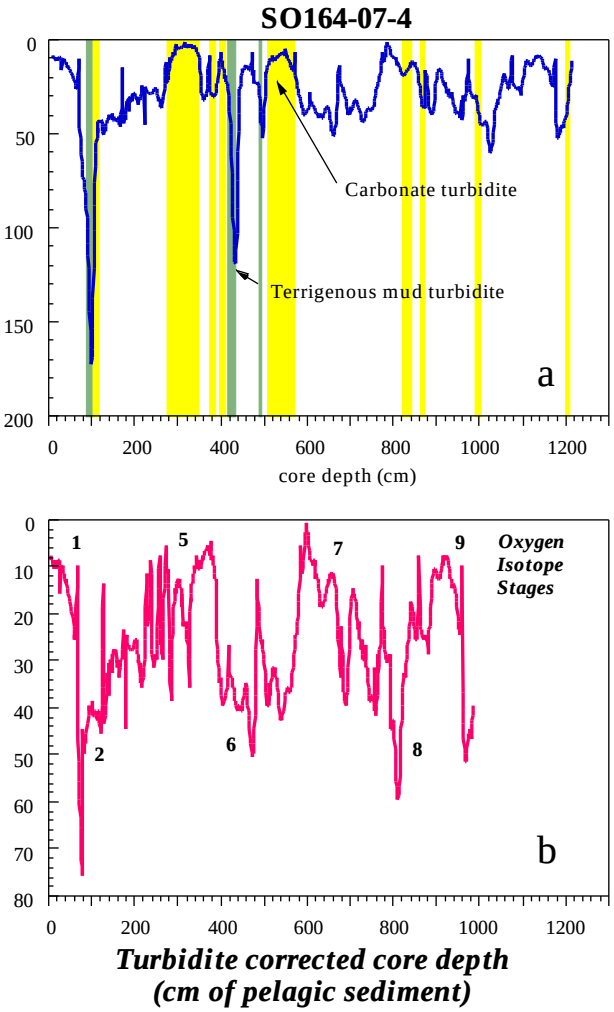

Fig. 37 a) Downcore magnetic susceptibility of core SO164–07–4. Carbonate turbidites and terrigenous mud turbidites are indicated by grey bars. b) Magnetic susceptibility record of core SO164–07–4 versus turbidite-corrected core depth.

6.3 Florida Straits

The piston core SO164–17–2 deployment recovered a 11.76 m long core. It shows a monotonous succession of strangly bioturbated silty clays. With the exception of a single, thin turbidite, no indications of erosion or redeposition were recognized. The magnetic susceptibility log and ist correlation to the Specmap stacked record (Imbrie et al., 1984) revealed that this core may go back in time until Marine Oxygen Isotope Stage 10, i.e. 341 ka. The average sedimentation rate should be in the order of 3.5 cm per thousand years. The uppermost two meters of the core was therefore routinely sampled in 2 cm intervals, and in 4 cm intervals below. Physical properties and carbonate content were determined in 10 cm intervals (Fig. 39).

Core recovery and basic sedimentological information from surface samples and sediment cores reveals that it is possible to describe the impact of the bottom-near current on sedimentary structures, composition and benthic biota. The long sediment core depicts most likely a continuous record. The last Glacial to Holocene environmental change will be revealed by applying a dense sampling scheme that keeps up with the low sedimentation rate.

6.4 Stratigraphic implications of calcareous nannoplankton

H. Kinkel

Smear slides made abord R/V SONNE were screened for biostratigraphic marker species of calcareous nannoplankton by using a transmittent and cross polarized light microscope, 1000x magnification. The cores SO164–02–4, –07–4, –17–2, and –19–2 were chosen for a first age determination. The standard calcareous nannoplankton zonation was used to identify the nannoplankton zones (Martini and Müller, 1986) including the most recent modifications by Young (1998). The preservation of calcareous nannofossils is good to excellent. The assemblages are very rich and show typical species from the equatorial Atlantic and Caribbean Sea.

SO164–02–4

The lowermost sample, 830 cm, showed small *Gephyrocapsa* as dominat species. *G. carribeanica* and *Helicoshaera inversa* were also found. *Pseudoemiliania lacunosa* was absent. Age: possibly NN20 (270 to 470 ka). The sample may be slightly older than the first occurrence of *E. huxleyi*, but this is almost impossible to assess with light microscopy. *H. inversa* appears just after the last occurrence of *P. lacunosa.*

SO164–07–4

The uppermost sample, 64cm, revealed *P. lacunosa*, *Discoaster brouweri*, and *Discoaster variabilis*. Age: appearently NN17 (2.2 to 2.4 ma). Pleistocene forms were also present. This indicates heavy reworking or winnowing. Sample 1010 cm showed *Discoaster pentaradiatus*, *Cyclococcolithus cristatus*, *Cyclococcolithus telesmus*, *Cyclococcolithus pelagicus* and *Helicoshaera macroporus*. Age: NN17 to NN18 (2.4 to 1.6 ma). Sample 1180cm revealed *D. pentaradiatus, P. lacunosa, D. brouweri*, and *Discoaster variabilis*. *R. pseudoumbillicus* and *S. abies* were missing. Age: NN16 to NN17 (3.4 to 2.2 ma).

SO164–17–2

The lowermost sample showed small *Gephyrocapsa* and possibly also *Emiliania huxleyi*. *P. lacunosa* was not recorded. Age: very likely NN21 (270 ka to present). First occurrence of *E. huxleyi* in this core is unclear, however, and needs further studies with the SEM.

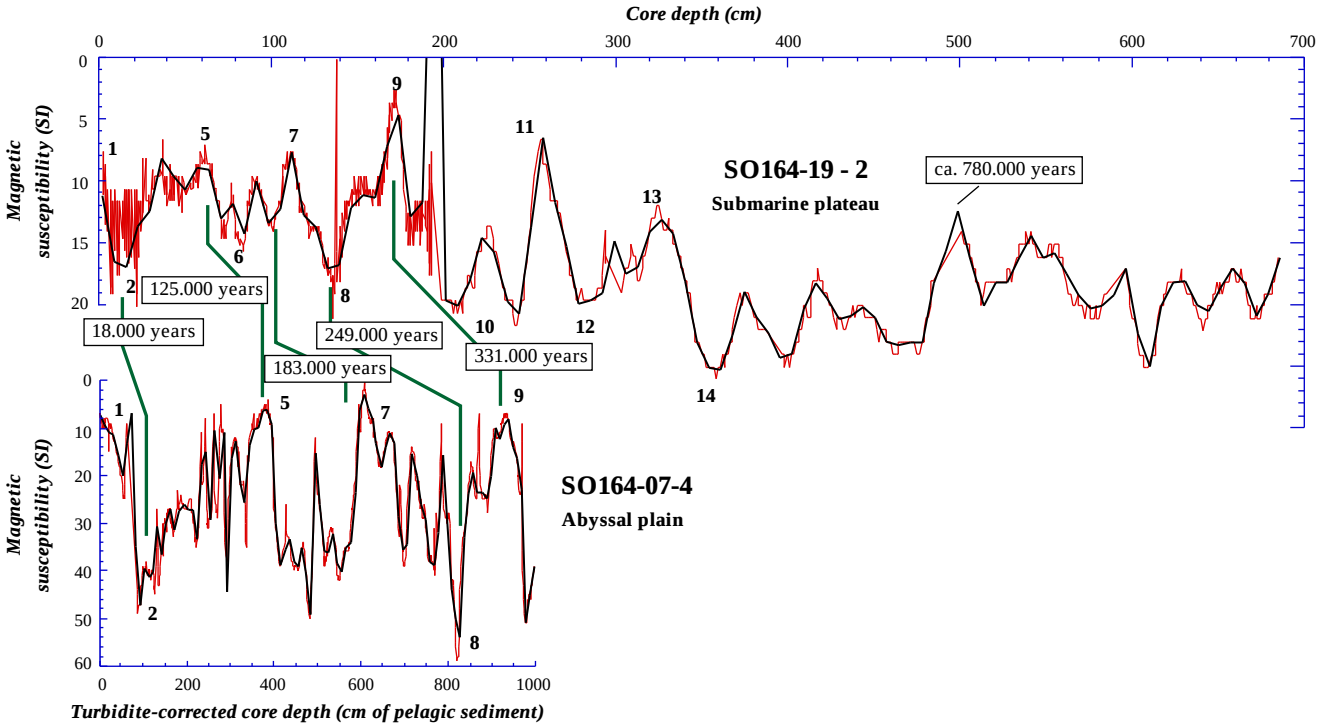

Fig. 38 Core-correlation between piston cores SO164–07–4 and SO164–19–2 based on the (turbidite-corrected) magnetic susceptibility records. Thin lines depict the original data. Thick lines indicate the smoothed records. Intersite-correlation is marked by thick tie lines. Marine Oxygen Stages (numbers) and age datums are indicated, based on our tentative stratigraphical approach.

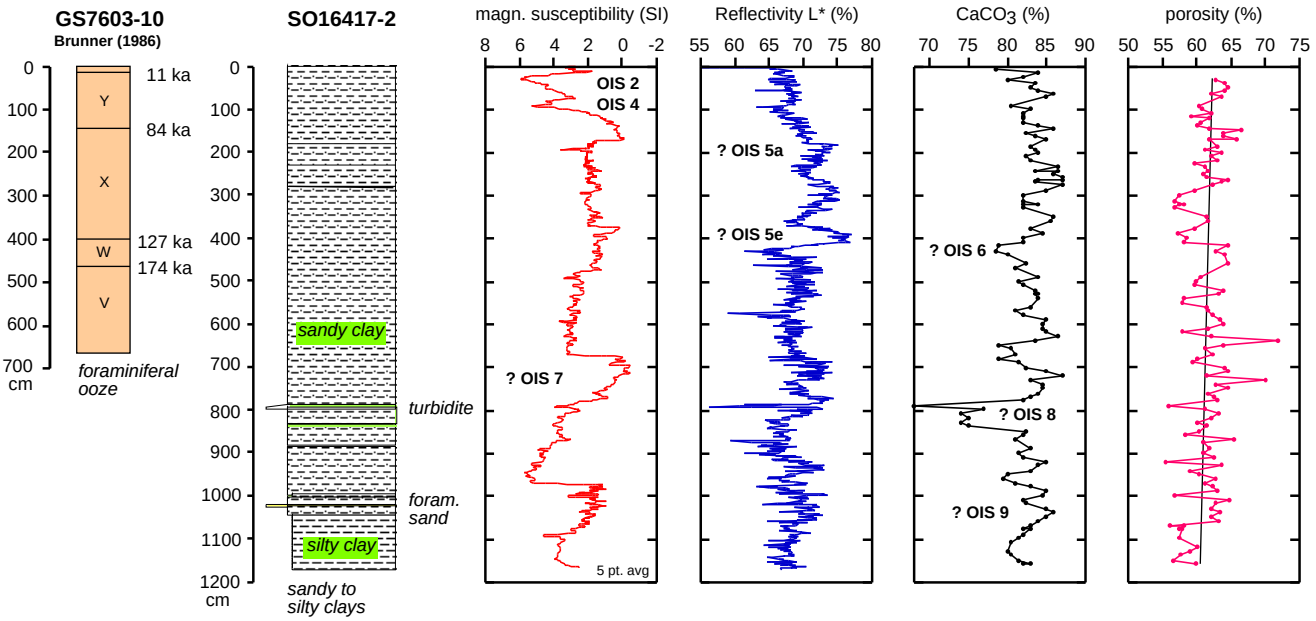

Fig. 39 Lithostratigraphy, magnetic susceptibility, reflectivity, carbonate content and porosity records of core SO164–17–2, southern Florida Straits. Core GS7603-10 (Brunner, 1986) from the same locality is given for comparison.

SO164–19–2

The uppermost sample at 20 cm showed a *Discoaster* rich assemblage similar to the assemblage ob-served in SO164–07–4, but Pleistocene species were present as well. This indicates most likely heavy reworking or winnowing.

6.5 Sedimentary facies distribution of drowned volcanic structures in the French Lesser Antilles: Banc Columbie, East of Marie Galante, and northern shelf off Martinique

W.-Chr. Dullo, A. Freiwald, G. Camoin, H. Westphal, T. Beck

The Banc Colombie is located 10 km east of Marie Galante. A 220 m deep channel separates both the volcanic island and the submerged bank. As most islands and submerged banks and shoals of the Lesser Antilles, also the Banc Columbie represents a drowned volcanic structure with a characteristic oval shaped outline and an extended plateau between 60 to 70 m water depth. Shallowest depths are found in the western area of the bank with 43 m, respectively.

During Sonne Cruise SO164 Leg 2, the Banc Colombie was one of the major sites to cover a broad scope of scientific topics:

1. Surveying the morphological features of a drowned tropical submerged bank which can be related to former sea level fluctuations and emergence periods.
2. Mapping the sedimentary environment with box corer (GKG) and, wherever possible, gravity corer (GC).
3. Collecting lithified carbonate crusts in order to understand microbially driven diagenetic processes.

Sampling strategy: Box corer (GKG) and gravity corer (GC)

The Banc Colombie was surveyed using the GKG with a total of 17 stations which were aligned along a N – S transect from the deeper water in the south of Banc Colombie to the shallow bank top (266 to 55 m water depths) and ending in deeper waters of the northern flank at 380 m water depth. A SW – NE transect from the bank top down the slope in NE direction (77 to 146 m water depths) completed the survey (Fig. 40). For comparative purposes, the sound between Marie Galante and Guadeloupe was sampled with 7 GKG stations (Fig. 41). The sedimentary facies of the shelf bank off northern Martinique was surveyed with ten GKGs, from 70 to 1350 m water depth, respectively (Tab. 12). Gravity cores cover the deeper area to the NE of Banc Colombie. One gravity core was taken on the northern toe of slope of Banc Colombie (30–2) at 383 m water depth, about 3.8 km off the bank margin. Three cores were taken in the north of Marie Galante in distal settings to Banc Colombie. Two closely spaced gravity cores (29–2 and 34–1) were taken at about 14 km off the bank margin in a NE direction at 829 and 836 m water depth, respectively. Core 48–3 represents a more open Atlantic setting with a distance to Banc Colombie of 50 km. However, recovery was always poor because of the large admixture of volcanoclastic components.

Tab. 12 Box corer station list (Lesser Antilles).

GKG-Station	Site	Latitude	Longitude	Depth [m]	Recovery [cm]
26-1	Guadeloupe shelf	16°11.490N	61°09.430W	32.1	22
28-1		16°28.300N	61°11.270W	993	14
29-1		16°05.160N	61°18.970W	829	25
30-1	Banc Colombie	16°01.754N	61°25.926W	380	35
32-1		15°57.51N	61°26.02W	73	20
33-1		15°58.01N	61°25.49W	55	10
33-2		15°58.00N	61°25.50W	55	15
37-1		15°54.14N	61°26.21W	226	10
38-1		15°55.46N	61°26.27W	185	8
39-1		15°55.61N	61°26.27W	178	----
39-2		15°55.60N	61°26.26W	179	poor
40-1		15°59.29N	61°24.40W	93	10
40-2		15°59.28N	61°24.41W	93	10
41-1		15°58.97N	61°24.43W	77	10
41-2		15°58.98N	61°24.43W	77	15
42-1		15°59.39N	61°63.91W	149	poor
43-1		15°59.23N	61°24.16W	117	8
43-2		15°59.24N	61°24.14W	118	poor
44-1		15°59.11N	61°24.28W	94	10
44-2		15°59.12N	61°24.28W	95	5
47-1	Guadeloupe sound	16°02.870N	61°11.800W	995	13
51-1	N Martinique	15°00.260N	60°56.070W	465	20
52-1		15°03.270N	60°58.930W	813	14
53-1		15°04.970N	60°04.980W	1328	45
54-1		14°59.070N	60°54.950W	80.2	12
54-2		14°59.070N	60°54.930W	80.2	10
55-3		14°55.120N	60°54.800W	343	12
57-1		15°00.310N	60°41.680W	1009	38

GKG-Station	Site	Latitude	Longitude	Depth [m]	Recovery [cm]
59-1		14°54.660N	60°52.040W	90	18
59-2		14°54.640N	60°52.040W	86.3	21
60-1		14°54.300N	60°52.030W	70.5	15

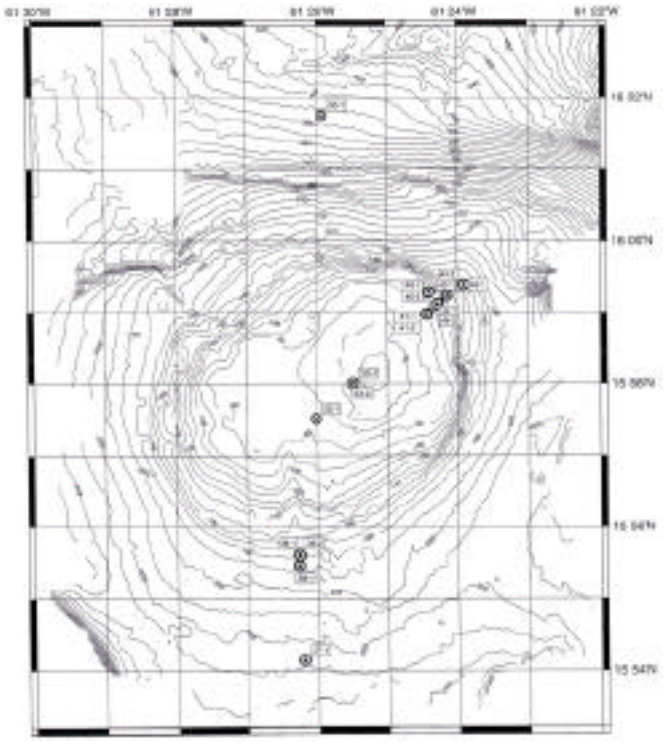

Fig. 40 Hydrosweep map of Banc Colombie, West of Marie Galante, generated during the SONNE cruise. Indicated are the GKG stations collected from the flat summit and adjacent flanks.

Sedimentary facies distribution

The GKGs were analysed for determining the sedimentary facies distribution and faunal composition.

Morphology of Banc Colombie

The submerged Banc Colombie is situated between the islands of Guadeloupe and Marie Galante. It extends from 16°00 N to 15°55.50 W and is oval shaped with its longest extension of 6.6 km in a NE – SW direction (Fig. 40). In NW – SE extension, the bank measures about 4 km. In analogy to other banks in this area, the origin of Banc Colombie is assumed to be volcanic. However, carbonate productivity overprinted the morphology of the bank.

The bank has a flat top in typically 70 to 80 m water depth. The NW part of the bank top reveals numerous elevated seabed structures that could be interpreted as drowned reefs. The top of Banc Colombie further shallows in the NE part, where the bank reaches water depths of less than 50 m. From the bank top, the bank slopes dip down to about 180 m where the slope dip decreases. Only to the E of the bank the slope then becomes steeper again towards the North Atlantic Basin. The slopes of Banc Colombie show a clear distinction between the northeastern windward and the southwestern leeward side, the latter being characterized by gentle slopes. The steepest slope is observed in the NE of the bank where water depth increases from 100 to 160 m within a distance of about 250 m. In the rest of the eastern part of the bank, the increase in water depth from 100 to 160 m extends over 500 m to 1 km, whereas in the W of the bank, up to 2.5 km are required for this depth increase. This difference in slope morphology reflects the dominant direction of winds (trade winds) causing offbank transport from the carbonate-producing bank.

Several submerged terraces are superimposed on the overall morphology of Banc Colombie. Around all of Banc Colombie, terraces were identified that occur in recurring water depths of 90 m and 120 to 130 m. Another characteristic terrace is found in 140 to 150 m water depth. These terraces are thought to represent old strand lines and reef structures formed during past sea-level stands (e.g. the 140 to 150 m terrace possibly during the Last Glacial Maximum, the 90 m terrace during Marine Isotopic Stage 3).

In addition, the sound between Guadeloupe and Marie Galante was also surveyed (Fig. 41). The approximately W – E tending sound deepens towards the Atlantic Basin with 550 m water depth in the eastern sector and 1100 m water depth in the western sector mapped. The slope of the Guadeloupe shelf is highly structured by a narrow and deeply incised canyon system. The slope off Marie Galante was not fully covered during the survey.

6.5.1. Banc Colombie

Preliminary analysis of the surface sediments demonstrates the existence of at least three major facies with a clear bathymetric and biologic zonation of autochthonous carbonate secreting organisms.

Platy coral and calcareous algal facies

This facies was found at the base of the shallow summit region of Banc Columbie at 55 m water depth. Shallower areas were not sampled in order to avoid a destructive impact to the thriving coral reef community. In GKG 33–1 and 33–2 platy scleractinian corals with *Montastrea* and *Agaricia* as the dominant genera were found (Fig. 42). These platy coral skeletons were cemented and thus stabilised by encrusting coralline algae. Dead coral skeletons are deeply excavated by boring sponges *(Cliona* spp.) whereas living corals are infested by endolithic cyanobacteria. The platy growth habit of the coral colonies is indicative for reduced irradiation at those depths for compensating the limited illumination for the phototrophic symbionts. The shaded parts of the platy coral substrate serves as

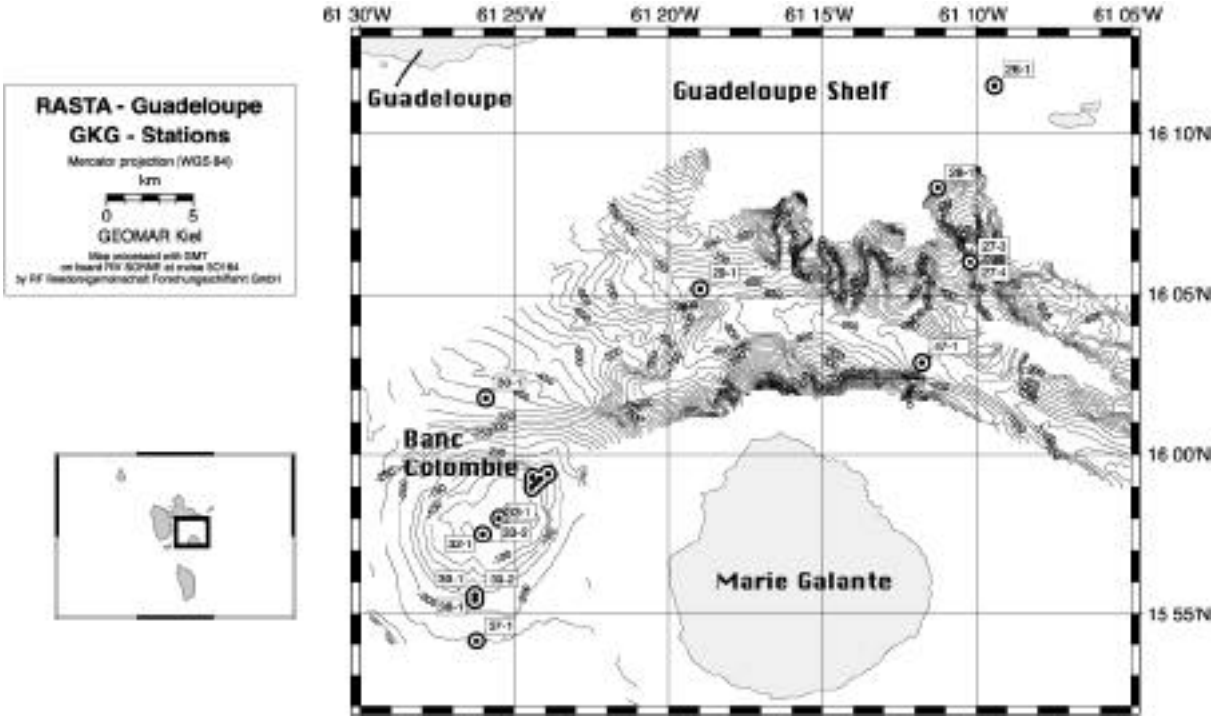

Fig. 41 The sound between Guadeloupe and Marie Galante with GKG stations indicated. Station 48-3 was taken just out of the shown area in South-east prolongation of the sound.

substrate for a diverse epibenthic sponge community, serpulids, vermetids, stylasterids, and foraminifers. A few solitary azooxanthellate *Thalamnophyllia cf. riisei* occur on the shaded undersides in shallower water GKGs but on the exposed sides in deeper water areas down to at least 226 m water depth. In places, the thalli of phaeophyte *Lobophora variegata* and the important sediment producing *Halimeda discoidea* are attached to dead exposed parts of the coral skeleton. If platy corals were not present, 20 to 25 cm-large coralline algal boulders were found (GKG 41–1 and 41–2). The concentric coralline algal laminae were grown around nuclei consisting of platy coral fragments. Towards greater water depth, this facies develops into rhodolith pavements admixed with free-lying bryozoans (GKG 43–1). In general the sediments are extremely coarse-grained and often form thin veneer above a Pleistocene cemented and karstified surface, presumably formed during the Last Glacial sea level lowstand at a period when Banc Colombie formed an island.

Foraminifer-mollusc facies

This facies is developed at the central southern slope of the Banc Colombie at least between 186 to 226 m water depth (GKG 37–1, 38–1). The transition to the shallower sedimentary facies was not covered by the GKGs available. The sediments generally are medium- to coarse-grained calcareous sands admixed with volcanoclastic pebbles. The shallower sample is predominantly a mollusc shell hash whereas the deeper sample displays a clear dominance of benthic agglutinated for aminifers (Fig. 43). The mollusc sands are mixed with imported coral and calcareous algal grains from the shallow facies. The bivalves contain recent deeper water associations but also the shallow water *Glycymeris* that may represent a Pleistocene low-stand indicator (Tab. 13). The shallower GKG 38–1 station (186 m) differs from the deeper GKG 37–1 station (226 m) in a more diverse gastropod and bivalve assemblage, a high amount of sand-dollar echinoid remains and lesser amounts of pteropods. Four species of azooxanthellate solitary corals were found in this facies (Tab. 13).

Foraminifer-pteropod facies

All sediments from water depths beyond 380 m consist of a bioturbated sandy foraminifer-pteropod facies often with dense colonisation by phoronids (GKG 30–1 and GKG 28–1, 29–1, 47–1 from the Guadeloupe sound). The calcareous sand is variably diluted by volcanoclastic sand (Fig. 44). Transported shallow water sedimentary particles are scarce thus indicating a reduced downslope mobilisation from the adjacent island shelves.

7.4.2 Northern Martinique shelf

An unnamed bank at the northern shelf off Martinique was surveyed with ten GKG stations from 70 to 1350 m water depth (Tab. 13). Except the shallow 70 to 90 m-water depth stations, all sediments sampled are highly diluted by volcanoclastic sand and gravel (Fig. 45). Two basic sedimentary facies are developed off Martinique.

Peyssonnellid algal framework facies

The thin and foliose peyssonnelid algae form a fragile and highly open-spaced skeletal framework that provides habitat for a diverse sponge community and for *Halimeda*. The associated molluscs show a very diverse portion of sponge-eating gastropods of the *Emarginula* group (Tab. 13). Zooxanthellate corals are sparsely distributed *(Madracis* sp.).

Volcanoclastic-foraminifer-pteropod facies

In water depths beyond 300 m, volcanoclastic sediments become dominant, but are admixed with both benthic and planktonic foraminifers, and pteropods Fig.46).

Tab.13 Preliminary faunal list of skeletal cnidaria and molluscs of selected samples.

		43-1	**37-1**	**38-1**	**30-1**	**40-1**	**44-1**	**47-1**	**57-1**	**54-1**
		117m	226m	186m	380m	93m	94m	995m	1013m	80m
Hydrocorallia	Stylaster roseus	X				X				X
Scleractinia	Caryophyllia ambrosia				X					
	Caryophyllia sp.			X						
	Deltocyathus calcar			X						
	Guynia annulata		X	X						
	Madracis sp.					X				
	Schizocyathus fissilis		X	X						
	1 gen. et sp. indet.				X					
Scaphopoda	Cadulus parvus						X			
	Dentalium didymum				X					
	Dentalium disparile		X	X						
	Dentalium sp.	X								
Gastropoda (p)	Atlanta sp.		X		X	X				
	Cavolina longirostris	X	X			X	X		X	
	Cavolina sp.	X	X		X			X		
	Clio pyramidata			X	X					
	Creseis aciculata							X	X	
	Creseis virgula						X	X		
	Cuvierina columnella		X		X			X	X	
	Diacria trispinosa	X	X		X			X		
	Peracle sp.							X	X	
	Styliola subula							X	X	
Gastropoda (b)	Aceton sp.	X								
	Acmaea sp.									X
	Addisonia lateralis									X
	Aemea sp.						X			
	Alvanica acuticostata							X		
	Arene sp.		X							
	Astraea caelata	X								
	Astraea sp.					X				
	Atys carbaea									
	Bellaspira pentagonalis			X						
	Caecum sp.					X	X			
	Cerithiopsis sp.		X	X	X	X	X			X
	Conus sp.	X		X						
	Cyclostrema amabile						X			
	Cytiscus sp.									X
	Diodora sp. A	X					X			X
	Diodora sp. B									

		43-1	37-1	38-1	30-1	40-1	44-1	47-1	57-1	54-1
		117m	226m	186m	380m	93m	94m	995m	1013m	80m
Gastropoda (b)	Diodora viridula					X				
	Emarginula sp.					X				X
	Emarginula pamila									X
	Emarginula sicula						X			X
	Emarginula tuberculosa									X
	Emarginula tumidula					X				
	Euchelus guttarosa									X
	Eulimidae indet.					X				
	Ficus atlanticus			X						
	Glyphostoma gratula				X					
	Granulina sp.						X			X
	Hyalina albolineata					X	X			X
	Hyalina sp.									X
	Janthina janthina				X					
	Litiopa melanostoma							X		
	Maginella sp.					X				
	Mangelia sp.						X			X
	Mathilda sp.									X
	Mitra sp.									X
	Mitrella sp.									X
	Naticidae indet				X					
	Nassarius sp.	X		X						
	Nesta atlantica						X			
	Olivella sp.	X	X	X	X					
	Opalia pumillo						X			
	Parviturbo comptus									X
	Pedicularia decussata	X								
	Polyspira sp.			X						
	Polystira sp.					X				
	Rissoina sp.						X			X
	Scaphander watsoni				X					
	Scissurella cingulata					X	X			
	Scissurella crispata						X			
	Siliquaria squamata	X				X				X
	Skenea sp.						X	X		
	Solariella infundibulum							X		
	Solariella cf. lamellosa				X					
	Solariella lubrica				X					
	Solariorbis sp.		X							
	Strombiformis auricinctus									X
	Strombiformis bilineatus						X			
	Tricolia sp.									X
	Triphora elvirae						X			X
	Triphora sp.									X
	Turbo sp.					X	X			X
	Turbonilla sp.					X				
	Vitrinella sp.									X
	Xenophora sp.	X								
Gastropoda (b)	Zeidora cf. Naufraga						X			
Bivalvia	Arca sp.					X	X			X
	Barbatia sp.					X				X

		43-1	**37-1**	**38-1**	**30-1**	**40-1**	**44-1**	**47-1**	**57-1**	**54-1**
		117m	226m	186m	380m	93m	94m	995m	1013m	80m
Bivalvia	Bathyarca inaequalis							X		
	Cardiomya sp.									X
	Chama sp.	X				X				
	Corbula contracta					X				
	Crenella sp.									X
	Cuspidaria jeffreysi			X						
	Dacrydium sp.									X
	Gastrochaena hians					X				
	Glycymeris sp.		X	X						
	Lima sp.						X			
	Limatula setifera		X	X				X		X
	Limea bronniani	X				X				X
	Limopsis anthillensis						X			X
	Limopsis sp.		X	X				X		
	Lucinoma sp.			X						
	Myonera sp.			X						
	Nucula sp.							X		
	Nuculana sp.		X							
	Pecten sp.	X								X
	Plectodon granulatus			X						
	Poromya rostrata		X							
	Poromya sp.	X								
	Pseudamussium sp.			X						
	Spondylus sp.	X								
	Verticordia fischeriana		X	X						
	Verticordia ornata		X	X		X	X			
	Verticordia sp.		X							
	Yoldia sp.		X							

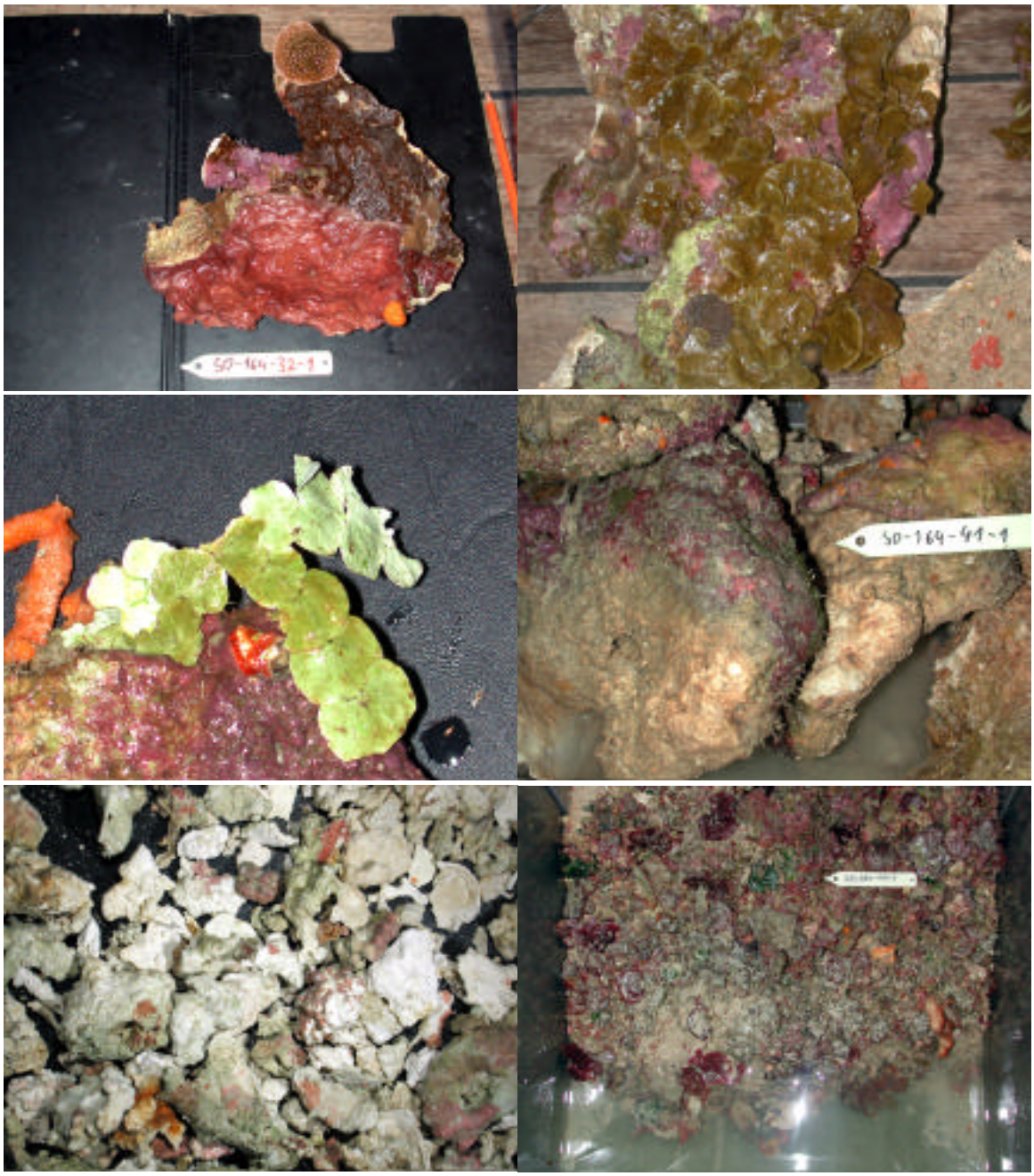

Fig. 42 Platy coral and calcareous algal facies (55 to 95 m water depth): Living platy coral assemblage (upper left). Platy corals overgrown by crustose coralline algae, and *Lobophora variegata* (upper right). Coralline algal boulder with living *Halimeda* (central left). Accumulation of coralline algal boulders consisting of concentric algal encrustations (central right). Rhodolith and calcareous arenites (lower left). Foliose pessonnelid algae and sponges (lower right).

Fig. 43 Foraminifer-mollusc facies: The 2 mm-sieve fraction shows the marked shallower mollusc-dominated (right) and the deeper foraminifer-dominated (left) sedimentary compositional styles of this mid-depth facies

Fig. 44 The 2.5 mm-sieve fraction of the foraminifer-pteropod facies represents the deepest sedimentary facies around Banc Colombie and is also developed in the Guadeloupe Sound.

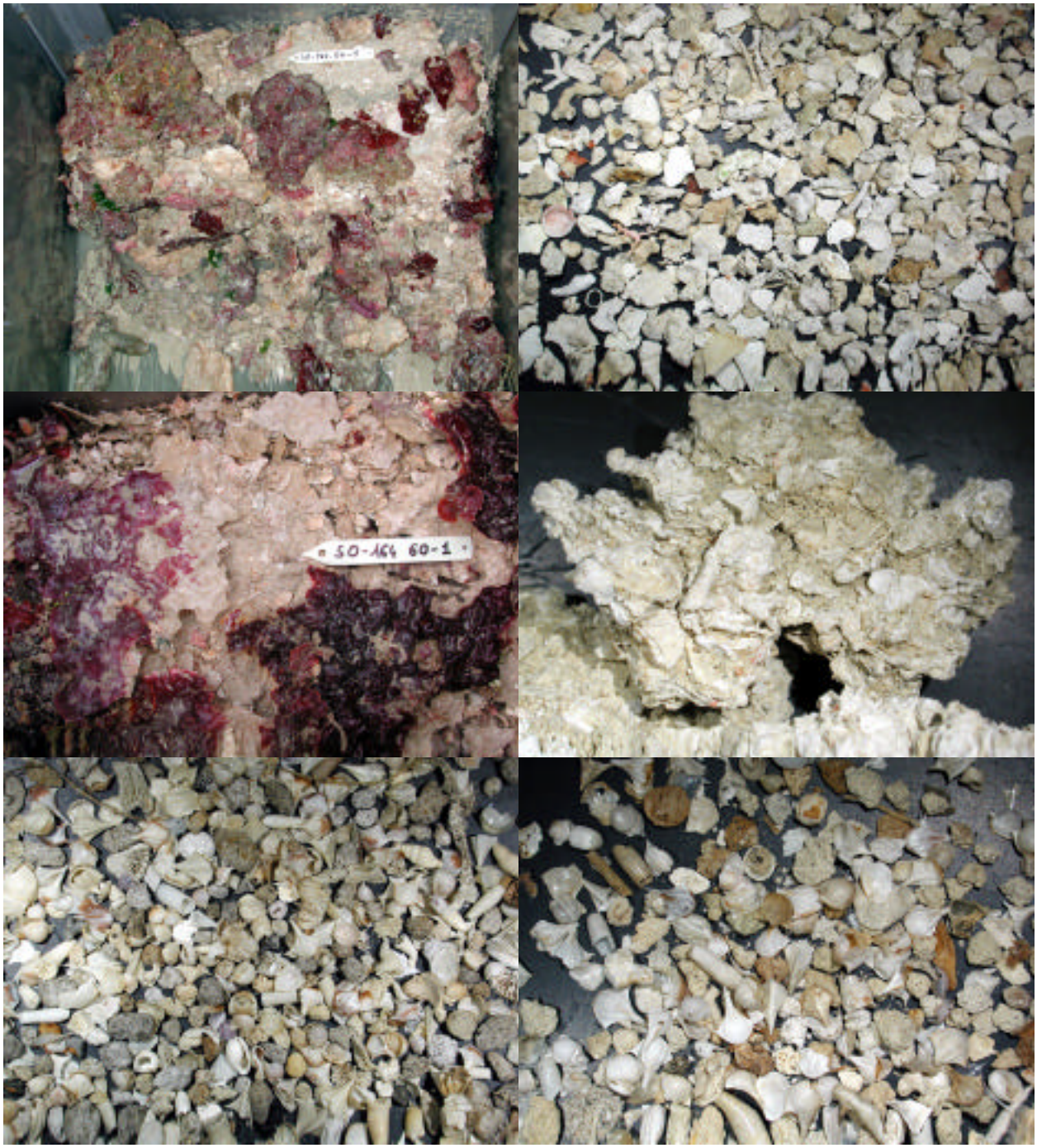

Fig. 45 Sediments off northern Martinique: Foliose framework of peyssonnelid algae (upper left) and the 2.5 mm-sieve fraction (upper right) rich in abraded coralline algal and *Halimeda* fragments (GKG 51–1, 80 m depth). At 70 m water depth, the foliose framework becomes thicker and more lithified (central images of GKG 60–1). The deep-water volcanoclastic-foraminifer-pteropod sands (2.5 mm sieve-fraction) dominate in water depths beyond 300 m (lower left: GKG 52–1, 810 m; lower right: GKG 55–3, 343 m).

7. Acknowledgements

Cruise SO164 was funded by the German Ministry of Education and Research (BMBF) under project No. 03G0164 to GEOMAR within the continued support for marine geosciences with the research vessel SONNE. Project review and scheduling of the SONNE Cruise 164 was handled efficiently by the Projektträger PTJ Forschungszentrum Jülich GmbH, Aussenstelle Rostock-Warnemünde. On behalf of all participants we wish to thank the agency and staff for their support.

The Reedereigemeinschaft Forschungsschifffahrt, RF Bremen, provided technical support on the vessel in order to accommodate the variety of technical, electronic, and navigational challenges required for the seagoing operations. We warmly thank master Hartmut Andresen and his crew for their hospitality and excellent support in all work done, in particular when difficulties arose or unforseen maintenance had to be done. We also acknowledge the splendid working atmosphere throughout the entire journey that greatly promoted the success of our mission. The submersible team Karen Hissmann and Jürgen Schauer provided an outstanding service. They always showed great enthusiasm although sea surface conditions were not calm at all. Their support is greatly acknowledged.

We thank the Governments of Barbados, Bahamas, Colombia, Dominican Republic, France, Jamaica, Panama, The Ne-therlands, United States of America, and Venezuela (in alphabetical order) for granting permission to work within their exclusive economic zones and territorial waters. We gratefully acknowledge the advice and continuous support of Jür-gen Lang and Rolf-Dieter Preyer, Auswärtiges Amt Berlin, in this matter. Alexander Barthold and Axel Hein, Bogotá, Margit Besser, Caracas, Hermann-Josef Hermanns, Nassau, Luis Fernando Lanzziano, Bonn, E. Rost, Paris, Monica de Salazar, Port of Spain, and Katharina Wilhelm, Panama, facilitated an efficient communication with the concerned authorities and gave auxiliary advice for which we thank them.

Scientific cooperation and cruise preparation largely benefited by the input of and encouragement of Hernán Pérez Nieto, Caracas, Gilbert Camoin, Nouvelle Caledonie, Jean Lynch-Stieglitz, New York, Bernhard Winters, Hamburg, and Rainer Zahn, Barcelona. Technical advice and loans of equipment were provided by Gerhard Bohrmann, John Reijmer, Bettina Domeyer, and Klaus von Broeckel, Kiel, Helmut Kawohl, Uetze, Hermann-Rudolf Kudrass and Rainer Goergens, Hannover, Sergej Neufeld and Brigitte Salomon, Kiel, and Götz Ruhland, Bremen. Their help is gratefully acknowledged.

8. References

Alley, R.B., and MacAyeal, D.R. (1994): Ice-rafted debris associated with binge/ purge oscillations of the Laurentide ice sheet. Paleoceanography 9, 503-511.

Alley, R.B., Meese, D.A., Shuman, C.A., Gow, A.J., Taylor, K.C., Grootes, P.M., White, J.W.C., Ram, M., Waddington, E.D., Mayewski, P.A., and Zielinski, G.A. (1993): Aprupt increase in Greenland snow accumulation at the end of the Younger Dryas event. Nature 362, 527-529.

Bard, E., Hamelin, B., Arnold, M., Montaggioni, L.F., Cabioch, G., Faure, G., and Rougerie, F. (1996): Deglacial sea level record from Tahiti corals and the timing of global meltwater discharge. Nature 382, 241-244.

Bard, E., Hamelin, B., Fairbanks, R.G., and Zinder, A. (1990): Calibration of the ^{14}C timescale over the past 30.000 years using mass spectrometric U/Th ages from Barbados corals. Nature 345, 405-410.

Bard, E., Rostek, F., and Sonzogni, C. (1997): Interhemispheric synchrony of the last deglaciation inferred from alkenane palaeothermometry. Nature 385, 707-710.

Bard, E., Rostek, F., Turon, J.-L., and Gendreau, S. (2000): Hydrological impact of Heinrich Events in the subtropical northeast Atlantic. Science 289, 1321-1324.

Barlow, R.G., Cummings, D.G, and Gibb, S.W. (1997): Improved resolution of mono- and divinyl chlorophylls a and b and zeaxanthin and lutein in phytoplankton extracts using reverse phase C-8 HPLC. Marine Ecology Progress Series 161, 303-307.

Beck, J.W., Edwards, R.L., Ito, E., Taylor, F.W., Recy, J., Rougerie, F., Joannot, P., and Henin, C. (1992): Sea surface temperature from coral skeletal Strontium/Calcium ratios. Science 257, 644-647.

Beck, J.W., Recy, J., Taylor, F., Edwards, R.L., and Cabioch, G. (1997): Abrupt changes in early Holocene tropical sea surface temperatures derived from coral records. Nature 385, 705-707.

Bertram, M.A., and Cowen, J.P. (1999): Temporal variations in the deep-water colonization rates of small benthic foraminifera: the results of an experiment on Cross Seamount. Deep-Sea Res. 1 (46), 1021-1049.

Blum, P. (1997): Physical properties handbook: a guide to the shipboard measurement of physical properties of deep-sea cores. ODP Technical Note 26. Online available at http://www.odp.tamu.edu/publications/tnotes/tn26/index.htm.

Blunier, T., Chappellaz, J., Schwander, J., Dällenbach, A., Stauffer, B., Stocker, T.F., Raynaud, D., Jouzel, J., Clausen, H.B., C.U., H., and Johnson, S.J. (1998): Asynchrony of Antarctic and Greenland climate change during the last glacial period. Nature 391, 739-743.

Bond, G., Broecker, W. S., Johnsen, S., McManus, J., Labeyrie, L., Jouzel, J., and Bonani, G. (1993): Correlations between climate records from North Atlantic sediments and Greenland ice. Nature 365, 143–147.

Boyce, R.E. (1976): Definitions and Laboratory techniques of compressional sound velocity parameters and wet-water content, wet bulk density, and porosity parameters by gravimetric and gamma ray attenuation techniques. Initial Reports DSDP 33, 931-958.

Boyle, E. A., and Keigwin, L. D. (1987): North Atlantic Thermohaline Circulation during the past 200,000 years linked to high-laditude surface temperature. Nature 330, 35-40.

Brachert, T.C., and Dullo, W.-Chr. (2000): Shallow burial diagenesis of skeletal carbonates: selective loss of aragonite shell material (Miocene to Recent, Queensland Plateau and Queensland Trough, NE Australia) – implications for shallow cool-water carbontes. Sedim. Geol. 136, 169-187.

Braithwaite, C.J.R., Montaggioni, L.F., Camoin, G.F., Dalmasso, H., and Dullo, W.-Chr. (2000): The origins and development of Holocene reefs: a revisited model based on boreholes in the Seychelles, Western Indian Ocean. Intern. Journal Earth Sci. Geologische Rundschau 89, 431-445.

Brassell, S.C., Eglinton, G., Marlowe, I.T., Pflaumann, U., and Sarnthein, M. (1986): Molecular stratigraphy: a new tool for climatic assessment. Nature 320, 129-133.

Broecker, W.S., and Denton, G.H. (1989): The role of ocean-atmosphere reorganizations in glacial cycles. Geochim. Cosmochim. Acta 53, 2465-2501.

Broecker, W.S., and Denton, G.H. (1990): What drives glacial cycles? Scientific American 262, 49-56.

Broecker, W.S., Peteet, D.M., and Rind, D. (1985): Does the ocean-atmosphere system have more than one stable mode of operation? Nature 315, 21-26.

Brunner, C.A. (1986): Deposition of a muddy sediment drift in the southern Straits of Florida during the late Quarternary. Mar. Geol., 69: 235-249.

Bryden, H.L., and Kinder, T.H. (1991): Recent progress in strait dynamics. Rev. Geophys., Suppl., (U.S. Nat. Rep. Intern. Union Geodesy Geophys. 1987-1990), 617-631.

Busalacchi, A.J., and J. Picaut (1983): Seasonal variability from a model of the tropical Atlantic Ocean. J. Phys. Ocean. 13, 1564-1588.

Cane, M. A., and Molnar, P. (2001): Closing of the Indonesian seaway as a precursor to east African aridification around 3-4 million years ago. Nature 411, 157-162.

Chapman, M.R., and Shackleton, N.J. (1998): What level of resolution is attainable in a deep-sea core? Results of a spectrophotometer study. Palaeoceanography 13, 311-315.

CLIMAP Project Members (1981): Seasonal reconstructions of the Earth's surface at the last glacial maximum. Geological Society of America Map Chart series MC-36.

Cofer-Shabica, N., and Peterson, L. (1986): Caribbean carbon isotope record for the last 300.000 years. Geol. Soc. Am. Abstr. with programs 18, 567.

Colonna, M., Casanova, J., Dullo, W.-Chr., and Camoin, G. (1996): Sea level changes and $\delta^{18}O$ record for the past 34.000 years from Mayotte reef, Indian Ocean. Quaternary Research 46, 335-339.

Conte, M. H., Thompson, A., Lesly, D., and Harris, R. P. (1998): Genetic and physiological influences on the alkenone/alkenoate versus growth temperature relationship in Emiliania huxleyi and Gephyrocapsa oceanica. Geochim. Cosmochim. Acta 62, 51–68.

Curry, W. B., Duplessy, J. C., Labeyrie, L. D., and Shackleton, N. J. (1988): Changes in the distribution of $\delta^{13}C$ of deep water CO_2 between the last glacial and the Holocene. Paleoceanography 3, 317-341.

Curry, W.B., and Oppo, D.W. (1997): Synchronous, high-frequency oscillations in tropical sea-surface temperatures and North Atlantic deep water production during the last glacial cycle. Paleoceanography 12 (1), 1-14.

De Menocal, P.B., Oppo, D.W., Fairbanks, R.G., and Prell, W.L. (1992): Pleistocene $\delta^{13}C$ variability of North Atlantic Intermediate Water. Paleoceanography 7, 229-250.

Driscoll, N.W., and Haug, G.H. (1998): A short circuit in thermohaline circulation: a cause for Northern Hemisphere glaciation? Science 282, 436-438.

Dullo, W.- Chr., Moussavian E., and Brachert T.C. (1990): The foralgal crust facies of the deeper forereefs in the Red Sea: A deep diving survey by submersible. Géobios 23 (3), 261- 281.

Dullo, W.-Chr., Camoin, G.F., Blomeier, D. Colonna, M., Eisenhauer, A., Faure, G., Casanova, J., and Thomassin, B.A. (1998): Morphology and sediments of the foreslopes of Mayotte, Comoro Islands: Direct observations from submersible. In: Camoin, G., Bergerson, D. and Davies, P.: Carbonate Platforms of the Indo Pacific Region. In: Camoin, G.F. & Davies, P.J. (eds): Reefs and carbonate platforms of the Pacific and Indian Ocean.- IAS Spec. Publ. 25, 219-236.

Duplessy, J.-C., Bard, E., Labeyrie, L., Duprat,J., and Moyes, J. (1993): Oxygen isotope records and salinity changes in the northeastern Atlantic ocean during the last 18.000 years. Paleoceanography 8, 341-350.

Duplessy, J.-C., Shackleton, N. J., Fairbanks, R. G., Labeyrie, L. D., Oppo, D., and Kallel, N. (1988): Deepwater source variations during the last climatic cycle and their impact on the global deepwater circulation. Paleoceanography 3, 317-341.

Eisenhauer, A., Wasserburg, G.J., Chen, J.H., Bonani, G., Collins, L.B., Zhu, Z.R., and Wyrwoll, K.H. (1993): Holocene sea-level determination relative to the Australian continent: U/Th (TIMS) and ^{14}C (AMS) dating of coral cores from the Abrolhos Islands. Earth Planet. Sci. Lett. 114, 529-547.

Elliot, M., Labeyrie, L., and Duplessy, J.-C. (2002): Changes in North Atlantic Deep-Water formation associated with the Dansgaard-Oeschger temperature oscillations (10-60 ka). Quat. Sci. Rev. 21, 1153-1163.

Fairbanks, R.F. (1989): A 17,000-year glacio-eustatic sea levle record: influence of glacial melting rates on the younger Dryas event and deep-ocean circulation. Nature, 342, 637-642.

Fairbanks, R.G., Evans, M.N., Rubenstone, J.L., Motlock, R.A., Broad, K., Moore, M.D., and Charles, C.D. (1997): Evaluating climate indices and their geochemical proxies measured in corals. Coral Reefs 16, 93-100.

Faugères, J.-C., Gonthier, E., and Stow, D.A.V. (1984): Contourite drift molded by deep Mediterranean outflow. Geology 12, 296-300.

Froehlich, J.P., Lakatta, E.G., Beard, E., Spurgeon, H.A., Weisfeldt, M.L., Gerstenblith, G. (1978): Studies of sarcoplasmic reticulum function and contraction duration in young adult and aged rat myocardium. J Mol Cell Cardiol 10, 427-438.

Ganopolski, A., and Rahmstorf, S. (2001): Rapid changes of glacial climate simulated in a coupled climate model. Nature 409 (6817), 153-158.

Ganopolski, A., Rahmstorf, S., Petoukhov, V., and Claussen, M. (1998): Simulation of modern and glacial climates with a coupled global model of intermediate complexity. Nature 391, 351-356.

Gordon, A.L. (1967): Circulation of the Caribbean Sea. Journal of Geophysical Research 72, 6207-6223.

Grammer, G.M., and Ginsburg, R.N. (1992): Highstand vs. lowstand deposition on carbonate platform margins: Insight from quaternary foreslopes in the Bahamas. Marine Geology 103, 125-136.

Grossmann, E. E., Ill, C. H. F., and Richmond, B. M. (1998): The Holocene sea-level highstand in the equatorial Pacific: analysis of the insular paleosea-level database. Coral Reefs 17, 309-327.

Haddad, G. A., and Droxler, A. W. (1996): Metastable $CaCO_3$ dissolution at intermediate water depths of the Caribbean and western North Atlantic: Implications for intermediate water circulation during the past 200,000 years. Paleoceanography 11, 701– 716.

Hall, M. M., and Bryden, H. L. (1982): Direct estimates and mechanisms of ocean heat transport. Deep-Sea Res. 29, 339-359.

Hanebuth, T., Stattegger, K., and Grootes, P. M. (2000): Rapid flooding of the Sunda shelf: A late-glacial sea-level record. Science 288, 1033-1035.

Hastings, D. W., Russell, A. D., and Emerson, S. R. (1998): Foraminiferal magnesium in *G. sacculifer* as a paleotemperature proxy in the equatorial Atlantic and Caribbean surface oceans, Paleoceanography 13 (2), 161-169.

Heiss, G.A., and Dullo, W.-Chr. (1997): Stable isotope record from recent and fossil *Porites* sp. in the nothern Red Sea. In: Poll, K, and Strauch, F. (Eds.): Contributions to coral research and museum efforts: Commemorative volume for the 60th birthday of Prof. Dr. Klemens Oekentorp. Coral Research Bulletin 5, 161-169.

Hernandez-Guerra, A., and Joyce, T. (2000): Water masses and circulation in the surface layer of the Caribbean at 66°W. Geophysical Research Letters 27 (21), 3497-3500.

Hinrichsen, H.-H., Rhein, M., Käse, R.H., and Zenk, W. (1989): The Mediterranean Water tongue and its chlorofluoro-methane signal in the Iberian Basin in early summer 1989. J. Geophys. Res. 98, 8405-8412.

Hogg, N.G and Johns, W.E. (1995): Western boundary currents. US. National Report to IUGG 1991-1994, Suppl. Rev. Geophys., 1311-1344.

Hüls, C.M. (2000): Millennial-scale SST variability as inferred from planktic foraminiferal census counts in the western subtropical Atlantic. Geomar Report 95, 118 pp.

Hüls, M., and Zahn, R. (2000): Millennial-scale sea surface temperature variability in the western tropical North Atlantic from planktic foraminiferal census counts. Paleoceanography 15, 659-678.

Imbrie, J., Hays, J.D., Martinson, D.G., McIntyre, A., Morley, J.J., Pisias, N.G., Prell, W.L., and Shackleton, N.J. (1984): The orbital theory of Pleistocene climate: support from a revised chronology of the marine d18O record. In: Berger, A., Imbrie, J., Hays, J., Kukla, G., and Saltzman, B. (Eds.): Milankovitch and Climate, Part I: NATO ASI Series C 126, 269-305; D. Reidel Publishing Co; Dordrecht (Netherlands).

Johns, W.E., Townsend, T.L., Fratantoni, D.M., and Wilson, W.D. (2002): On the Atlantic inflow to the Caribbean Sea. Deep-Sea Research 49, 211-243.

Jung, S. J. A. (1996): Wassermassenaustausch zwischen NE-Atlantik und Nordmeer während der letzten 300.000/ 80.000 Jahre im Abbild stabiler O- und C-Isotope. Ph.D. Thesis, Christian-Albrechts-Universität, Kiel, 104 pp.

Kawase, M., and Sarmiento, J.L. (1986): Circulation and nutrients in middepth Atlantic waters. J. Geophys. Res. 91, 9749-9770.

Keigwin, L.D., Jones, G.A., and Lehman, S.J. (1991): Deglacial meltwater discharge, North Atlantic deep circulation, and abrupt climate change. J. Geophys. Res. 96, 16.811-16.826.

Kennedy, J.F. (1964): The formation of sediment ripples in closed rectangular conduits and in the desert. Journal of Geophysical Research 69, 1517-1524.

Kennett, J.P., Keller, G., and Srinivasan, M.S. (1985): Miocene planktic foraminiferal biogeography and paleoceanographic development of the Indo-Pacific region. In: Kennett, J.P. (Ed.): The Miocene Ocean: Paleoceanography and Biogeography. Geol. Soc. Am. Mem. 163, 197-236.

Kennett, J.P., Sarnthein, M., and SCOR-IMAGES W.G. 117 (2001): Decadal to millennial-scale climate variability - Chronology and mechanisms. Summary and recommendations.1117-1280.

Kroon, D., Reijmer, J.J.G., and Rendle, R. (2000): Mid- to Late-Quaternary variations in the oxygen isotope signature of *Globigerinoides ruber* at Site 1006 in the western subtropical Atlantic. In: Swart, P.K., Eberli, G.P., Malone, M.J., and Sarg, J.F. (Eds.): Proceedings of the Ocean Drilling Program, Scientific Re-

sults. 4, Ocean Drilling Program, College Station, 166, 13-22.

Kroon, D.,Alexander, I., Little, M., Lourens, L.J., Mathewson,A., Robertson,A.H.F., and Sakamoto, T. (1998): Oxygen isotope and sapropel stratigraphy in the Eastern Mediterranean during the last 3.2 million years. Proceedings of the Ocean Drilling Program, Scientific results,Volume 160, 81-189.

Lamb, P.J. (1981): Estimate of annual variation of Atlantic Ocean heat transport. Nature 290, 766-768.

Lambeck, K., and Nakada, M. (1992): Constraints on the age and duration of the age and duration of the last interglacial period and on sea-level variations. Nature 357, 125-128.

Larsen, J.C. (1992): Transport and heat flux of the Florida Current at 27°N derived from cross-stream voltages and profiling data: Theory and observations. Philos. Trans. R. Soc. London, A, 338, 169-236.

Lea, D., Pak, D. K., and Spero, H.W. (2000): Climate impact of Later Quaternary equatorial Pacific sea surface temperature variations. Science 289, 1719-1724.

Leaman, K.D., Molinari, R.L., and Vertes, P.S. (1987): Structure and variability of the Florida Current at 27°N: April 1982 to July 1984. J. Phys. Oceanogr. 17, 565-583.

Levitus, S., and Boyer, T.P. (1994): World Ocean Atlas 1994. Volume 4 : Temperature. NOAA ATLAS NESDIS 4, 117 pp.

Linke, P., and Lutze, G.F. (1993): Microhabitat preferences of benthic foraminifera - a static concept or a dynamic adaptation to optimize food acquisition? In: M.R. Langer (Ed.), Foraminiferal Microhabitats. Mar. Micropaleontol. 20, 215-234.

Lutze, G.F., and Thiel, H. (1989): Epibenthic foraminifera from elevated microhabitats: *Cibicidoides wuellerstorfi* and *Planulina ariminensis*. J. Foram. Res. 19, 153-158.

Lynch-Stieglitz, J., Curry, W.B., and Slowey, N. (1998): Reconstructing upper-ocean density structure and circulation during the Last Glacial Maximum. Abstract, 6th International Conference on Paleoceanography, Lissabon (Portugal), 23.-28. August 1998.

Lynch-Stieglitz, J., Curry, W.B., and Slowey, N. (1999): Weaker Gulf Stream during the last Glacial Maximum. Nature 402, 644-648.

Mackensen, A., Sejrup, H.P., and Jansen, E. (1985): The distribution of living benthic foraminifera on the continental slope und rise off southwest Norway. Mar. Micropaleontol. 9, 275-306.

Manabe, S., and Stouffer, R.J. (1997): Coupled ocean-atmosphere model response to freshwater input: Comparision to Younger Dryas event. Paleoceanography 12, 321-336.

Manabe, S., and Stouffer, R.J. (1988): Two stable equilibria of a coupled ocean-atmosphere model. J. Clim. 1, 841-866.

Martini, E., and Müller, C. (1986): Current Tertiary and Quaternary calcareous nannoplankton stratigraphy and correlations. Newsletter Stratigraphy 16, 99-112.

Martinson, D.G., Pisias, N.G., Hays, J.D., Imbrie, J., More, T.C., Jr., and Shackleton, N.J. (1987): Age dating and the orbital theory of the ice ages: development of a high-resolution 0 to 300.000-year chronostratigraphy. Quaternary Research 27, 1-29.

Mazzullo, J.M., Meyer, A., and Kidd, R.B. (1988): New sediment classification scheme for the Ocean Drilling Program. In: Mazzullo, J., and Graham, A.G. (Eds.): Handbook for Shipboard Sedimentologists. ODP Tech. Note 8, 45-67.

McCave, I.N. (1984): Erosion, transport and deposition of fine-grained marine sediments. In: Stow, D.A.V., Piper, D.J. (Eds.): Fine-Grained Sediments. Deep-Water Processes and Facies. Geological Society Special Publication 15, 35-70.

McCulloch, M.T., Mortimer, G.E., Esat, T., Xinhua, L., Pillans, B., and Chapell, J. (1996): High resolution windows into early Holocene climate: Sr/Ca coral records from the Huon Peninsula. Earth Planet. Sci. Lett. 138, 169-178.

McIntyre, A., and Molfino, B. (1996): Forcing of Atlantic equatorial and subpolar millennial cycles by precession. Science 274, 1867-1870.

Metcalf, W.G. (1976): Caribbean-Atlantic water exchange through the Anegada-Jungfern Passage. J. Geophys. Res. 81, 6401-6409.

Milliman, J.D., and Meade, R.H. (1983): World-delivery of river sediment to the oceans. J. Geol. 91, 1-21.

Min, G.R., Edwards, R.L., Taylor, F.W., Recy, J., Gallup, C.D., and Beck, J.W. (1995): Annual cycles of U/Ca in coral skeletons and U/Ca thermometry. Geochim. Cosmochim. Acta 59 (10), 2025-2042.

Minolta Co. Ltd. (1995): Spectrophotometer CM-508d Instruction Manual, 32 pp.

Mitrovica, J.X., and Peltier, W.R. (1991): On postglacial geoid subsidence over the equatorial oceans. J. Geophys. Res. 96 (B12), 20053-20071.

Molinari, R. L., Maul, G.A., Chew, F., Wilson, W.D., Bushnell, M., Mayer. D., Leaman, K., Schott, F., Lee, T., Zantopp, R., Larsen, J.C., and Sanford, T.B. (1985a): Subtropical Atlantic climate studies: Introduction. Science 227, 292-295.

Molinari, R. L., Wilson, W. D., and Leaman, K. D. (1985b): Volume and heat transports of the Florida Current: April 1982 through August 1983. Science 227, 295-297.

Montaggioni, L.F., Cabioch, G, Camoin, G.F., Bard, E., Ribeaux, A., Faure, G., Déjardin, P., and Recy, J. (1997): A 14,000 years continous record of reef growth in a mid Pacific island. Geology 25, 555-558.

Morrison, J., and, Nowlin, W. (1982): General distribution of water masses within the eastern Caribbean

Sea during the winter of 1972 and fall of 1973. Journal of Geophysical Research 87, 4207-4229.

Müller, P.J., Kirst, G., Ruhland, G., von Storch, I., and Rosell-Melé, A. (1998): Calibration of the alkenone paleotemperature index $U^{K'}_{37}$ based on core-tops from the eastern South Atlantic and the global ocean (60°N-60°S). Geochim. Cosmochim. Acta 62, 1757-1772.

Mullineaux, L.S., and Butman, C.A. (1990). Recruitment of encrusting benthic invertebrates in boundary-layer flows: a deep water experiment on Cross Seamount. Limnology and Oceanography 35, 409-423.

Niiller, P.P., and Richardson, W.S. (1973): Seasonal variability of the Florida Current. J. Mar. Res. 31, 144-167.

Nürnberg, D. (2000): Taking the temperature of past ocean surfaces. Science 289, 1698-1699.

Nürnberg, D., Müller, A., and Schneider, R. (2000): Paleo-sea surface temperature calculations in the equatorial east Atlantic from Mg/Ca ratios in planktic foraminifera - A comparison to sea surface temperature estimates from $U^{K'}_{37}$, oxygen isotopes, and foraminiferal transfer function. Paleoceanography 15 (1), 124-134.

Oppo, D.W., and Fairbanks, R.G. (1987): Variability in the deep and intermediate water circulation of the Atlantic Ocean during the past 25.000 years: Northern Hemisphere modulation of the Southern Ocean. Earth Plan. Sci. Lett. 86, 1-15.

Oppo, D.W., and Fairbanks, R.G. (1990): Atlantic thermohaline circulation over the last 150.000 years: Relationship to climate and atmospheric CO_2. Paleoceanography 5, 277-288.

Oppo, D.W., Raymo, M.E., Lohmann, G.P., Mix, A.C., Wright, J.D., and Prell, W.L. (1995): A $\delta^{13}C$ record of Upper North Atlantic Deep Water during the past 2.6 million years. Paleoceanography 10, 373-394.

Pätzold, J. (1984): Growth rhythms recorded in stable isotopes, and density bands in the reef coral *Porites lobata* (Cebu, Philippines). Coral Reefs 3, 87-89.

Peltier, W.R. (1991): The ICE-3G model of Late Pleistocene deglaciation: construction, verification and applications. In: Sabadini R. (Ed.): Glacial Isostacy, Sea Level and Mantle Rheology, 95-119.

Pickard, G.L., and Emery, W.J. (1982): Descriptive physical oceanography. Pergamon, Oxford, 249 pp.

Prahl, F.G., and Wakeham, S.G. (1987): Calibration of unsaturation patterns in long-chain ketone compositions for paleotemperature assessment. Nature 330, 367-396.

Prahl, F.G., Muehlhausen, L.A., and Zahnle, D.L. (1988): Further evaluation of long-chain alkenones as indicators of paleoceanographic conditions. Geochimica et Cosmochemica Acta 52 (9), 2303-2310.

Prell, W.L., and Hays, J.D. (1976): Late Pleistocene faunal and temperature patterns of the Colombia Basin, Caribbean Sea. Memoir, Geological Society of America. 145, Investigation of late Quaternary paleoceanography and paleoclimatology, 201-220.

Price, J., O'Neil Barringer, M., Lueck, R.G., Johnson, G.C., Ambar, I., Parrilla, G., Cantos, A., Kennelly, M.A., and Sanford, T.B. (1993): Mediterranean outflow mixing and dynamics. Science 259, 1277-1282.

Rahmstorf, S. (1994): Rapid climate transitions in a coupled ocean-atmosphere model. Nature 372, 82-85.

Rendle, R., Alexander, I., Reijmer, J.J.G., and Kroon, D. (1998): Mineralogy and sedimentology of the Pliocene/Pleistocene on the leeward side of Great Bahama Bank (ODP Leg 166). In: Canaveras, J.C., Garcia del Cura, M.A., Soria, J., Melendez Hevia, A., and Soria, A.R.: 15th international sedimentological congress: Sedimentology at the dawn of the third millenium: Abstracts. Univ. Alicante, Spain, 657 pp.

Revel, M., Cremer, M., Grousset, F.E., and Labeyrie, L. (1996): Grain-size and Sr-Nd isotopes as tracers of paleo-bottom current strength, Northeast Atlantic Ocean. Marine Geology 132, 233-249.

Richardson, P.L., and T.K. McKee (1984): Average seasonal variation of the Atlantic equatorial currents from historical ship drifts. J. Phys. Ocean. 14, 1226-1238.

Richardson, W.S., Schmitz, W.J. Jr., and Niiler, P.P. (1969): The velocity structure of the Florida Current from the Straits of Florida to Cape Fear. Deep-Sea Res., Suppl. to 16, 225-231.

Rosell-Mélé, A., Bard, E., Emeis, K.-C., Farrimond, P., Grimald, J., Müller, P.J., and Schneider, R. (1998): Project takes a new look at past sea surface temperatures. EOS, Transactions, AGU 79 (33), 393-394.

Rühlemann, C., Mulitza, S., Müller, P. M., Wefer, G., and Zahn, R. (1999): Warming of the tropical Atlantic Ocean and slowdown of thermohaline circulation during the last deglaciation. Nature 402, 511-514.

Sarnthein, M., Kennett, J.P., Allen, J.R.M., Beer, J., Grootes, P., Laj, C., McManus, J., Ramesh, R., and SCOR-IMAGES Working Group 117 (2002): Decadal-to-millennial-scale climate variability--chronology and mechanisms: summary and recommendations. Quaternary Science Reviews 21 (10), 1121-1128.

Sarnthein, M., Pflaumann, U., Vogelsang, E., Working group Kiel SFB-313, Pätzold, J., Wefer, G., Working group Bremen SFB-261, Spielhagen, R., and Working group Kiel-GEOMAR (1998): Atlantic sea-surface temperatures during the LGM - First Results of the German Project “Climap 2000“. EOS, Transactions, AGU 79 (45).

Sarnthein, M., Winn, K., Duplessy, J.-C., Labeyrie, L., Erlenkeuser, H., Ganssen, G., and Jung, S. (1994): Changes in east Atlantic deep-water circulation over the last 30.000 years an eight-time-slice record. Paleoceanography 9, 209-267.

Sato, O.T., and Rossby, T. (1995): Seasonal and low frequency variations in dynamic height anomaly and

transport of the Gulf Stream. Deep-Sea Res. Part L, 42, 149-164.

Schmitz, W.J., and McCartney, M.S. (1993): On the North Atlantic circulation. Rev. Geophys. 31, 29-49.

Schmitz, W.J., Luyten, J.R., and Schmitt, R.W. (1993): On the Florida Current T/S envelope. Bull. Mar. Sci. 53, 1048-1065.

Schönfeld, J. (1997): The impact of the Mediterranean Outflow Water (MOW) on Benthic foraminiferal assemblages and surface sediments at the southern Portuguese continental margin. Mar. Micropaleontol. 29, 211-236.

Schönfeld, J. (1998): Recent benthic foraminiferal assemblages in deep high-energy environments from the Gulf of Cadiz (Spain). Newsl. Micropalaeontol. 58, 16-17.

Schönfeld, J. (2002). Recent benthic foraminiferal assemblages in deep high-energy environments from the Gulf of Cadiz (Spain). Marine Micropal. 44, 141-162.

Schönfeld, J. (2002a): A new benthic foraminiferal proxy for near-bottom current velocities in the Gulf of Cadiz, northeastern Atlantic Ocean. Deep-Sea Res. 49, 1853-1875.

Schönfeld, J., and Zahn, R. (2000): Late Glacial to Holocene history of the Mediterranean Outflow. Evidence from benthic foraminiferal assemblages and stable isotopes at the Portuguese Margin. Palaeogeogr., Palaeoclimatol., Palaeoecol. 159, 85-111.

Schott, F., and Zantop, R. (1985): Florida Current: seasonal and interannual variability. Science 227, 308-311.

Sicre, M-A., Bard, E., Ezat, U., and Rostek, F. (2002): Alkenone distributions in the North Atlantic and Nordic sea surface waters. Geochem. Geophys. Geosyst. 3, 10.1029/2001GC000159.

Southard, J.B., and Boguchwal, L.A. (1990): Bed configurations in steady unidirectional water flows. Part 2. Synthesis of flume data. Journal of Sedimentary Petrology 60, 658-679.

Stalcup, M.C., and Metcalf, W.G. (1972): Current measurements in the passages of the Lesser Antilles. J. Geophys. Res. 77, 1032-1049.

Sturges, W. (1975): Mixing of renewal water flowing into the Caribbean Sea. J. Mar. Res. 33, 117-130.

Tomczak, M., and Godfrey, J. S. (1994): Regional Oceanography: An Introduction. Pergamon, New York.

Van Andel, T.H., Hearth, G.R., and Moore, T.C. (1975): In: Cenozoic history and paleoceanography of the central equatorial Pacific Ocean: A regional synthesis of Deep Sea Drilling data. Geological Society of America, Memoir 143, 49-72.

Van Kreveld, S., Sarnthein, M., Erlenkeuser, H., Grootes, P., Jung, S., Nadeau, S.J., Pflaumann, U., and Voelker, A. (2000): Potential links between surging ice sheets, circulation changes, and the Dansgaard-Oeschger cycles in the Irminger Sea. Paleoceanography 15, 425-442.

Westphal, H. (1998): Carbonate platform slopes - a record of changing conditions: The Pliocene of the Bahamas. In: Bhattacharji, S., Friedman, G.M., Neugebauer, H.J., and Seilacher, A. (Eds.): Lecture notes in earth sciences. Springer, Berlin-Heidelberg-New York, 75, 195 pp.

Worthington, L.V. (1971): Water circulation in the Caribbean Sea and its relationship to North Atlantic circulation. Symposium on Investigation and Resources of the Caribbean Sea and Adjacent Region. UNESCO, Paris, 181-191.

Worthington, L.V. (1976): On the North Atlantic circulation. Johns Hopkins Oceanographic Studies 6, 110 pp.

Wüst, G. (1964): On the stratification and the circulation in the cold water sphere of the Antillean-Caribbean basins. Deep-Sea Res. 10, 165-187.

Wüst, G. (1964): Stratification and circulation in the Antillean-Caribbean Basins. Columbia University Press, New York.

Young, J.R. (1998): Neogene. In: Bown, P.R. (Ed.): Calcareous Nannoplankton Stratigraphy. Kluwer Dordrecht, 225-265.

Zahn, R., Sarnthein, M., and Erlenkeuser, H. (1987): Benthic isotope evidence for changes of the Mediterranean outflow during the late Quaternary. Paleoceanography 2, 543-559.

Zanke, U. (1982): Grundlagen der Sedimentbewegung. Springer, Berlin, 402 pp.

Zenk, W., and L. Armi (1990): The complex spreading pattern of Mediterranean Water off the Portuguese continental slope. Deep-Sea Res. 37, 1805-1823.

Zenk, W., K. Schultz Tokos, and O. Boebel (1992): New observations of meddy movement south of the Tejo Plateau, Geophys. Res. Lett. 19, 2389-2392.

Zinke, J., Reijmer, J. J.G., Thomassin, B. A., Dullo, W.-Chr., Grootes, P. M., and Erlenkeuser, H. (2003): Postglacial flooding history of the Mayotte lagoon (Comoro archipelago, SW Indian Ocean). Marine Geology in press.